LICENTIATE THESIS

FRP Strengthening of Concrete Walls with Openings

Cosmin Popescu

LULEÅ UNIVERSITY OF TECHNOLOGY

FRP strengthening of concrete walls with openings

COSMIN POPESCU

Luleå 2015

Luleå University of Technology
Department of Civil, Environmental and Natural Resources Engineering
Division of Structural and Construction Engineering – Structural Engineering
SE-971 87 Luleå, Sweden
www.ltu.se

Printed by Luleå University of Technology, Graphic Production 2015

ISSN 1402-1757
ISBN 978-91-7583-453-5 (print)
ISBN 978-91-7583-454-2 (pdf)

Luleå 2015

www.ltu.se

Academic thesis

for the Degree of Licentiate (Tech. Lic.) in structural engineering, which by due of the Technical Faculty Board at Luleå University of Technology will be publicly defended in:

Room F1031, Luleå University of Technology,
Monday, December 7th, 2015, 10:00

Opponent:	Professor Joaquim António Oliveira de Barros, University of Minho
Principal supervisor:	Professor Björn Täljsten, Luleå University of Technology
Assistant supervisor:	Associate Senior Lecturer Gabriel Sas, NORUT Northern Research Institute
	Associate Senior Lecturer Thomas Blanksvärd, Luleå University of Technology

PREFACE

The ongoing PhD program is jointly managed under a cooperative agreement by the Northern Research Institute Narvik AS (Norut) and Luleå University of Technology (LTU).

I would like to acknowledge The Research Council of Norway (RFF), Development Fund of the Swedish Construction Industry (SBUF) and Skanska for largely financing the presented work and associated, ongoing project. Other financial contributions from LTU, NORUT, Elsa and Sven Thysells' Foundation, Nordea Bank and the Norwegian Concrete Association (Norsk Betongforening) are also gratefully acknowledged.

Many people have contributed to this thesis, the research it is based upon, and my professional development. First and foremost I would like to thank the supervisory team from LTU and NORUT consisting of my main supervisor Prof. Björn Taljsten, and assistant supervisors Dr. Gabriel Sas and Dr. Thomas Blanksvärd, who gave me the freedom to explore while always guiding me. Dr. Gabriel Sas provided me with valuable advice and fruitful discussions almost every day. Dr. Thomas Blanksvärd is acknowledged for his support throughout my studies and critically reviewing my work. Besides scientific guidance, Prof. Björn Taljsten is a visionary who taught me valuable lessons about project management and thinking ahead.

I would also like to express thankfulness to those who provided help during this research program. Special thanks are due to the technicians of CompLab, the structural engineering laboratory at LTU, Dr. Dan Diaconu from Politehnica University Timisoara for the help provided with the strengthening work and PhD student Cristian Sabău and Dr. Mohammed Salih from LTU for providing help with optical measurements.

My first steps into the research started at Politehnica University Timisoara under the supervision of Prof. Valeriu Stoian, to whom I am eternally grateful. My former colleagues and dear friends from the same university, Dr. Tamás Nagy-György, Dr. Sorin-Codruţ Floruţ, and Dr. Cosmin Dăescu are also acknowledged for the fruitful collaboration we had during my PhD studies. I look forward to our continued collaboration.

A big thanks to my colleagues at the Division of Structural and Construction Engineering are also due for making the working days enjoyable. Special thanks to Tekn. Lic. Niklas Bagge, PhD students Jens Häggström and Cristian Sabău for all the time we spent together.

Above all I would like to thank my wife Adriana for her love, endless support and encouragement. You are the force behind me who's always pushing me forward.

Cosmin Popescu
Luleå, December 2015

SUMMARY

The thesis deals with the axial strength of axially and eccentrically loaded concrete walls with cut-out openings strengthened by fiber-reinforced polymers (FRPs).

Background: Functional modifications of concrete structures are common because existing structures must often be adapted to comply with current living standards. Such modifications may include the addition of new windows or doors and paths for ventilation and heating systems, all of which require openings to be cut into structural walls. These openings are a source of weakness and can size-dependently reduce the structures' stiffness and load-bearing capacity, thus, requiring the element to be repaired.

Aim and objectives: The main aim of this project was to develop a toolbox containing solutions for strengthening concrete walls with existing or newly created openings using FRP materials. The two immediate objectives sought are: (1) An assessment of the research level on concrete walls with and without openings; (2) An experimental and numerical investigation of the structural behavior of the FRP strengthened walls with openings.

Methods of investigation: The experimental program was defined by reviewing the relevant tests performed to date. The literature review revealed research gaps that the current study aims to fill. Moreover, preliminary nonlinear finite element analyses were performed prior to the experimental program in order to gain insight into the structural behavior of these elements. Nine specimens designed to represent typical wall panels in residential buildings, at half-scale, were constructed for testing to failure. The two types of openings examined comprised symmetric half-scaled single door-type openings, and symmetric half-scaled double door-type openings. The test matrix was divided into three stages, namely: (1) Reference specimens, (2) Pre-cracked specimens strengthened by FRP and (3) Un-cracked specimens strengthened by FRP. The strengthening method used was FRP-confinement with the aid of mechanical anchorages.

Results: The results indicate that the 25% and 50% reductions in cross-sectional area of the solid wall caused by introducing the small opening and large opening reduced its load carrying capacity by nearly 36% and 50%, respectively. The application of the FRP confinement increases the capacity and the stiffness of the specimens with cut-out openings. The axial strengths were between 85-94.8% and 56.5-63.4% for specimens having a small and large opening, respectively, of that of a solid wall.

Conclusion: The FRP-confinement together with the mechanical anchorages was able to partly restore the capacity of a solid wall. Better results might have been possible if longitudinal FRP strips or bi-directional fibers were used. The effects of steel anchorages were not investigated and it is believed that they might have had positive influences. However, the optimal distance in-between the anchors should be further investigated. Moreover, the influence of the prestressing force of the anchorages may also be an important parameter that has led to an increase in capacity.

Keywords: Strengthening, Fiber-reinforced polymers, Concrete walls, Openings, Axial load, Eccentricity, Out-of-plane behavior, Two-Way

TABLE OF CONTENTS

1 Introduction

This section gives a brief overview of the research problem investigated. The section ends by presenting the research questions, limitations and the original contributions published as journal papers.

1.1 Background

One of the most significant current discussions about sustainable development of our society is that it always has to be supported by a safe, functional and durable built environment. Concrete structures have a high share of the total number of structures in the world. These structures are degrading continuously and the need for repair and rehabilitation increases annually as shown in Table 1. This increase is closely connected to the worldwide population growth so that new structures are being built and existing structures are still needed to be used.

Functional modifications of these structures are common because existing structures often have to be adapted to comply with current living standards and/or legislation. Such modifications may include the addition of new windows or doors and paths for ventilation and heating systems, all of which require openings to be cut into structural walls. These openings are essential in order to redesign the building for space efficiency and reuse for long-term conditions.

The openings are a source of weakness and can size-dependently reduce the structures' stiffness and load-bearing capacity. Numerous experimental studies have examined the behavior of solid concrete walls, but the performance of walls with openings has been studied much less intensively. Exceptions include contributions by (Ali and Wight 1991, Taylor 1998, Wang, et al. 2012, Mosoarca 2014, Todut, et al. 2014). However, the cited studies focused on structural walls subjected to seismic forces; effects of openings in walls that are only designed to withstand axial compression loads have received much less attention.

Table 1. Investment trends in rehabilitation and maintenance in Europe (FIEC 2014)

	Mln. € fixed prices	Per cent variation of production in real terms on previous year				
Country	**2013**	**2010**	**2011**	**2012**	**2013**	**2014**
Sweden	6931	18.0	-2.2	-3.3	-1.3	1.4
Norway	3763	2.1	1.9	5.1	3.1	3.0
Denmark	3995	0.2	13.2	-1.4	-2.2	3.5
Finland	5441	5.7	3.0	3.1	3.0	3.0
European Union	**266201**	**2.1**	**1.2**	**2.1**	**-0.1**	**1.9**

In the research literature, walls that are subjected to axial loads are described as one-way (OW) or two-way (TW) walls, respectively. Walls restrained along top and bottom edges are referred to as OW action panels. Walls that are restrained in this fashion tend to develop a single out-of-plane curvature in parallel to the load direction, and are usually encountered in tilt-up concrete structures. Panels restrained along three or four sides are referred to as TW action panels. Walls restrained in this way generally deform along both the horizontal and vertical directions and are usually encountered in monolithic concrete structures. Typical crack patterns for walls both with and without openings are shown in Fig. 1.

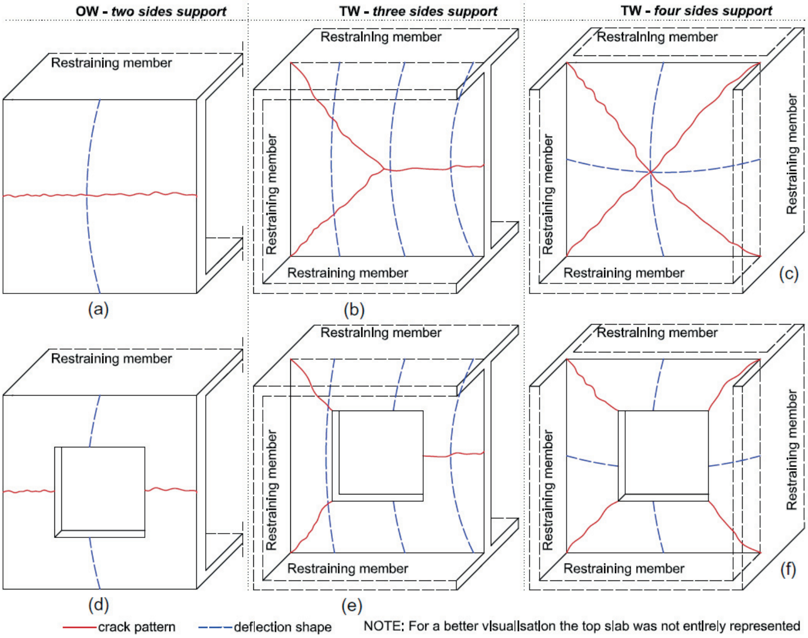

Fig. 1. Typical crack pattern and deflection shape of axially loaded RC walls (Popescu, et al. 2015b)

As shown by many research studies, restraining members along the side edges can provide significant increases in load-bearing capacity. Even so, EN1992-1-1 (2004) and AS3600 (2009) are the only major codes which recognize the contributions of the side restraints.

In all major design codes a distinction is made between reinforced and unreinforced walls. It should be noted that unreinforced members does not only refer to plain concrete but also when the reinforcement provided is less than the minimum required for reinforced concrete, also referred to as lightly reinforced members.

When the walls are subjected to axial loads with small eccentricities recommendations as for unreinforced members can be applied. However, the eccentricity should not be of significance, and the value is described in ACI318 (2011), AS3600 (2009) and CAN/CSA-A23.3 (2004) as being one sixth of the wall thickness (i.e. the resultant of all loads on the wall must be located within the middle third of its overall thickness). Within these limits, design codes provide some empirical formulas for predicting the ultimate capacity. Results obtained from these empirically developed design models may deviate from real values in cases where there is greater eccentricity.

Since the simplified methods assume that the walls are unreinforced elements, the contribution of any steel reinforcement is disregarded. This occurs regardless of the location of the steel mesh layer, or if the reinforcement is placed in one or two layers. For centrally reinforced walls this seems to be valid (Pillai and Parthasarathy 1977), although in some cases it may bring some ductility at higher loads. For walls with reinforcement placed in two layers, however, the enhanced capacity should be accounted for, even when the steel ratio is at a minimum level required by design codes.

The majority of all studies performed to date concerned walls with designed openings (i.e. with diagonal bars around the opening corner to avoid premature cracking). Walls with cut-out openings (i.e. openings sawn in a solid panel) are still unexplored yet; to the best knowledge of the author, just one research study (Mohammed, et al. 2013) has focused on this problem type. The findings showed that the presence of the opening in a solid OW panel led to disturbance zones. The discontinuities causing high stresses will force the cracks to firstly occur at the corners due to insufficient reinforcement. Therefore, the vicinity of the openings needs to be strengthened.

In order to restore the capacity of concrete walls prior to cutting the opening, two methods are commonly used. These are either to create a frame around the opening using reinforced concrete/steel members (Engel n.d.) or to increase the cross-sectional thickness (Delatte 2009). Nowadays, intervention in existing buildings must be minimal in order to reduce inconvenience due to limited use of the structure during repairs. Other drawbacks of these traditional methods are: the methods may not be architecturally convenient, may result in increases in the weight of the elements strengthened and that they are time consuming. As a consequence, an alternative that has been used successfully in the last decades is to use FRP as the externally bonded material.

1.2 Hypothesis, aim and research questions

<u>Hypothesis</u>: Strengthening concrete walls with cut-out openings by FRP enhances their structural performances, i.e. axial strength, stiffness and energy dissipation.

<u>Aim</u>: Developing a toolbox containing solutions for strengthening concrete walls with existing or newly created openings using FRP materials. The two immediate objectives are sought: (1) Assess the current research level carried out worldwide on concrete walls with and without openings; (2) Investigate experimentally and numerically the structural behavior of the FRP strengthened walls with openings.

<u>Research questions</u>: From a scientific point of view, there are several unknowns that cannot be addressed from only a limited number of experimental tests. In order to comply with the aim of this research project these unknowns are to be identified based on the following research questions:

i. *Do existing models accurately predict the ultimate capacity of axially loaded concrete walls with and without openings?*

ii. *How to delineate small and large openings in walls, and where the transition from RC walls to RC frames should occur in the design of structural elements?*

iii. *Does the failure mechanism of a concrete wall with an opening change after strengthening with FRP?*

1.3 Limitations

The literature study considered the performances of design models found in scientific articles published since 1990 onwards and indexed in databases such as Scopus and Web of Science.

Therefore, it is possible that some relevant models may have been unintentionally overlooked.

The experimental study involved short-term tests and newly cast specimens, therefore the results may not be fully representative of walls from existing structures, which are always subject to a relatively high sustained load and effects of degradation due to aging.

In an attempt to perform all the rehabilitation work at once, the pre-cracked specimens were removed from the test setup, thus, the formed cracks were nearly closed before strengthening was applied.

Having a complex test protocol, the duration of one test varied from 30 minutes to 2 hours. This could have affected the data collected by the digital image correlation system since the ambient light (subjected to fast changes) may have influenced the readings.

Indeed, some choices made by the author such as the number of specimens, amount of eccentricity, the aspect and slenderness ratio, boundary conditions or the loading protocol, may be regarded as limitations. However, these choices were imposed by the study idea and more obviously, financial resources availability.

1.4 Scientific approach

The research was performed by following the conventional methodological approach in order to accomplish the research objectives. The process started with a critical literature review of the existing knowledge on concrete walls with and without openings, with an emphasis on the latter. The study indicated areas where further testing is required in order to enhance the reliability of current design models. Moreover, research questions were formulated in accordance with the research gaps identified.

Previous experience from experimental tests was used to calibrate a finite element model (FEM) useful in finding important information such as crack development, strain/stress patterns for steel reinforcement and concrete, deformation behavior, failure mode and ultimate capacity. The information gathered was used to answer the question: "What is to be measured in order to obtain reliable data that would form the basis to formulate answers for the research questions?"

The instrumentation scheme was the first important outcome from this investigation. The second outcome was the design of the test-rig able to reproduce the as-build boundary conditions and to facilitate the loading regime wanted. The third outcome was to design a reliable test matrix using design of experiments (DoE) technique (Box, et al. 1978).

The strengthening method proposed was designed according to analytical methods found in the research literature and the results obtained were then verified in laboratory experiments.

1.5 Outline of the thesis

This book is an article-based thesis, in which printed or reprinted journal articles are appended to an overall summary of their content. The structure of this summary is comprised of *Chapters 1-3* and briefly described below:

Chapter 1 sets the background, aim and limitations of the work, and describes previous work related to the research subject.

Chapter 2 defines the research design and presents the laboratory-based experimental program.

Chapter 3 presents the conclusions based on findings related to the aim of the research and answers the research questions.

1.6 Appended papers

The core of this thesis incorporates four journal papers. My contribution to these papers was the design of the experiments including the test setup design, performing the experiments and numerical analyses, data collection and analysis, and finally writing the manuscripts.

PAPER I

Popescu, C., Sas, G., Blanksvärd, T., & Täljsten, B. (2015). Concrete walls weakened by openings as compression members: A review. *Engineering Structures, 89*(0), 172-190. doi: http://dx.doi.org/10.1016/j.engstruct.2015.02.006

Paper I is a review of the advances that have been made in the design of concrete walls, both with and without openings that are subjected to eccentric axial loads. A statistical analysis of available models from design codes and research studies from across the world was performed on a database collected by the first author.

PAPER II

Popescu, C., & Sas, G. (2014). The Development of an Experimental Program through Design of Experiments and FEM Analysis: A Preliminary Study. *Nordic Concrete Research, 51*, 14.http://www.nordicconcrete.net/ikbViewer/Content/918170/NCR%20vol%2051%20ec%22014.pdf

Paper II presents the design of the current experimental program using DoE method. A FEM model able to predict the behavior of TW axially loaded walls was calibrated with past experimental results. It was then possible to decide the instrumentation scheme and to design the test setup.

PAPER III

Popescu, C., Sas, G., Sabău, C., & Blanksvärd, T. (2016). Effect of cut-out openings on the axial strength of concrete walls [*under review*]

Paper III presents the experimental results on un-strengthened walls with and without openings. Aspects such as the effects of the size of cut-out openings and steel reinforcement on the axial strength of concrete walls is evaluated. The results were also used to assess the accuracy of current design models.

PAPER IV

Popescu, C., Sas, G., Blanksvärd, T., & Täljsten, B. (2016). Concrete walls with cut-out openings strengthened by FRP-confinement [*to be submitted*]

Paper IV investigates the effectiveness of FRP-confinement to increase the axial strength of concrete walls damaged by cut-out openings. Comparisons were made between un-strengthened and strengthened elements in order to evaluate the global and local performances such as cracking, demands on the steel reinforcement and utilization of the composite fibers.

1.7 Additional publications

Besides the research project described in this thesis, the author had the opportunity to collaborate with other researchers in different projects that are related, direct or indirect, to the current research project. This work was materialized by publication of several journal, reports and conference papers. These papers are stated here, but not appended to the thesis.

Journal papers

[1] Floruţ, S.-C., Sas, G., **Popescu, C.**, & Stoian, V. (2014). Tests on reinforced concrete slabs with cut-out openings strengthened with fibre-reinforced polymers. *Composites Part B: Engineering, 66C*. doi: http://dx.doi.org/10.1016/j.compositesb.2014.06.008

[2] Sas, G., Dăescu, C., **Popescu, C.**, & Nagy-György, T. (2014). Numerical optimization of strengthening disturbed regions of dapped-end beams using NSM and EBR CFRP. *Composites Part B: Engineering, 67*, 381-390.
doi: http://dx.doi.org/10.1016/j.compositesb.2014.07.013

[3] **Popescu, C.**, Dăescu, C., Tamás, N-G. & Sas, G. (2013). Disturbed regions in dapped-end beams: numerical simulations of strengthening techniques. *Nordic Concrete Research*, 48(2), 14-26

Conference papers

[1] **Popescu, C.**, Sas, G., Sabău, C., & Blanksvärd, T. & Täljsten, B. (2015) Experimental tests on RC walls with openings strengthened by FRP. Accepted in *The 12th International Symposium on Fiber Reinforced Polymers for Reinforced Concrete Structures (FRPRCS-12) & The 5th Asia-Pacific Conference on Fiber Reinforced Polymers in Structures (APFIS-2015),* Joint Conference, 14-16 December 2015, Nanjing, China

[2] **Popescu, C.**, Sas, G., Täljsten, B. & Blanksvärd, T. (2014). A state of the art review on walls with openings strengthened by use of fiber reinforced polymers. *Proceedings of The 7th International Conference on FRP Composites in Civil Engineering (CICE 2014)*. El-Hacha, R. (ed.). Vancouver, British Columbia, Canada: International Institute for FRP in Construction (IIFC), 6 p. #128

[3] **Popescu, C.**, Sas, G., Täljsten, B. & Blanksvärd, T. (2014) Experimental Program for Axially Loaded RC Walls with Openings Strengthened by FRP. *XXIIth Symposium on Nordic Concrete Research & Development*, Reykjavik, Iceland. (Conference paper published in Proceedings of Nordic Concrete Research). 50, 285-288

[4] Dăescu, C., Nagy-György, T., Sas, G., Barros, J. & **Popescu, C.** (2013) Numerical Assessment of Dapped Beam Ends Retrofitted with FRP Composites. *FRPRCS-11: 11th International Symposium on Fiber Reinforced Polymer for Reinforced Concrete Structures*. Barros, J. & Sena-Cruz, J. (eds.). Guimarães, Portugal, 9 p.

Technical reports

[1] Sas, G., Daescu, C., Sæther, I., **Popescu, C.**, Arntsen, B. (2013). MÅLSET DAM - Finite element analysis assisted by tests, Technical report no.: 2013/3

[2] **Popescu, C.**, Sas, G., Sand, B. (2013) Composite slabs with profiled steel decking - numerical simulations, Technical report no.: 2012/12

2 Concrete walls with openings strengthened with fiber-reinforced polymers

Discussions of the approaches to design walls according to international codes and research literature are given in this section. The research design and the quantitative approaches employed in collecting data will also be presented. Results from the laboratory tests are then briefly described.

2.1 Literature review

2.1.1 Axially loaded concrete walls with and without openings

Several researchers have put a tremendous effort into understanding the behavior of concrete walls treated as compression members. A summary of all these studies is given herein and presented in more detail in Paper I.

The first studies related to walls subjected to axial loads were performed by Seddon (1956) and Larsson (1959). Oberlender and Everard (1977) investigated solid walls in one-way action and derived an empirical design model. The reinforcement layers were arranged at different depths in order to determine the effect of reinforcement location in response to either concentric or eccentric loading conditions. Another purpose of the program was to determine the load capacities of the OW panels with respect to their aspect and slenderness ratio. In an attempt to observe any differences from varying the steel reinforcement ratio as well as slenderness ratios Pillai and Parthasarathy (1977) developed an experimental program on testing OW walls and provided a new empirical design equation. Swartz, et al. (1974) pointed out that reinforced concrete panels are usually simply supported along all sides in which biaxial buckling may occur. Therefore, the buckling loads were monitored for several panels tested in which steel reinforcement ratio and the number of steel mesh layers was varied. A formula predicting the average stress in concrete at the onset of buckling was derived.

Based on the abovementioned studies the parameters that have an influence on the ultimate capacity are analyzed and presented in Paper I. The results from these experimental tests are gathered in the database collected by the author and used to assess the performances of existing design models. However, some of these researchers developed design models but those are not evaluated here nor in Paper I (Popescu, et al. 2015b). The reader is referred to (Fragomeni, et al. 1994). The performances of the design models developed more recently (i.e. after 1990) are included in the analysis presented in Paper I. A short summary is also given in the following paragraphs.

The first systematic study of concrete walls with and without openings tested in OW and TW action was reported by Saheb and Desayi (1989), (1990a, b). The study investigated the influence of aspect, thickness and slenderness ratio as well as vertical and horizontal steel reinforcement ratio on the ultimate load. For OW action the authors combined experimental results from their own tests and from test results reported by Oberlender and Everard (1977), Pillai and Parthasarathy (1977) and Zielinski, et al. (1982) to suggest modifications to existing design equation. Until that time no equations for predicting the ultimate strength of wall panels in TW were available. Hence, the authors suggested two methods in this direction: (1) the empirical method based on their own data and the one published by Swartz, et al. (1974); (2) a semi-empirical method developed from a modification of the buckling strength theory of thin rectangular metal sheets proposed by Timoshenko and Gere (1961) (see Paper I for further details). For walls with openings all the above parameters were kept constant in order to allow the study to account for the influence of type and location of opening(s). Saheb and Desayi (1990a) have also proposed an equation for predicting the ultimate load of such walls. The experimental program undertaken by the Fragomeni (1995) focused on investigating the axial load capacity of OW normal and high-strength concrete walls. The authors suggested a change to the design formula to account for the increase in wall strength when high strength concrete is used. Following the suggestions made by Fragomeni (1995) where the high concrete strength values have to be taken into account in order to increase the wall strength, Doh (2002) performed an extensive experimental program on OW and TW concrete walls in order to modify the existing equation in design codes. Further on Doh and Fragomeni (2006) enriched their experimental program by testing also concrete walls with opening(s). Based on the equation proposed for solid walls (Doh and Fragomeni 2005) and following the same methodology for walls with openings proposed by Saheb and Desayi (1990a), the authors developed a new formula for concrete walls with openings. In order to provide useful information for further improvement of the code equation, an extensive experimental program was undertaken by Lee (2008). Both OW and TW walls with openings having different slenderness ratios and concrete compressive strength were investigated. The experimental results were used to validate the design model of Doh and Fragomeni (2006). In two recent studies, (Ganesan, et al. 2012, Ganesan, et al. 2013) the axial strength of OW wall panels made out of steel fiber reinforced concrete and geo-polymer concrete, was studied. The key parameters in these studies were slenderness and aspect ratio. The findings were used to modify the equation proposed by Saheb and Desayi (1989). Robinson, et al. (2013) proved that current methodologies (ACI318 2011, AS3600 2009, EN1992-1-1 2004) have a significant conservationism when assessed through experimental results obtained in a series of tests for OW slender wall panels. Therefore, those authors devised a new theoretical model by using the application of the ''lumped plasticity'' through the semi-empirical semi-probabilistic DAT (Design Assisted by Testing) methodology, enabled within the European design code. The theoretical model has been validated against experimental data and by applying statistical techniques the authors were able to propose a design method suitable for its purpose.

As can be seen a considerable amount of literature has been published on the study of the behavior of wall panels with and without openings. An up-to-date database collected by the author has shown that 41.1% and 26.1% from the tests included in the database was referred to OW and TW solid walls, respectively. Little attention has yet been given to the study of walls with openings: 19.4% and 13.4% from the tests included in the database was referred to OW and TW walls with openings, respectively. The database can be found in Paper I (Popescu, et al. 2015b) appended to this thesis.

Numerous design-oriented models have been developed by researchers and their performances were reviewed by Fragomeni, et al. (1994) (studies until 1990) and Popescu, et al.

(2015b) (studies since 1990). Both of these reviews concluded that the performance of walls with openings has not been thoroughly addressed, and some results are conflicting, thus more experimental tests are needed. Fewer tests exist on walls under TW action, walls with openings or different load eccentricities, and more tests are required in these experimental conditions to facilitate the development of appropriate design models. An overview of the performance of current design models through a statistical analysis based on the database collected by the author is published in Paper I of this thesis (Popescu, et al. 2015b).

2.1.2 Axially loaded concrete walls with openings strengthened with FRP

Sustainable social development requires a safe, functional and durable built environment. Structures are continuously degrading and the need of repair increases exponentially. There are many reasons for strengthening, however, one can identify a number of common features such us: changes in use combined with an increase in imposed load, structures ageing due to material degradation and external environment, structural alterations who requires openings to be cut into slabs or walls. Nowadays, intervention in existing buildings must be minimal in order to reduce inconvenience due to limited use of the structure during repairs. As a consequence, an alternative that has been used successfully in the last decades is to use FRP materials as the externally bonded material. The technique implies that thin composite sheets, plates or bars are bonded through an adhesive to the concrete surface or inside the concrete cover (near surface) to improve the strength and behavior of the structural element (Täljsten, et al. 2003).

FRP composites are comprised of fibres with high tensile strength within a polymer matrix. The fibres are generally made from carbon, glass, aramid and basalt. Typical mechanical values for all types of fibres are shown in Fig. 2. The adhesives used for supporting the fibers can be of organic or inorganic nature. Organic adhesives, such as epoxy, are the most common type and their application have shown good behavior in terms of strength, bond and creep properties (Blanksvärd 2009). However, there are some drawbacks such as diffusion tightness, poor thermal compatibility with concrete or regulations on how to handle the epoxy bonding agents (Blanksvärd, et al. 2009). Moreover, low fire resistance of FRP-strengthened structural elements may also be seen as poor performance. Thus, more recently inorganic (mineral) binders started to gain more attention from the research community as it may be a better alternative in terms of compatibility with the base layer, i.e. concrete.

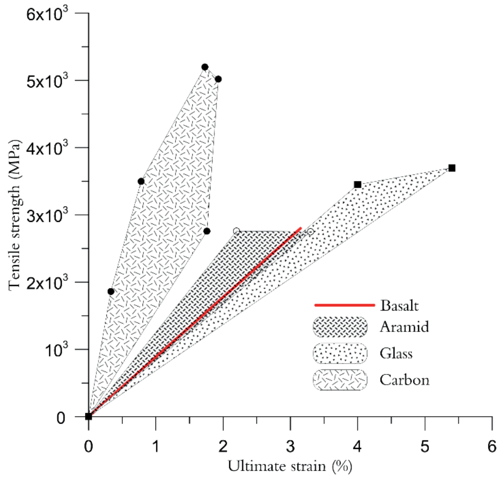

Fig. 2. Typical mechanical properties range of carbon, glass aramid and basalt fibers

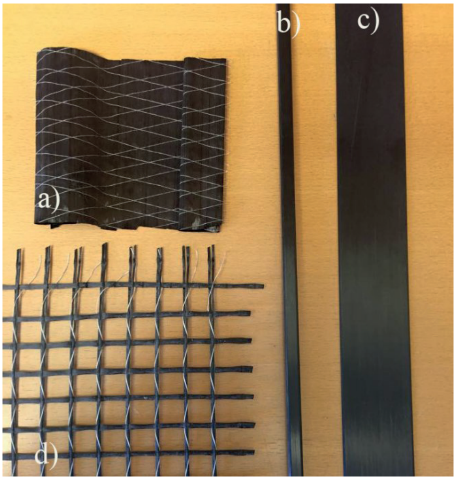

Fig. 3. FRP products: a) sheets; b) bars; c) plates and d) textile reinforcement grids

The FRP products can be found in different shapes such as: sheets, bars, plates and grids, see Fig. 3. For strengthening purposes, FRP bars and plates are only uni-directional while FRP sheets and grids can be produced as uni-, bi- or multi-directional fibers. These fibers are aligned parallel to the principal tensile stresses when structural elements are shear or flexural deficient. Axial strength can also be enhanced by wrapping transversally the fibers, method known as FRP-confinement. Some particular cases in which the FRPs are successfully employed can be seen in Fig. 4.

The research conducted so far on strengthening large structural members with openings, such as slabs or walls, using FRPs is promising (Todut, et al. 2015, Floruţ, et al. 2014, Li, et al. 2013, Demeter 2011, Enochsson, et al. 2007). The alignment of the fibres was based on observations of the failure modes of the un-strengthened elements. Usually the FRP material is placed around openings in a vertical, horizontal or inclined alignment, or a combination of these. The studies regarding walls were focused on seismic retrofitting. The proposed strengthening schemes, therefore, may not be suitable for the repair of gravitationally loaded walls, and more research is required with the loads applied vertically. For non-seismically designed walls with openings, Mohammed, et al. (2013) was the first who investigated their performances when FRP-strengthened. One-way, 1/3-scale RC walls with size opening varying from 5% to 30% of the total wall area were strengthened using CFRP sheets. The CFRP sheets were placed around opening edges in two different configurations and the capacity was increased as the principal stresses on the opening corners were reduced. Given the failure mode (i.e. concrete crushing) observed in experimental tests – Paper III (Popescu, et al. 2015c) for un-strengthened TW walls with openings, the strengthening configuration proposed by Mohammed, et al. (2013) would not be suitable. It is believed that a better configuration would be to strengthen the walls by confinement.

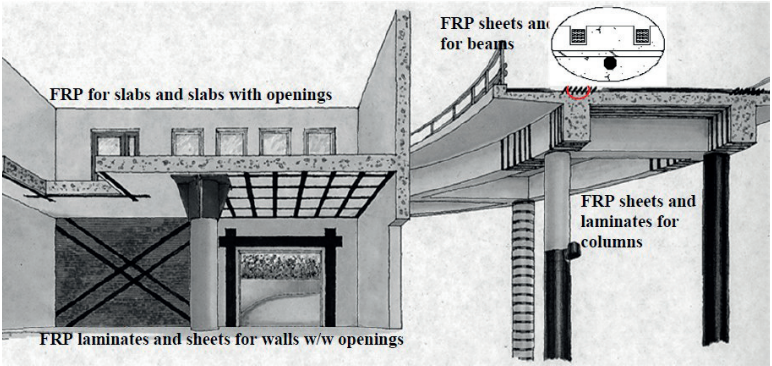

Fig. 4. FRP strengthening configurations in different contexts (Täljsten, et al. 2012)

The confinement has proved to be a viable solution where ductility and/or axial strength are concerned. The method is highly dependent on the cross-section geometry: a uniform confinement effect is obtained for circular cross-sections whereas only part of the cross-section is effectively confined for rectangular cross-sections (Mirmiran 1998, Pessiki 2001, Wu and Wei 2010, Liu, et al. 2015). Numerous design/analysis-oriented models have been developed by researchers and their performances were reviewed in Lam and Teng (2003), Rocca, et al. (2008). These studies showed that as the aspect ratio of the cross-section increases the enhancement in compressive strength decreases. Therefore, for high aspect ratios the simple wrapping of the element by the FRP will not significantly increase the axial strength. To overcome this problem, further actions are sought, these being either to increase the cross-section by adding additional material (i.e. high-strength mortar) or by using FRP or steel anchors. Several methods were presented and studied in the literature and these are briefly described. Tan (2002) used fiber anchor spikes placed along the wider faces of the column while an increase in the cross-sectional area by adding semi-cylindrical attachments (high-strength mortar) was used by Tanwongsval, et al. (2003) for a strength increase of more than 30%; Prota, et al. (2006) used a quadri-directional CFRP, however, with no significant improvement unless seismic performances are required. The usefulness of having fibre anchor spikes and cross-section enlargement in combination with circumferential FRP was studied also by Triantafillou, et al. (2015). It was concluded that by adding heavy fibre anchor spikes the confining effect was doubled. Light anchor spikes failed prematurely having the same effect as without anchors. The increase in cross-section using high-strength mortar was as efficient as using heavy anchors.

Increasing the cross-section cannot always be a viable solution, i.e. due to spatial, esthetical or structural limitations and therefore, using anchors remains the only available solution. Consequently, the anchors are introduced to create shorter distances which are confined between bolts (Karbhari and Seible 1998).

2.2 Design of experimental program

The current study started with the aim to develop a toolbox containing solutions for strengthening concrete walls with existing or newly created openings using FRP materials. The strengthening configuration proposed has to be able to fully or partially restore the axial strength of concrete walls with openings prior to cutting the opening.

The specimens were designed to represent typical wall panels in residential buildings. Half-scale walls with and without cut-out openings (1800 mm long, 1350 mm tall and 60 mm thick), were constructed for testing to failure. Details about the design and fabrication process are given in Paper III and Paper IV. In order to determine mechanical characteristics of the concrete (compressive strength and fracture energy), cubes and beams with standardized sizes were cast and cured in identical conditions to the specimens. The average cubic compressive strength of the concrete was determined in accordance to (SS-EN 12390-3:2009 2009). The fracture energy was determined following the RILEM TC 50-FMC (1985) standard's recommendations. Coupons were taken from the reinforcing steel meshes and tested according to SS-EN ISO 6892-1:2009 (2009) in order to determine their stress-strain properties. Average values and their corresponding coefficients of variations can be found in Paper III (Popescu, et al. 2015c).

A quantitative approach has been used to design the laboratory investigation based on DoE method. This technique was applied in order to plan a realistic test-matrix such that the response of the FRP-strengthened concrete walls with openings could be evaluated effectively. According to the theory behind DoE, past experience should contribute in choosing the right parameters and these should be varied at maximum of two levels. For the current study, size opening and degradation state of the wall (i.e. pre-cracked and un-cracked) were selected as the most influential parameters. For the first parameter (size opening) small (450 mm x 1050 mm) and large opening (900 mm x 1050 mm) was set as the min/max level. The minimum level represents the width of a typical door opening in a residential building whereas the maximum level corresponds to a double-door opening. For the second parameter, pre-cracked and un-cracked condition was established as the min/max level. The minimum level represents the wall in a pre-cracked state (loaded until 75% of the peak load, prior to applying the strengthening) whereas the maximum level corresponds to the un-cracked condition. The test-matrix designed according to the DoE technique is shown in Fig. 5. The entire matrix was divided into three stages, namely:

1) Reference specimens, loaded until failure in order to evaluate the cut-out effect on the axial strength.

2) Pre-cracked specimens strengthened with FRP. Comprised of two damaged specimens strengthened with FRP. The cracking load was obtained based on nonlinear finite element analyses and observations on the reference specimens (first stage) so as to acquire a significant crack width. It was decided on a load level of 75% of the un-strengthened axial capacity.

3) Un-cracked specimens strengthened with FRP. Comprised of two duplicated specimens from each type of size opening with the FRP system applied in an un-cracked state and then loaded to failure. For convenience, the naming system adopted consists the test stage described above (I, II or III where I refers to first stage, II and III refers to second and third stage, respectively) and the type of wall C, S, L (where C refers to a solid wall, S and L refers to a wall with small and large opening, respectively). In addition, the specimens from the third stage contains a serial number of the specimen. For example, II-S refers to a pre-cracked wall with small opening strengthened with FRP.

This process started with a preliminary study in which existing experimental tests from Lee (2008) were used to calibrate a FEM model. After calibration, the model was able to describe the structural behavior of such walls and to provide important information for the current experimental program such as: (1) the solid wall reactions decided the number of hydraulic jacks required to obtain a uniform distributed load along the wall length; the reactions resulted by loading to the full capacity of the hydraulic jacks were then used to design the test-rig; information regarding maximum displacements, strains in reinforcement/concrete and crack pattern were all used to decide the position of the strain gauges and linear displacement sensors.

The nonlinear analysis and design of the test rig is given in Paper II (Popescu and Sas 2014). The test-rig was designed to represent the as-built boundary conditions. The test rig had to simulate hinged connections at the top and bottom edges of the specimen and clamped side edges. All drawings used to build the test rig can be found in Appendix A.

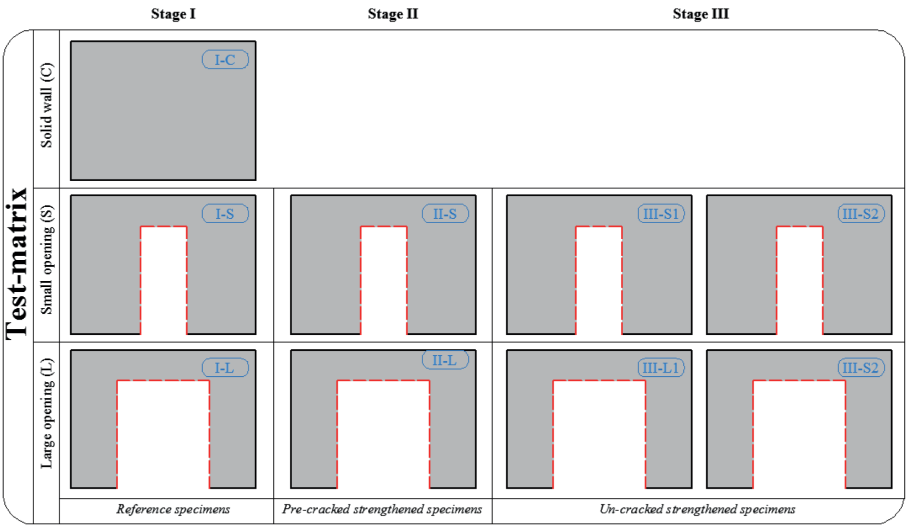

Fig. 5. Test-matrix

Fig. 6. General overview of the test setup

The strain gauges intercepting potential yield lines (resulting from nonlinear finite element analysis) were installed on the steel reinforcement, on FRPs, and on compression side of the concrete surface. Out-of-plane and in-plane displacements were monitored through linear displacement sensors, both on the tested specimens and on the test rig, respectively. In addition to a more classical way of measuring strains, three-dimensional measurements were also acquired by the digital image correlation (3D-DIC) technique. The method has been proven to be a reliable non-contact tool for monitoring strain and displacement fields in both laboratory environment (Blanksvärd, et al. 2009, Mahal 2015) and field tests (Sas, et al. 2012, Bagge, et al. 2014), just to mention a few. The instrumentation scheme is given in Paper III (Popescu, et al. 2015c) and Paper IV (Popescu, et al. 2015a).

The specimens were tested gravitationally with a small eccentricity (one sixth of the wall thickness). Four hydraulic jacks, each with a maximum capacity of 1.4 MN, were networked together to apply a uniformly distributed load along the wall length. A general view of the test setup is shown in Fig. 6.

2.3 Behavior of concrete walls with openings

Currently the practical design of RC walls, described in standards such as ACI318 (2011), AS3600 (2009) or CAN/CSA-A23.3 (2004) is based on empirical models whereas EN1992-1-1 (2004) is based on calibration against the results of non-linear analysis. Differences exist between design codes regarding how they deal with the following parameters: variation of the compressive forces within the stress block, eccentricities, slenderness and creep. For the sake of brevity the derivations of these models are presented elsewhere (Doh 2002) and their performances are evaluated in Paper I (Popescu, et al. 2015b).

The design codes that have been mentioned above (ACI318 2011, AS3600 2009, CAN/CSA-A23.3 2004, EN1992-1-1 2004) do not provide design equations to evaluate the axial strength of a concrete wall that contains openings. There is very limited information in the research literature compared to that available for beams, columns or slabs, probably due to the complex behavioral mechanisms of such elements. Only some guidelines are provided in the Australian and European standards (AS3600 2009, EN1992-1-1 2004). These state that if the walls are restrained on all sides, and enclose an opening with an area less than 1/10 of the total, the effects of this opening on the axial strength can be neglected. The height of the opening should also be less than 1/3 of the wall height. If these conditions are not met, the portion between restraining member and opening has to be treated as being supported on three sides, and the area between the openings (if more than one) has to be treated as being supported on two sides. This will give us the ultimate capacity of individual elements, independently of others. However, it is important to evaluate the reliability of the entire system (in this context walls with openings), but design codes do not provide such information. A simplified procedure is presented in Paper III (Popescu, et al. 2015c) together with a comparison between experimental values obtained from tests of the first stage and predictions using this simplified procedure. Besides this aspect, the tests on reference specimens were further analyzed to obtain important information to support the strengthening procedure. The results are briefly summarized as follows.

The walls behaved as predicted by numerical analysis, deflecting in both vertical and horizontal directions. The maximum load capacity, strains in steel reinforcement and concrete, displacements and crack pattern was monitored for each specimen. These measurements are presented in detail in Paper III (Popescu, et al. 2015c). For the sake of brevity only selected measurements are given herein. Displacements of all three specimens (recorded at the same position, D1) were plotted on the same graph (Fig. 7) to assess effects of the size of openings on the ultimate capacity. The results indicate that the 25% and 50% reductions in cross-sectional area of the solid wall caused by introducing the small opening and large opening reduced its load carrying capacity by nearly 36% and 50%, respectively.

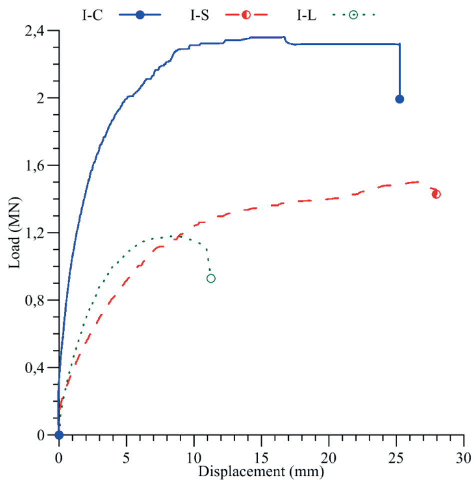

Fig. 7. Load-displacement diagrams for all specimens

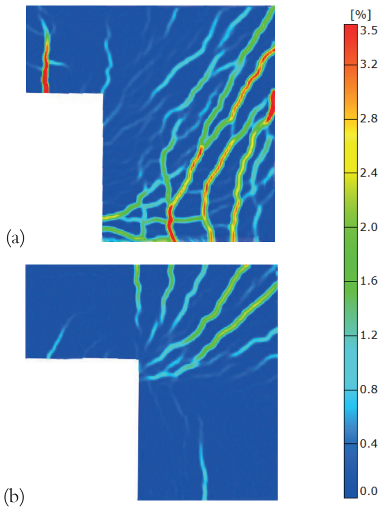

Fig. 8. Principal plane strain development on the tension side of the specimens at peak load: (a) specimen I-S; (b) specimen I-L

The 3D-DIC system captured well the strain development and distribution around the openings during loading of the specimens, as illustrated by the images in Fig. 8 showing strains at the peak load in the wall with a small opening (I-S) and large opening (I-L), respectively.

Although the minimum amount of reinforcement prescribed by design codes was used, the tensile or compressive strains that developed in the reinforcement were significant at higher loads, with yielding of some bars occurring at failure. Recorded strains in the steel reinforcement indicate that reinforcement has no significant contribution at serviceability limit states, but yielding may occur close to failure when second order effects start to be more active, thus contributing to the overall ductility. Yielding at ultimate also indicates that reinforcement might provide increased capacity, however this preliminary conclusion should be verified with tests on walls without any reinforcement.

In all cases the walls with openings had a brittle failure due to crushing of concrete with spalling and reinforcement buckling along the line between the corner of the wall and opening corner of one pier. The crack pattern at failure of both tension and compression side is shown in Fig. 9. When one of the piers failed, the other pier failed immediately thereafter and triggered the failure of the entire system. This failure mode was analyzed in detail in Paper III (Popescu, et al. 2015c) and a strengthening configuration was proposed in Paper IV (Popescu, et al. 2015a). Selected details are also given in Section 2.4.

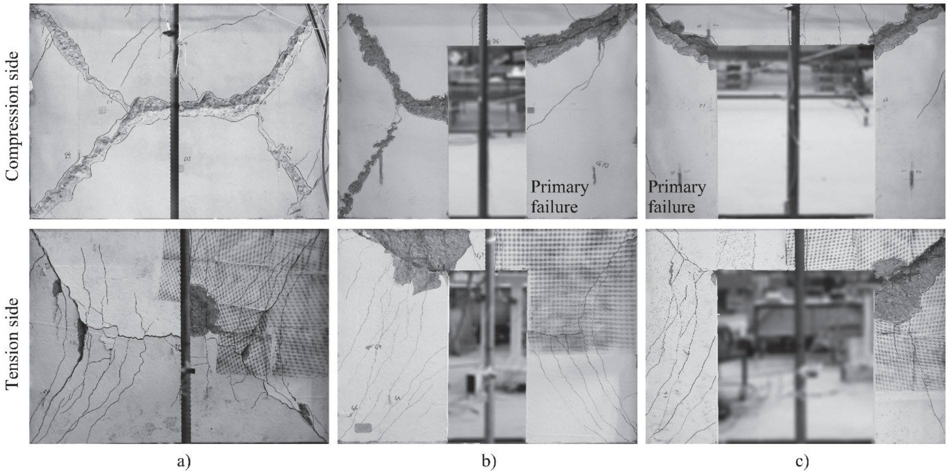

Fig. 9. Crack pattern and failure mode of the tested specimens: a) specimen I-C; b) specimen I-S and c) specimen I-L

2.4 Behavior of concrete walls with openings strengthened with FRP

In the current study anchor bolts were used to create virtual cross-sections with an aspect ratio limited to 2. The Lam and Teng (2003) model for confined concrete was then used to compute the number of FRP layers required to increase the axial strength. The design procedure is given in detail in Paper IV (Popescu, et al. 2015a).

The failure mode was by crushing of concrete followed by debonding of the CFRP in the areas between anchorage rows, see Fig. 10. The failure was concentrated in smaller regions than for the reference specimens, i.e. at the bottom of one pier. The strengthened specimens had lower deformations (thus increasing the stiffness) and higher capacity when compared with the un-strengthened ones as can be seen from Fig. 11. The increase in capacity was in range of 34 – 50% and 13 – 27% for specimens with small and large opening, respectively. Analysis of the test results are described in detail in Paper IV (Popescu, et al. 2015a). The peak loads, ductility index and energy dissipation for all specimens tested are given in Table 2. More details are given in Paper III and IV.

Table 2. Summary of test results

Specimen		Peak load (kN)	Ductility index	Energy dissipation (kNm)
Reference	I-C	2363	4.05	39.37
	I-S	1500	3.21	34.21
	I-L	1180	2.78	10.88
Pre-cracked and strengthened	II-S	2241	1.97	31.23
	II-L	1497	1.23	4.66
Un-cracked and strengthened	III-S1	2178	1.94	26.61
	III-S2	2009	3.38	29.89
	III-L1	1334	1.05	6.60
	III-L2	1482	2.18	9.66

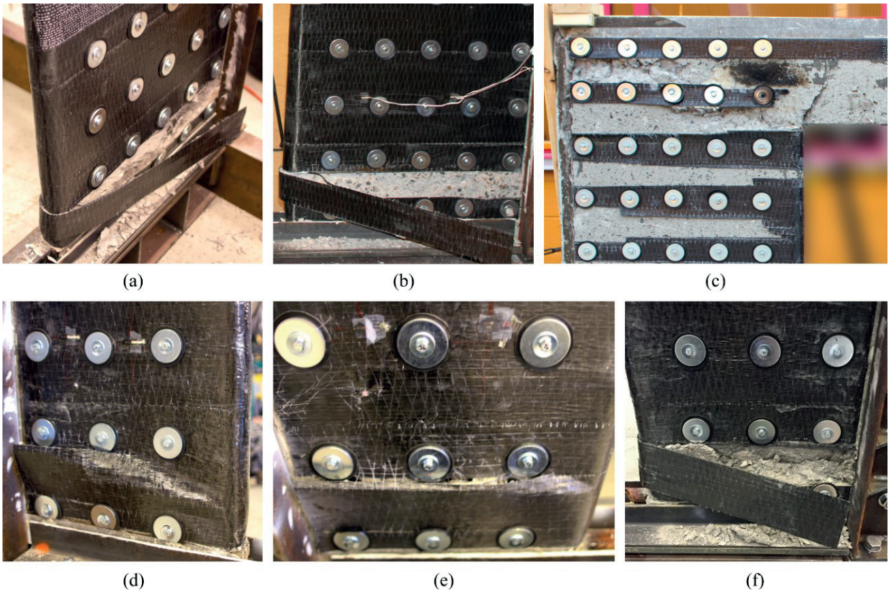

Fig. 10. Failure of the strengthened specimens: a) II-S; b) III-S1; c) III-S2; d) II-L; e) III-L1 and f) III-L2

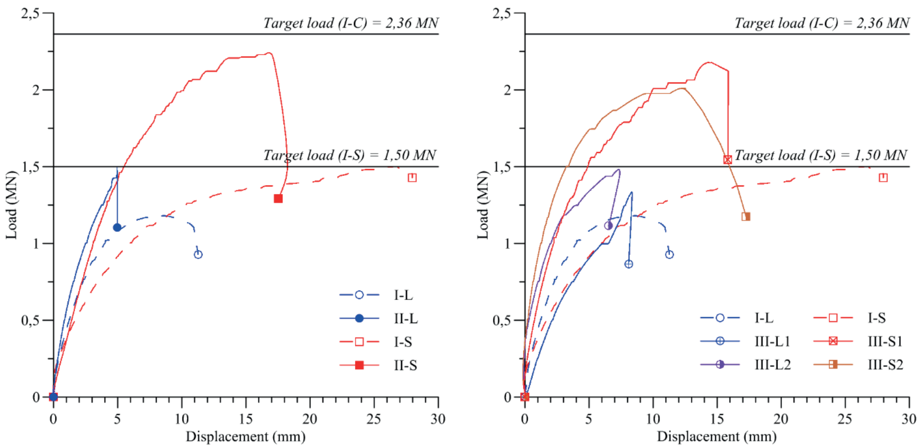

Fig. 11. Axial load-displacement diagrams of strengthened specimens: (a) pre-cracked specimens; (b) un-cracked specimens

3 Conclusions and future research

In this section the research questions formulated in the Introduction section will be addressed. Future research ideas will also be presented.

3.1 Conclusions

Three research questions were formulated in the beginning in order to comply with the aim of this research project. Based on the results of this research, these questions are addressed below:

i. Do existing models accurately predict the ultimate capacity of axially loaded concrete walls with and without openings?

Solid walls

Design models found in international standards provide conservative results, while those proposed in other studies showed a certain level of non-conservationism. This conclusion is formulated on the basis of the statistical analysis performed on a database collected by the author and presented in Paper I.

Walls with openings

There are no straightforward methods in design codes to evaluate the ultimate capacity. A simplified method by dividing the wall with openings into isolated columns connected by beams is adopted. The capacity of individual members is then computed and by idealizing the system (in this context wall with openings) as a hybrid, upon where the reliability of the entire system is found. Considering this procedure, design codes were in good agreement with test results. Empirical design formulas can be found in the research literature that aims to predict the ultimate capacity. These were derived using rather limited test results, thus, giving in some cases un-conservative predictions. The equations derived by Doh and Fragomeni (2005) and Doh and Fragomeni (2006), which address the axial strength of walls without and with openings, respectively, provided good performance when compared with test results.

ii. How to delineate small and large openings in walls, and determine where the transition from RC walls to RC frames should occur in the design of structural elements?

In order to classify an opening as small or large, different criteria should be taken into account.

Firstly, the failure mode should be investigated. It was found that regardless of size opening the failure mode is by concrete crushing along the diagonal line wall corner-opening corner accompanied by reinforcement buckling. The observed strain patterns measured with 3D-DIC indicate that the specimen with a large opening behaved more like an RC frame than an RC wall, with all major strains oriented towards the corner of the opening. As a consequence, the failure of the remaining part after introducing an opening (i.e. pier) has a typical crack pattern for panels restrained on three sides (for the wall with small opening) while no typical crack pattern was observed for the wall with large opening.

Secondly, the utilization of the steel reinforcement and failure initiation of the spandrel above the opening are another criteria. The trends, together with strain values measured at different locations on the reinforcement, were very similar for both small and large opening except the spandrel. The reinforcement bar above the opening was tensioned more than in the panel with a small opening, thus accelerating the redistribution of the forces to piers.

iii. How does the failure mechanism of a concrete wall with an opening change after strengthening with FRP?

In all cases, the walls had a brittle failure due to crushing of concrete with spalling and reinforcement buckling. However, after strengthening the crushing failure mode could not be avoided. The failure mode was not as explosive as the un-strengthened ones and no reinforcement buckling was noted. The position were the crushing occurred was, however, changed. While crushing appeared along the diagonal line from wall corner to opening corner for un-strengthened walls, crushing at the bottom part of the piers occurred for strengthened ones. The opening was placed symmetrically and the piers were theoretically equal in capacity. When one of the piers failed, the entire wall triggered failure of the other. It is therefore, difficult to predict the exact location where the failure will occur. Using random fields which can represent the variability of material and geometric properties in combination with stochastic rather than deterministic nonlinear finite element analysis might be a viable approach. For example, it is common to model the concrete properties, i.e. compressive or tensile strength, uniformly throughout an element while random fields would enable fluctuations within the standard deviation limits in a non-uniformly routine. A typical commercial software is SARA which is a combination of ATENA (advanced nonlinear finite element) software and FReET (multi-purpose probabilistic software for statistical, sensitivity and reliability analysis) (Cervenka Consulting 2015).

3.2 Future research

The limitations of this study were stated in the introduction mainly to identify what could be necessary to do in order to better understand the research field. Thus, those limitations are used here as recommendations for future research:

From the research literature study (Paper I) it was found that fewer tests exist on walls under TW action, walls with different size openings or higher eccentricities, and more tests are required in these experimental regimes to facilitate the development of appropriate design models. The influence of the steel reinforcement was only assessed, in this study, for a centrally placed layer while studies with the mesh distributed in two layers should be investigated.

The optimal distance between steel anchorages should be further investigated. Moreover, the influence of the prestressing force of the bolts may also be an important parameter that has to be studied.

The type of FRP sheet used to strengthen the specimens was uni-directional while it is believed that bi-directional fibers may have been more effective in order to better exploit the CFRP fibers and further increase the axial strength. Also, the FRP sheets should be anchored into the wall foundation and to the adjacent elements (i.e. transverse walls or floors). Perrone, et al. (2009) suggested a method in which FRP laminates are first introduced into pre-drilled holes to the specimen's foundation and slits at the base of the specimen prior to apply the CFRP sheet used to increase the concrete confinement.

The strengthening was done with the specimens unloaded. However, real walls are usually subjected to a relatively high sustained load. It is therefore necessary to take into account the effect of sustained loading when strengthening such elements.

It should be noted that "small" and "large" are used here as convenient designations rather than as clearly delimited terms with specific thresholds and implications. In order to determine the optimal transition point between RC walls and RC frames in design codes for structural elements, more tests are required including walls with intermediate size openings.

Experimental tests on walls are costly and time consuming due to the more complex test setup and mechanical behavior, therefore nonlinear finite element modeling could be a useful tool to assess effects of the aforementioned parameters. Important resources can be saved if a reliable FEM model can be calibrated against experimental tests performed.

The lateral restraints transformed the problem into a three-dimensional rather the one-dimensional problem. It is therefore necessary to develop a design model that can better describe current stress state. In the current study the design of the FRP strengthening was based on one-dimensional element with no load eccentricity assumptions. However, it may be possible to develop disk theory Nielsen (1999) to derive a theoretical model that provides better estimates of capacities of FRP-strengthened walls with openings.

References

ACI318 (2011). "Building code requirements for structural concrete and commentary (ACI 318–11)." American Concrete Institute (ACI), Farmington Hills, USA.

Ali, A., and Wight, J. (1991). "RC Structural Walls with Staggered Door Openings." *Journal of Structural Engineering*, 117(5), 1514-1531.

AS3600 (2009). "Concrete structures." Standards Australia, Sydney, Australia.

Bagge, N., Nilimaa, J., Blanksvärd, T., and Elfgren, L. (2014). "Instrumentation and Full-Scale Test of a Post-Tensioned Concrete Bridge." *Nordic Concrete Research*, 51, 63-83.

Blanksvärd, T., Täljsten, B., and Carolin, A. (2009). "Shear Strengthening of Concrete Structures with the Use of Mineral-Based Composites." *Journal of Composites for Construction*, 13(1), 25-34.

Blanksvärd, T. (2009). "Strengthening of concrete structures by the use of mineral-based composites." PhD Thesis, Luleå University of Technology.

Box, G. E. P., Hunter, W. G., and Hunter, J. S. (1978). *Statistics for experimenters: An introduction to design, data analysis, and model building*, John Wiley & Sons, Inc, New York.

CAN/CSA-A23.3 (2004). "Design of concrete structures." Canadian Standards Association, Mississauga, Ontario.

Cervenka Consulting (2015). <http://www.cervenka.cz/products/sara>. (2015.09.23).

Delatte, N. (2009). *Failure, Distress and Repair of Concrete Structures*, Woodhead Publishing.

Demeter, I. (2011). "Seismic retrofit of precast RC walls by externally bonded CFRP composites." Politehnica University of Timisoara, Romania: PhD Thesis.

Doh, J., and Fragomeni, S. (2005). "Evaluation of experimental work on concrete walls in one-way and two-way action." *Aust J Struct Eng*, 6, 37–52.

Doh, J. H. (2002). "Experimental and Theoretical Studies of Normal and High Strength Concrete Wall Panels." PhD Thesis, Griffith University, Australia.

Doh, J. H., and Fragomeni, S. (2006). "Ultimate load formula for reinforced concrete wall panels with openings." *Advances in Structural Engineering*, 9(1), 103-115.

EN1992-1-1 (2004). "Eurocode 2: design of concrete structures – Part 1–1: General rules and rules for buildings." Comité Européen de Normalisation (CEN), Brussels, Belgium.

Engel, P. (n.d.). "General rehabilitation techniques using steel." <http://www.constructalia.com/english/renovation_with_steel/ii_general_rehabilitation_techniques_using_steel#.VMPsNP6G9Wg>. (2015.01.23).

Enochsson, O., Lundqvist, J., Täljsten, B., Rusinowski, P., and Olofsson, T. (2007). "CFRP strengthened openings in two-way concrete slabs – An experimental and numerical study." *Construction and Building Materials*, 21(4), 810-826.

FIEC (2014). "Construction activity in Europe." European Construction Industry Federation (FIEC).

Floruţ, S.-C., Sas, G., Popescu, C., and Stoian, V. (2014). "Tests on reinforced concrete slabs with cut-out openings strengthened with fibre-reinforced polymers." *Composites Part B: Engineering*, 66C, 484–493.

Fragomeni, S. (1995). "Design of Normal and High Strength Reinforced Concrete Walls." PhD

Thesis, University of Melbourne, Australia.

Fragomeni, S., Mendis, P. A., and Grayson, W. R. (1994). "Review of reinforced concrete wall design formulas." *ACI materials journal*, 91(5), 521-529.

Ganesan, N., Indira, P. V., and Rajendra Prasad, S. (2012). "Strength and Behavior of SFRSCC and SFRC Wall Panels under One-Way In-Plane Action." *High Performance Fiber Reinforced Cement Composites 6*, G. Parra-Montesinos, H. Reinhardt, and A. E. Naaman, eds., Springer Netherlands, 279-286.

Ganesan, N., Indira, P. V., and Santhakumar, A. (2013). "Prediction of ultimate strength of reinforced geopolymer concrete wall panels in one-way action." *Construction and Building Materials*, 48(0), 91-97.

Karbhari, V. M., and Seible, F. (1998). "Design considerations for the use of fiber reinforced polymeric composites in the rehabilitation of concrete structures." *Proceedings of NIST Workshop on Standards Development for the Use of Fiber Reinbforced Polymers for the Rehabilitation of Concrete and Masonry Structures*, D. Duthinh, ed.Tucson, Arizona.

Lam, L., and Teng, J. G. (2003). "Design-Oriented Stress-Strain Model for FRP-Confined Concrete in Rectangular Columns." *Journal of Reinforced Plastics and Composites*, 22(13), 1149-1186.

Larsson, L.-E. (1959). "Bearing capacity of plain and reinforced concrete walls." PhD Thesis, Chalmers Tekniska Högskola, Göteborg, Sweden.

Lee, D.-J. (2008). "Experimental and theoretical study of normal and high strength concrete wall panels with openings." Griffith University, Australia: PhD Thesis.

Li, B., Kai Qian, and Tran, C. T. N. (2013). "Retrofitting earthquake-damaged RC structural walls with openings by externally bonded FRP strips and sheets." *Journal of composites for construction*, 17(2), 259-270.

Liu, H.-X., Liu, G.-J., Wang, X.-Z., and Kong, X.-Q. (2015). "Effect of cross-sectional aspect ratio and basalt fiber-reinforced polymer-confined number on axial compression behavior of short columns." *Journal of Reinforced Plastics and Composites*, 34(10), 782-794.

Mahal, M. (2015). "Fatigue Behaviour of RC beams Strengthened with CFRP." PhD Thesis, Luleå University of Technology.

Mirmiran, A., Shahawy, M., Samaan, M., Echary, H., Mastrapa, J., Pico, O. (1998). "Effect of Column Parameters on FRP-Confined Concrete." *Journal of Composites for Construction*, 2(4), 175-185.

Mohammed, B., Ean, L. W., and Malek, M. A. (2013). "One way RC wall panels with openings strengthened with CFRP." *Construction & building materials*, 40, 575-583.

Mosoarca, M. (2014). "Failure analysis of RC shear walls with staggered openings under seismic loads." *Engineering Failure Analysis*, 41(0), 48-64.

Nielsen, M. P. (1999). *Limit analysis and concrete plasticity, Second Edition*, CRC Press.

Oberlender, G. D., and Everard, N. J. (1977). "Investigation of reinforced concrete walls." *ACI Structural Journal*, 74, 256-263.

Perrone, M., Barros, J. A. O., and Aprile, A. (2009). "CFRP-based strengthening technique to increase the flexural and energy dissipation capacities of RC Columns." *Journal of Composites for Construction*, 13(5), 372-383.

Pessiki, S., Harries, K., Kestner, J., Sause, R., Ricles, J. (2001). "Axial Behavior of Reinforced Concrete Columns Confined with FRP Jackets." *Journal of Composites for Construction*, 5(4), 237-245.

Pillai, S. U., and Parthasarathy, C. V. (1977). "Ultimate strength and design of concrete walls." *Building and Environment*, 12(1), 25-29.

Popescu, C., Sas, G., Blanksvärd, T., and Täljsten, B. (2015a). "Concrete walls with cut-out openings strengthened by FRP-confinement." *Working paper*, Luleå University of Technology.

Popescu, C., Sas, G., Blanksvärd, T., and Täljsten, B. (2015b). "Concrete walls weakened by openings as compression members: A review." *Engineering Structures*, 89, 172-190.

Popescu, C., and Sas, G. (2014). "The Development of an Experimental Program through Design of Experiments and FEM Analysis: A Preliminary Study." *Nordic Concrete Research*, 51, 14.

Popescu, C., Sas, G., Sabău, C., and Blanksvärd, T. (2015c). "Effect of cut-out openings on the axial strength of concrete walls " *Submitted*, Luleå University of Technology.

Prota, A., Manfredi, G., and Cosenza, E. (2006). "Ultimate behavior of axially loaded RC wall-like columns confined with GFRP." *Composites Part B: Engineering*, 37(7–8), 670-678.

RILEM TC 50-FMC (1985). "Determination of the fracture energy of mortar and concrete by means of three-point bend tests on notched beams." *Materials and Structures*, 18(4), 287-290.

Robinson, G., Palmeri, A., and Austin, S. (2013). "Design methodologies for one way spanning eccentrically loaded minimally or centrally reinforced pre-cast RC panels." *Engineering structures*, 56, 1945-1956.

Rocca, S., Galati, N., and Nanni, A. (2008). "Review of design guidelines for FRP confinement of reinforced concrete columns of noncircular cross sections." *Journal of Composites for Construction*, 12(1), 80-92.

Saheb, M., and Desayi, P. (1990a). "Ultimate strength of RC wall panels with openings." *Journal of structural engineering*, 116(6), 1565-1578.

Saheb, M., and Desayi, P. (1990b). "Ultimate Strength of R.C. Wall Panels in Two-Way In-Plane Action." *Journal of Structural Engineering*, 116(5), 1384-1402.

Saheb, M., and Desayi, P. (1989). "Ultimate strength of RC wall panels in one-way in-plane action." *Journal of structural engineering*, 115(10), 2617-2630.

Sas, G., Blanksvärd, T., Enochsson, O., Täljsten, B., and Elfgren, L. (2012). "Photographic strain monitoring during full-scale failure testing of Örnsköldsvik bridge." *Structural Health Monitoring*, 11(4), 489-498.

Seddon, A. E. (1956). "The strength of concrete walls under axial and eccentric loads." *In: Andrew RP, editor. Symposium on the strength of concrete structures: Cement and Concrete Association, London, UK;*, 445-486.

SS-EN 12390-3:2009 (2009). "Testing hardened concrete – Part 3: Compressive strength of test specimens." Swedish Standards Institute (SIS), Stockholm, Sweden.

SS-EN ISO 6892-1:2009 (2009). "Metallic materials – Tensile testing – Part 1: Method of test at room temperature (ISO 6892-1:2009)." Swedish Standards Institute (SIS), Stockholm, Sweden.

Swartz, S. E., Rosebraugh, V. H., and Rogacki, S. A. (1974). "A method for determining the buckling strength of concrete panels." *Experimental Mechanics*, 14(4), 138-144.

Tan, K. (2002). "Strength Enhancement of Rectangular Reinforced Concrete Columns using Fiber-Reinforced Polymer." *Journal of Composites for Construction*, 6(3), 175-183.

Tanwongsval, S., Maalej, M., and Paramasivam, P. (2003). "Strengthening of RC wall-like columns with FRP under sustained loading." *Materials and Structures*, 36(5), 282-290.

Taylor, C. P. (1998). "Design of slender reinforced concrete walls with openings." *ACI structural journal*, 95(4), 420-433.

Timoshenko, S. P., and Gere, J. M. (1961). *Theory of Elastic Stability*, McGRAW-HILL International Book Co., New York.

Todut, C., Dan, D., and Stoian, V. (2015). "Numerical and experimental investigation on seismically damaged reinforced concrete wall panels retrofitted with FRP composites." *Composite Structures*, 119, 648-665.

Todut, C., Dan, D., and Stoian, V. (2014). "Theoretical and experimental study on precast reinforced concrete wall panels subjected to shear force." *Engineering Structures*, 80, 323-338.

Triantafillou, T. C., Choutopoulou, E., Fotaki, E., Skorda, M., Stathopoulou, M., and Karlos, K. (2015). "FRP confinement of wall-like reinforced concrete columns." *Materials and Structures*, 1-14.

Täljsten, B., Carolin, A., and Nordin, H. (2003). "Concrete Structures Strengthened with Near Surface Mounted Reinforcement of CFRP." *Advances in Structural Engineering*, 6(3), 201-213.

Wang, J., Sakashita, M., Kono, S., and Tanaka, H. (2012). "Shear behaviour of reinforced concrete structural walls with eccentric openings under cyclic loading: experimental study." *The Structural Design of Tall and Special Buildings*, 21(9), 669-681.

Wu, Y.-F., and Wei, Y.-Y. (2010). "Effect of cross-sectional aspect ratio on the strength of CFRP-confined rectangular concrete columns." *Engineering Structures*, 32(1), 32-45.

Zielinski, Z. A., Troitsky, M. S., and Christodoulou, H. (1982). "Full-Scale Bearing Strength Investigation of Thin Wall-Ribbed Reinforced Concrete Panels." *ACI Structural Journal*, 79(4), 313-321.

Appendix A

TECHNICAL DRAWINGS OF THE TEST-RIG

Test-rig - Lateral view

Scale 1:15

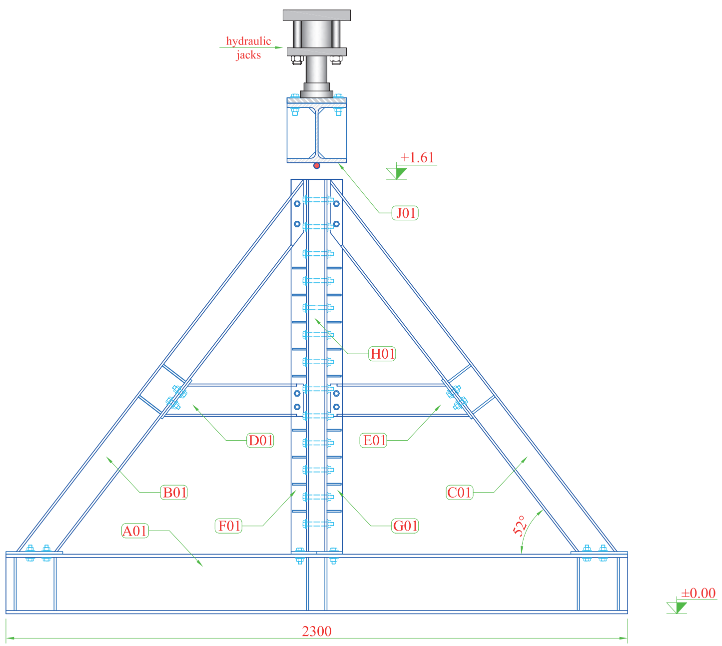

Test-rig - Front view

Scale 1:15

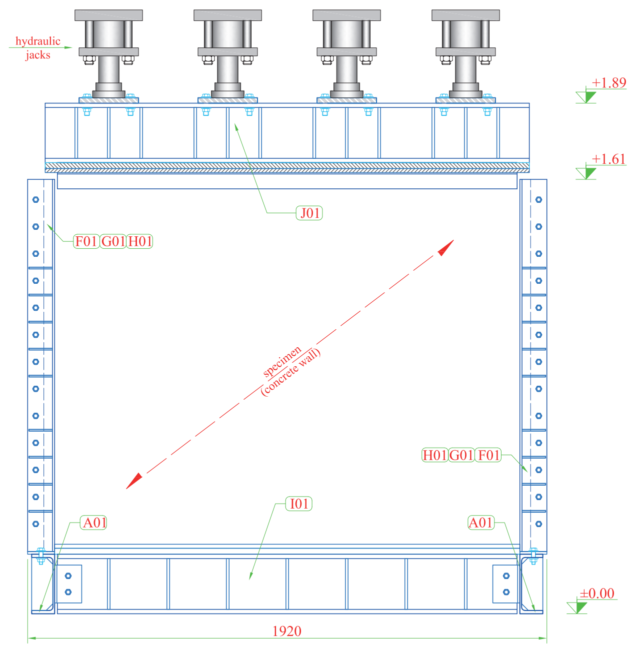

Luleå University of Technology		Client: *Luleå University of Technology*	Project no.
Designed by Cosmin Popescu	Scale: 1:15	Project title: Test-rig	R-01
Drawings by Cosmin Popescu	Date: 2014.10.02	Drawing title: General view of the test-rig	

Assembly A01 - Front view
Scale 1:10

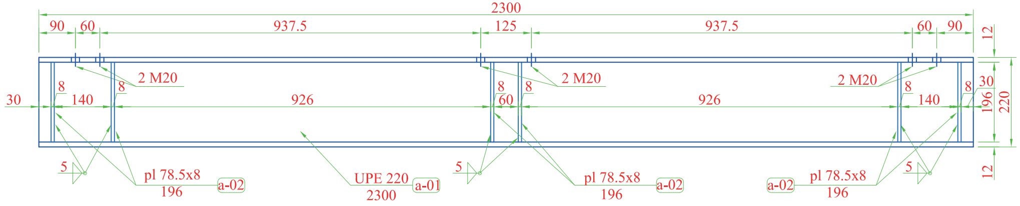

Assembly A01 - Lateral view
Scale 1:10

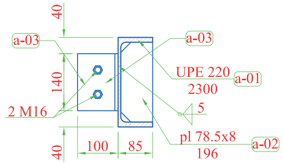

Assembly A01 - Rear view
Scale 1:10

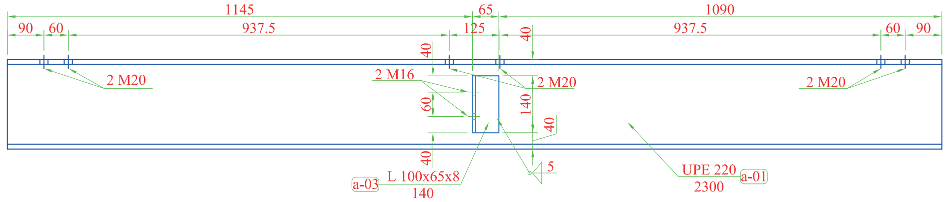

Profile a-01 - UPE 220
Scale 1:10

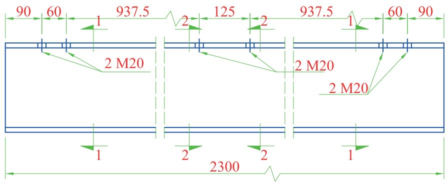

Section 1-1
Scale 1:10

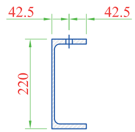

Section 2-2
Scale 1:10

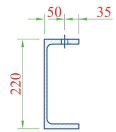

Plate a-02 - 78.5x8
Scale 1:10

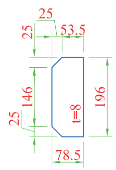

Profile a-03 - L 100x65x8
Scale 1:10

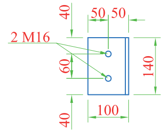

Luleå University of Technology			**Client:** *Luleå University of Technology*	Project no.
Designed by	Cosmin Popescu	Scale: 1:10	**Project title:** Test-rig	R-02
Drawings by	Cosmin Popescu	Date: 2014.10.02	**Drawing title:** Assembly A01. Details	

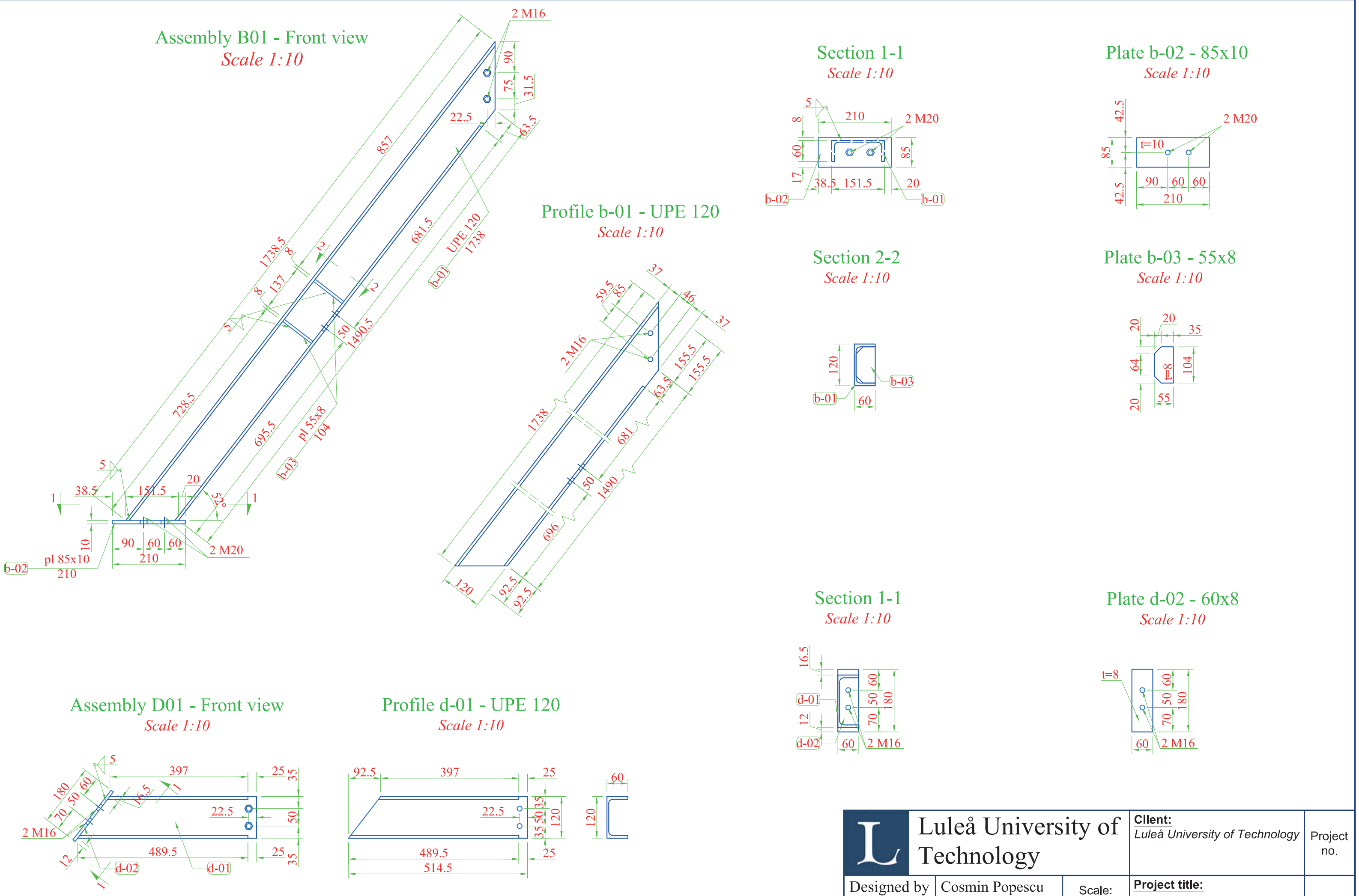

Luleå University of Technology			Client: *Luleå University of Technology*	Project no.
Designed by	Cosmin Popescu	Scale: 1:10	Project title: Test-rig	R-03
Drawings by	Cosmin Popescu	Date: 2014.10.02	Drawing title: Assembly B01 & D01. Details	

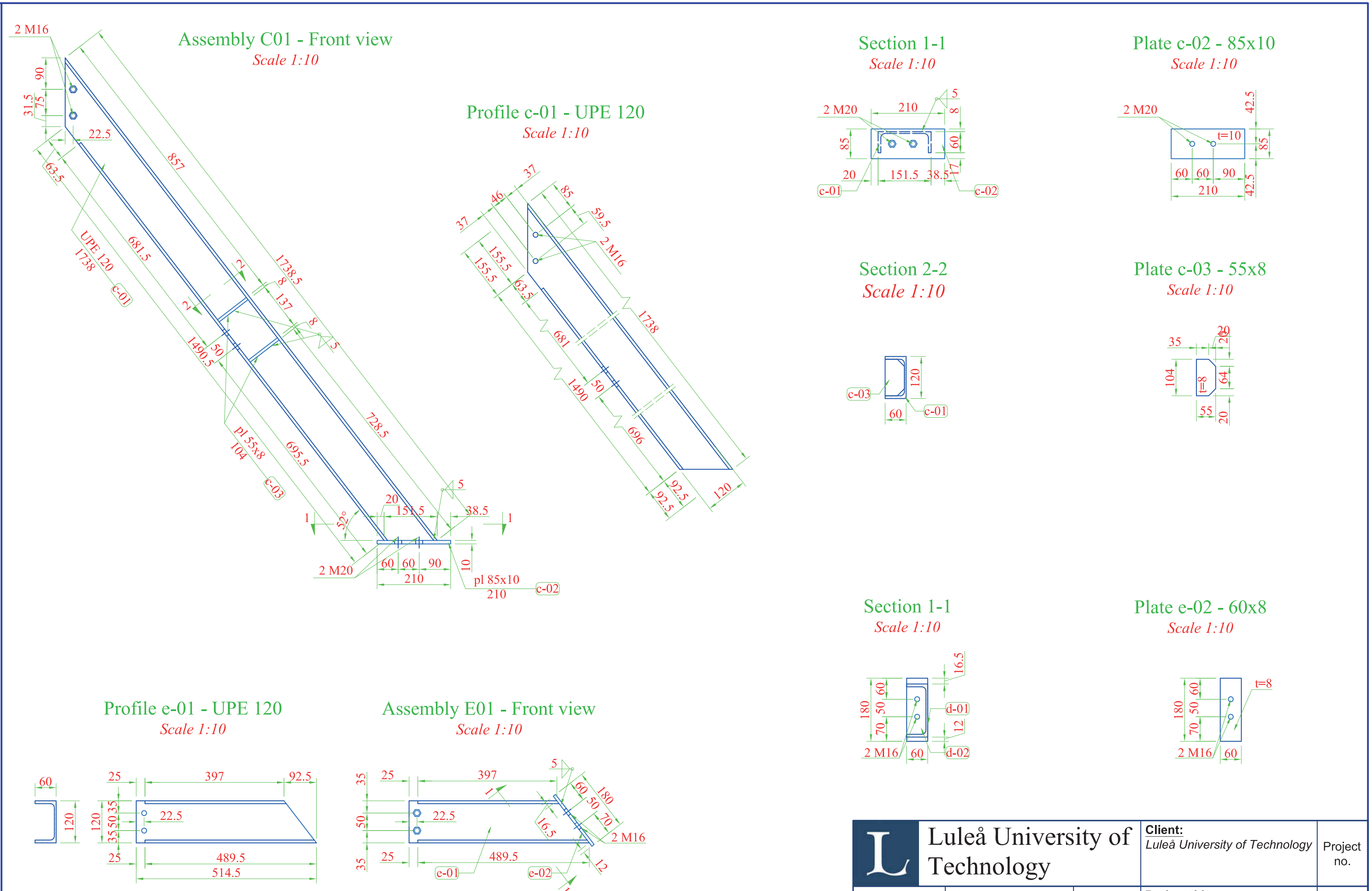

Luleå University of Technology			Client: *Luleå University of Technology*	Project no.
Designed by	Cosmin Popescu	Scale: 1:10	Project title: Test-rig	R-04
Drawings by	Cosmin Popescu	Date: 2014.10.02	Drawing title: Assembly C01 & E01. Details	

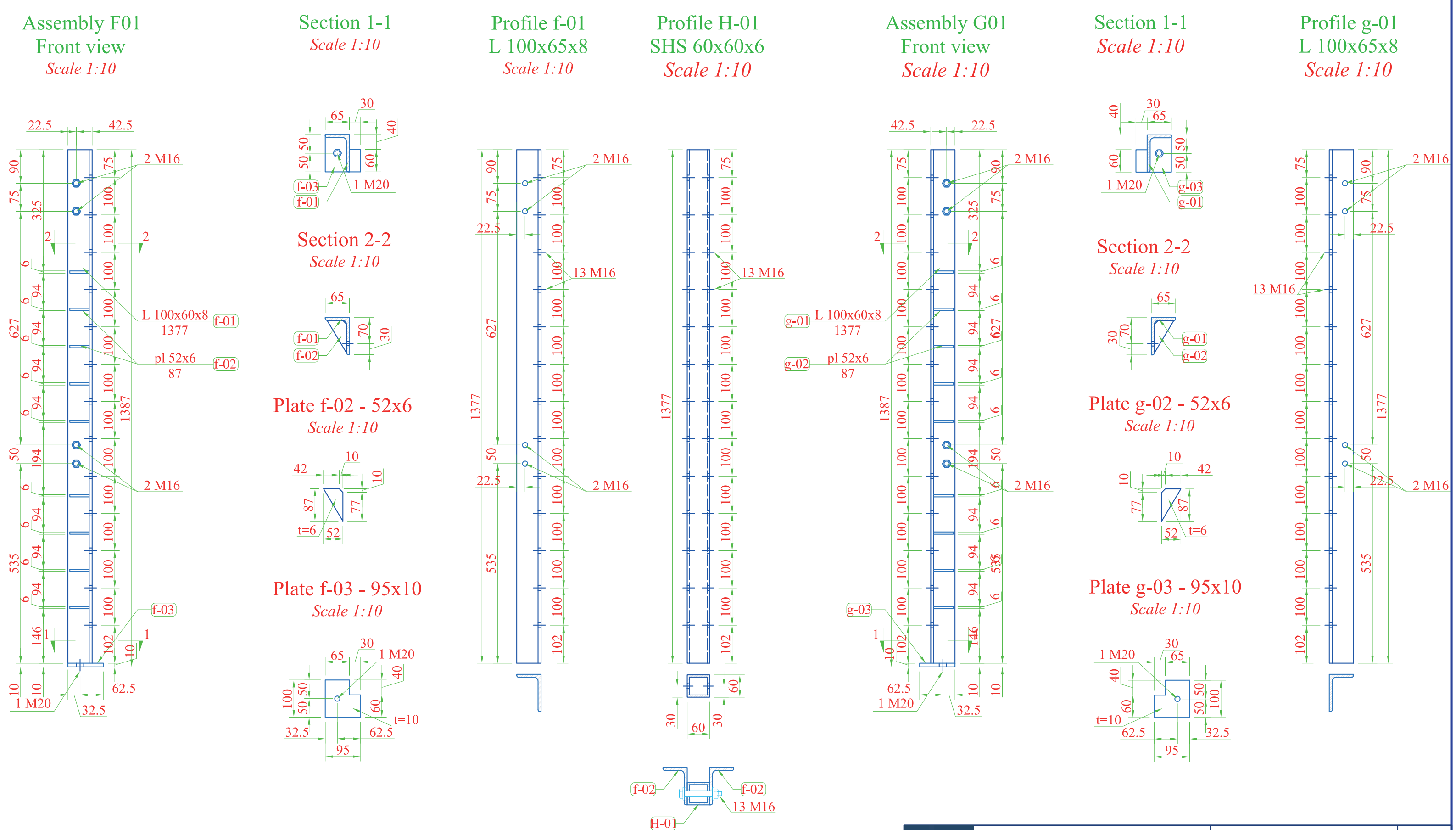

Luleå University of Technology			Client: *Luleå University of Technology*	Project no.
Designed by	Cosmin Popescu	Scale: 1:10	Project title: Test-rig	R-05
Drawings by	Cosmin Popescu	Date: 2014.10.02	Drawing title: Assembly F01, G01 & H01. Details	

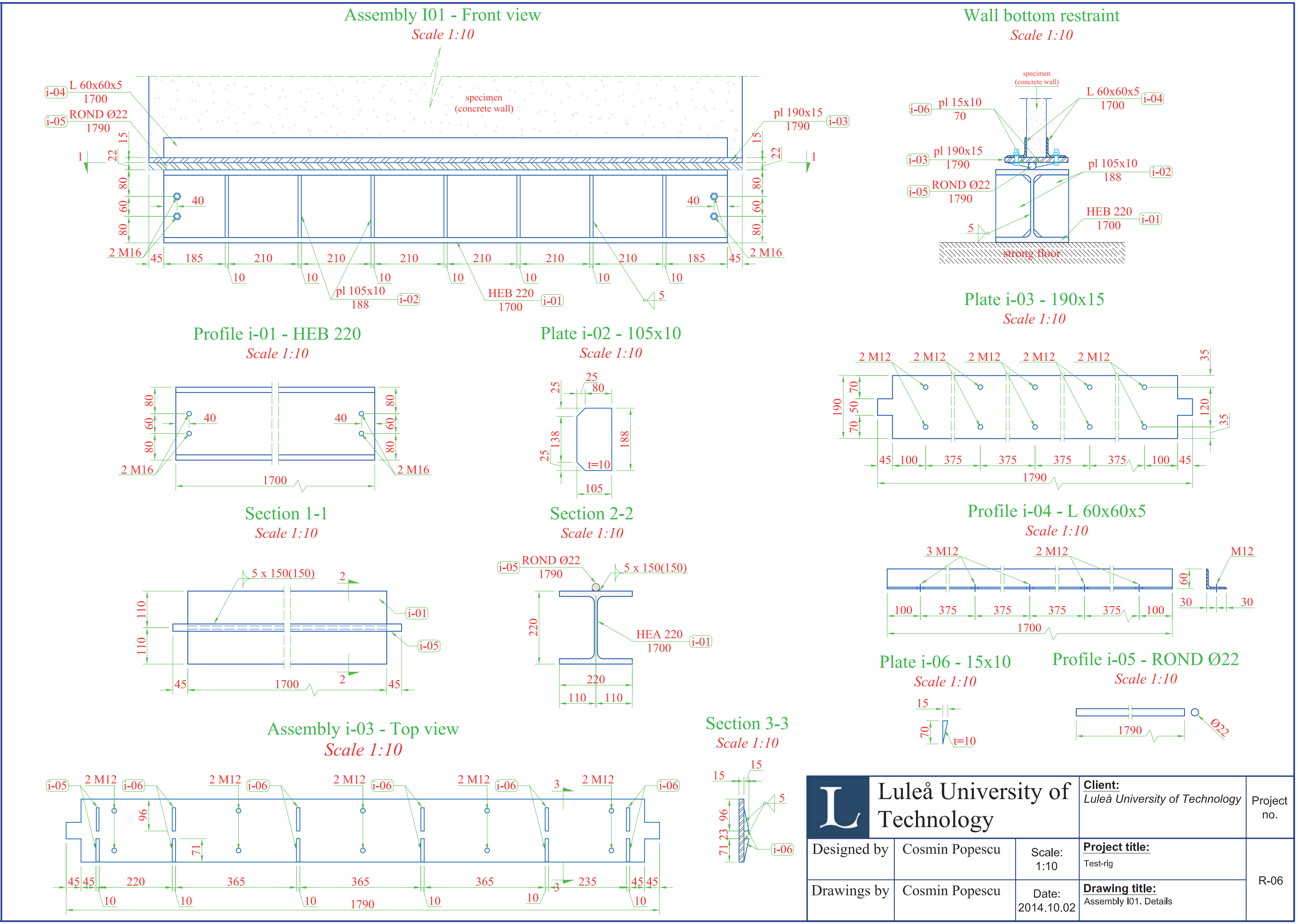

Luleå University of Technology		Client: Luleå University of Technology	Project no.
Designed by	Cosmin Popescu	Scale: 1:10	Project title: Test-rig	R-06
Drawings by	Cosmin Popescu	Date: 2014.10.02	Drawing title: Assembly I01. Details	

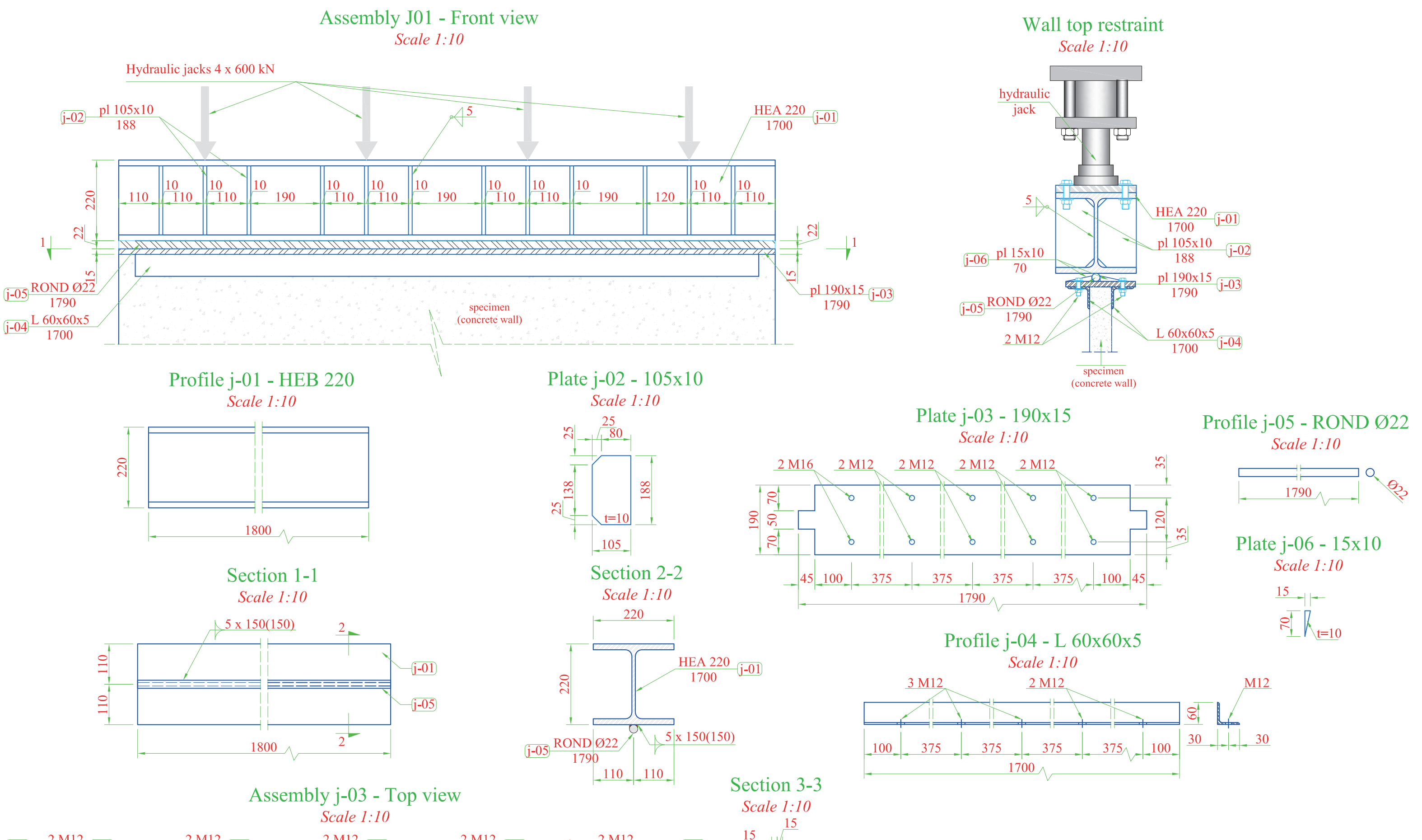

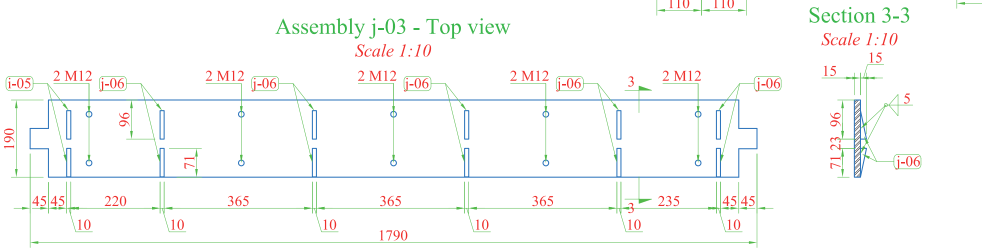

Luleå University of Technology			Client: Luleå University of Technology	Project no.
Designed by	Cosmin Popescu	Scale: 1:10	Project title: RC walls strengthened by FRP	R-07
Drawings by	Cosmin Popescu	Date: 2014.10.02	Drawing title: Assembly J01. Details	

Paper I

Concrete walls weakened by openings as compression members: A review

Cosmin Popescu, Gabriel Sas, Thomas Blanksvärd, Björn Täljsten

Published in:

Engineering Structures

Vol. 89, April 2015, pp. 172-190

Engineering Structures 89 (2015) 172–190

Contents lists available at ScienceDirect

Engineering Structures

journal homepage: www.elsevier.com/locate/engstruct

Review article

Concrete walls weakened by openings as compression members: A review

Cosmin Popescu [a,*], Gabriel Sas [b], Thomas Blanksvärd [a], Björn Täljsten [a]

[a] Luleå University of Technology, SE-97187, Sweden
[b] NORUT, Rombaksveien E-6 47, N-8517 Narvik, Norway

ARTICLE INFO

Article history:
Received 17 October 2014
Revised 4 February 2015
Accepted 5 February 2015
Available online 25 February 2015

Keywords:
Concrete walls
Openings
Axial load
Eccentricity
Out-of-plane behaviour
FRP
Strengthening

ABSTRACT

The purpose of this paper is to review the advances that have been made in the design of monolithic and precast reinforced concrete walls, both with and without openings, subject to eccentrically applied axial loads. Using the results of previous experimental studies, a database was assembled to enable statistical assessment of the reliability of existing design models. Several design aspects are highlighted, including the size and position of openings, and the roles of boundary conditions and geometric characteristics. In addition, the performance of fiber-reinforced polymers in strengthening wall openings is discussed. Overall it is found that design codes provide more conservative results than alternative design models that have been proposed in recent studies. Research into the strengthening of walls with openings is still in its early stages, and further studies in this area are needed. The paper therefore concludes by highlighting some areas where new investigations could provide important insights into the structural behaviour of strengthened elements.

Contents

* Corresponding author. Tel.: +46 702375433.
E-mail addresses: cosmin.popescu@ltu.se (C. Popescu), gabriel.sas@norut.no (G. Sas), thomas.blanksvard@ltu.se (T. Blanksvärd), bjorn.taljsten@ltu.se (B. Täljsten).

http://dx.doi.org/10.1016/j.engstruct.2015.02.006
0141-0296/

1. Introduction

Sustainable social development requires a safe, functional and durable built environment. Many structures around the world are made of reinforced concrete (RC), most of which were built before 1970 [1]. Functional modifications of these structures are common because existing structures must often be adapted to comply with current living standards. Such modifications may include the addition of new windows or doors and paths for ventilation and heating systems, all of which require openings to be cut into structural walls.

These openings can be divided into three types, namely already existing openings, existing openings that have been enlarged and newly created openings. Creating or modifying openings in walls may change the stress distribution within the wall, adversely influencing its behaviour. It is generally believed that the effects of small openings can often be neglected, while the presence of a large opening usually significantly alters the structural system [2]. However, in the existing literature there is currently no clear delimitation between small and large openings.

Experimental investigations have shown that cutting an opening into an RC wall decreases its ultimate load capacity, requiring the wall to be upgraded [3,4]. Traditionally, two methods have been used to strengthen RC walls with openings, these being either to create a frame around the opening using RC/steel members [5] or to increase the cross-sectional thickness [6]. Both methods increase the weight of the strengthened elements and may cause significant inconvenience by limiting the use of the structure during repairs. A superior alternative that has been used successfully in diverse contexts [7–10] is to use fiber-reinforced polymers (FRP) as the externally bonded material. This technique requires that thin laminates or bars be bonded to the surface of the structure using an adhesive to form a composite material.

The following sections provide a review of contemporary wall design methods that have been included in various design codes [11–14]. Two different design methods can be identified in these documents: (1) a simplified design method and (2) a method based on column theory; the latter is arguably the more rational approach. Although the simplified method is straightforward to implement, its applicability becomes limited when lateral loads need to be considered because in such cases the resultant of all loads on the wall must be located within the middle third of its overall thickness. As a result, the total load eccentricity must not exceed one sixth of the wall's thickness. In this way the walls may be considered as reasonably concentrically loaded [15]. The column method represents a viable alternative that provides more accurate results.

The purpose of this paper is to review the considerable advances that have been made in the design of concrete walls, both with and without openings that are subjected to eccentric axial loads. Additionally, the performance of FRP-strengthened walls is discussed on the basis of earlier studies. Design codes and research studies from across the world were taken into consideration in the analysis. Several aspects are highlighted, including the size and position of the openings, and the roles of boundary conditions and the wall's geometric characteristics (i.e. slenderness $\lambda = H/t$, aspect ratio $\delta = H/L$ and thickness ratio $\eta = L/t$, where H, L and t represent the wall's height, length and thickness, respectively).

A statistical analysis of available models was performed on a database collected by the authors, and is presented in this paper. The outcome of this study provides an overview of the performance of current design models and identifies research gaps. Overall, design codes were found to provide more conservative results than recent design models proposed in other studies. Research into the strengthening of RC walls with openings is still at an early stage, and further studies are undoubtedly required in this area. The findings presented herein will be used to define a new experimental programme that aims to characterize the behaviour of axially loaded RC walls strengthened with FRP; the results of these investigations will be presented in a future publication.

2. Previous experimental work

The results of 253 experimental tests on RC walls reported in the literature were compiled in a database, which is presented in Appendices A1–A3.

In line with the aim of this study, the database contains information on walls that were loaded gravitationally with uniformly distributed forces applied eccentrically at a maximum of 1/6 of their thickness. Tests on walls loaded gravitationally with eccentricities greater than 1/6 of their thickness have also been reported in the literature [16,17]. However, these results are omitted from the database because the design of such walls is not compatible with current industry standards. Data for walls that failed before reaching their ultimate capacity due to incorrect laboratory manipulation were also omitted.

2.1. Database description

The database is organized into six different sections:

(a) Name of authors and citation.
(b) Original description of the test as presented in the cited reference.
(c) Geometrical characteristics of the tested wall: height (H), length (L), thickness (t), number of steel reinforcement layers (n).

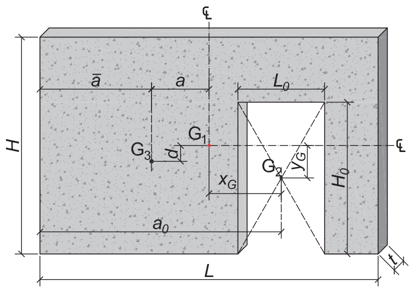

Fig. 1. Geometry of a wall with openings (G3 = centre of gravity of wall with opening, G1 = centre of gravity of solid wall, G2 = centre of gravity of opening) (adapted from [18]).

(d) Derived geometrical parameters of the tested wall: slenderness (λ), aspect ratio (δ) and thickness ratio (η).
(e) The location(s) of opening(s) in the wall, given in Cartesian coordinates relative to the point at which the wall's centre of gravity would have been located if were completely solid with no openings.
(f) Material properties of the tested wall: compressive strength of concrete (f_c), yield strength of steel reinforcement (f_y) and steel reinforcement ratio (ρ_h – horizontal, ρ_v – vertical).
(g) Ultimate axial capacity of the tested wall (N_u) as reported in the original reference.

It should be noted that some of these parameters are referred to by different names in the original references. However, as shown in Fig. 1, a unified naming system was adopted in this work for the sake of clarity.

Because both the experimental boundary conditions and the presence of openings influence the failure modes of stressed walls, the walls listed in the database were initially divided into four main categories: (1) one-way (OW) solid walls (41.1%); (2) two-way (TW) solid walls (26.1%); (3) OW walls with openings (19.1%) and (4) TW walls with openings (13.1%). Fig. 2 summarizes the ranges (frequency distributions between different types of walls) covered by some of the most important parameters

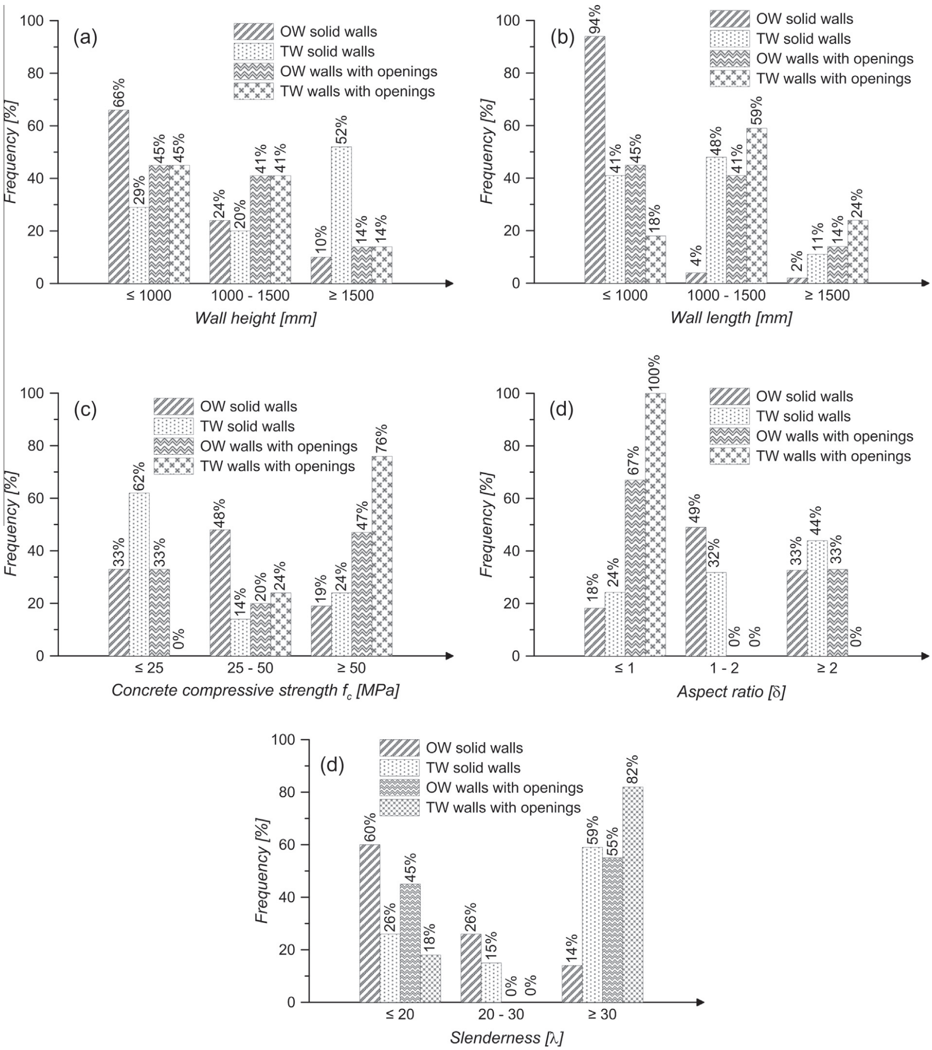

Fig. 2. Distribution of the main parameters included in the current database: (a) height; (b) length; (c) concrete strength; (d) aspect ratio; (e) slenderness ratio.

recorded in the database. For example, Fig. 2e shows that 60% of OW solid walls included in the database had slenderness values of less than 20, 26% had a slenderness between 20 and 30, and only 14% had a slenderness higher than 30.

2.2. Parameters that influence the wall's ultimate strength

2.2.1. Boundary conditions

Walls restrained along top and bottom edges are referred to as OW action panels. Walls that are restrained in this fashion tend to develop a single out-of-plane curvature in parallel to the load direction, and are usually encountered in tilt-up concrete structures. Panels restrained along three or four sides are referred to as TW action panels. Walls restrained in this way generally deform along both the horizontal and vertical directions and are usually encountered in monolithic concrete structures. In all experimental tests found in the literature, restraining elements that were applied along the top and bottom edges were designed as hinged connections that prevented translation while allowing free rotation. The restraining elements applied along the lateral sides were also fixed to prevent translation without restricting rotation.

Restraints can reduce the wall's deformation and increase its ultimate strength. The use of lateral restraints increased ultimate strength by up to 29% for walls with $\delta \leqslant 1$; increases of up to 68% were achieved for walls of $\delta > 1$ [19]. The data gathered in [20] suggest that even greater increases of up to 300% are possible when $\delta = 1$.

Boundary conditions have a dominant influence on cracking patterns and failure modes. Tests on OW walls usually reveal the development of a horizontal main crack along the middle of the wall. According to Swartz et al. [21], TW walls behave similarly to transversely loaded slabs with simple supports. Typical crack patterns for walls both with and without openings are shown in Fig. 3.

2.2.2. Slenderness and aspect ratio

In general, slender walls will have a lower ultimate strength [17,19,20,22–24]. Saheb and Desayi [22] and Saheb and Desayi [19] proved that increasing the slenderness ratio from 9 to 27 reduces strength by 35% for OW walls and 37% for TW walls. A separate study showed that the reduction in strength with increasing slenderness was more pronounced in walls made out of high-strength concrete than in those made of normal strength concrete [20]. El-Metwally et al. [25] subsequently showed that the failure mode is sensitive to both slenderness and end eccentricity.

In general, walls with a low slenderness may fail by crushing on the compressed face and bending on the tension face, while those with high slenderness may additionally fail through buckling. In either case, brittle types of failure have been observed in all experimental studies performed to date [15,16,19,20,22,24,26–29].

For OW walls the ultimate strength tends to decrease with an increase in aspect ratio, while for TW walls the opposite trend is found. For an increase in aspect ratio from 0.67 to 2, Saheb and Desayi reported a 16.6% decrease in the ultimate strength of OW walls, [22], and a 26% increase for TW walls [19].

2.2.3. Reinforcement ratio

When RC walls are subject to axial loads, reinforcement is mainly required to offset creep and shrinkage effects in the

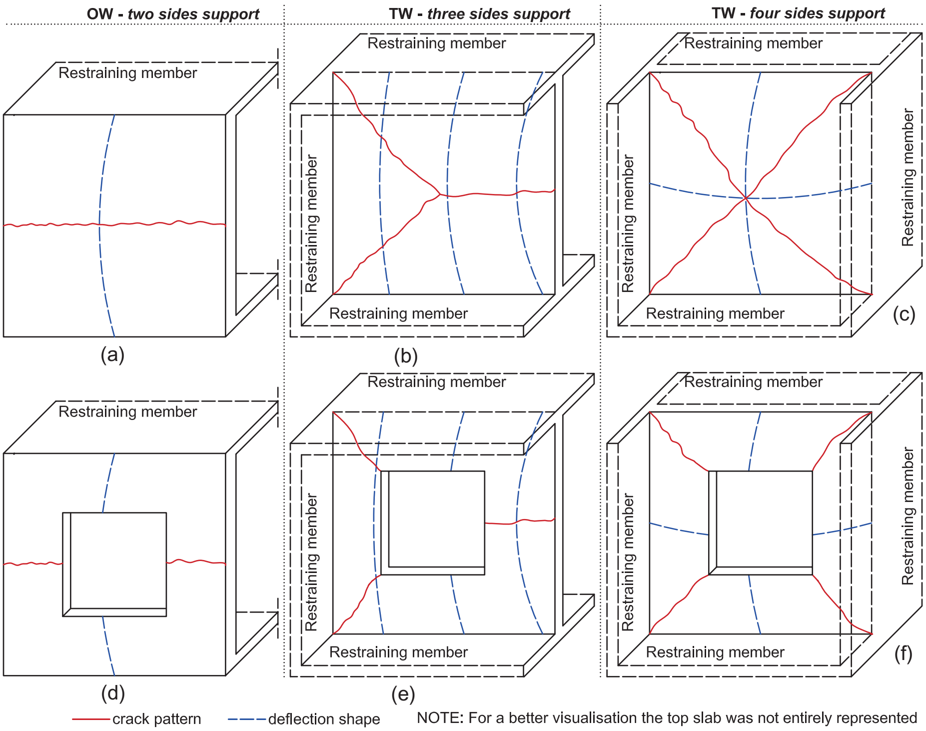

Fig. 3. Typical crack pattern and deflection shape of axially loaded RC walls.

concrete, and additionally due to accidental eccentricities in the applied loads [11–14]. When walls act as compression members it is generally believed that the contribution of the steel reinforcement should be neglected. Indeed, one of the first experimental studies conducted in Sweden [30] found that RC walls with the minimum level of steel reinforcement exhibited lower than expected ultimate strengths due to difficulties in compacting the concrete. However, no such effect was observed in subsequent studies on this phenomenon [2,15].

Pillai and Parthasarathy [15] found that varying the steel reinforcement ratio had a negligible influence on the ultimate strength when the reinforcement is placed centrally within one layer. When the reinforcement is placed in two layers, however, a significant increase in ultimate strength can be achieved [2,31]. With the reinforcement being placed in two layers it was found that an increase in vertical reinforcement ratio from 0.175% to 0.85% caused an increase in ultimate strength of 54–55% for panels with a slenderness of 12, and about 43–45% for slenderness equal to 24 [19,22]. Increasing the horizontal steel amount, on the other hand, has no influence on the ultimate strength of the walls [19,22]. These observations are valid for both OW and TW walls.

2.2.4. Openings

The presence of openings in a wall considerably reduces its ultimate load capacity relative to the equivalent solid wall. Saheb and Desayi [18] showed that although at 75% of the ultimate load cracking loads are higher for TW than OW walls, at ultimate load the presence of the openings negates the advantage of having restraints on all sides. On the other hand, Doh and Fragomeni [27] and Fragomeni et al. [28] observed that taking the side restraints into consideration could achieve significant gains in the ultimate capacity. It is believed that the differences between the above studies, even though they are studying the same parameter (the effects of restraints on walls with openings), can be explained in terms of the different layouts and opening sizes that the studies investigated. Furthermore, it is not clear whether the lateral restraints were able to function correctly in providing the desired restraining effect.

The magnitude of the ultimate load is governed by the premature failure of the column or beam strips that enclose the opening, however, how large the opening must be for the side restraints to play an important role in the ultimate capacity is currently unknown.

3. Design for ultimate strength

To the authors' knowledge, the design of axially loaded RC walls is generally based on column theory. This approach involves an analytical derivation that considers stress–strain compatibilities and the equilibrium of forces over the wall's cross section, as shown in Fig. 4. Two conditions are required for this method to be applicable: (1) the steel reinforcement ratio has to be higher than 1% and (2) the total amount of reinforcement has to be placed in two layers [17]. If treated as columns, walls can be regarded as compression members that carry mainly vertical loads. However, pure axial loads rarely occur in practice; a small eccentricity usually exists. In such cases the walls can still be regarded as compression members because compression forces control their failure. Fig. 4 shows a cross-section of an axially loaded wall with an eccentricity, e, from its centreline. The distribution of the strains along its thickness is also shown, together with the corresponding rectangular stress distribution proposed by Mattock et al. [32]. The width of the stress block is taken to be $0.85f_c$ acting on the uncracked depth, x.

The equilibrium between internal and external forces is described by Eq. (1), together with Eq. (2), which describes the equilibrium between internal and external moments. These expressions can be used to compute the interaction between the ultimate axial load, N_u, which is given by Eq. (3), and the capable moment, M_u, which is given by Eq. (4), at any eccentricity e.

$$\sum F = 0 \Rightarrow F_c + F_{sc} - F_{st} - N_u = 0 \tag{1}$$

$$\sum M = 0 \Rightarrow F_c\left(\frac{t}{2}-\frac{x}{2}\right) + F_{sc}\left(\frac{t}{2}-d_1\right) + F_{st}\left(\frac{t}{2}-d_2\right) - M_u = 0 \tag{2}$$

thus,

$$N_u = 0.85f_c(xL - A_{st}) + f_y A_{st} \tag{3}$$

and,

$$M_u = F_c\left(\frac{t}{2}-\frac{x}{2}\right) + F_{sc}\left(\frac{t}{2}-d_1\right) + F_{st}\left(\frac{t}{2}-d_2\right) \tag{4}$$

Eq. (3) is valid for walls whose slenderness does not significantly affect their ultimate capacity. These walls are generally described in the literature as stocky or short walls with a slenderness of less than 15. Macgregor et al. [33] indicated that 98% of the columns in braced frames have a slenderness of less than 12.5, while 98% of the columns in unbraced frames have a slenderness of less than 18. With the increased use of high-strength materials and advanced methods for dimensioning, however, slender elements are becoming more common in current building practices [28].

For slender elements, the predicted ultimate capacity has to be reduced through a second-order analysis that takes into consideration the material nonlinearity, cracking stages and member curvature. A second-order analysis that takes into account variable wall stiffness, as well as the effects of member curvature and lateral drift, is proposed in all international design codes [11–14]. As an alternative to the refined second-order analysis, design may be based on axial forces and moments obtained from the moment magnifier approach. Through this method, the total design moment according to EN 1992-1-1 [14] may be expressed as,

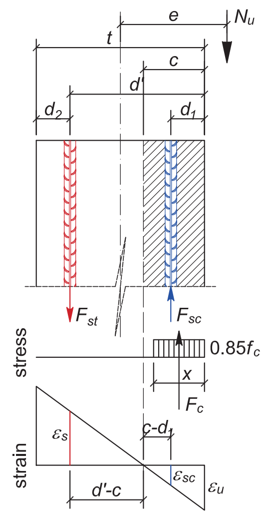

Fig. 4. Forces acting on the cross-section of a wall at equilibrium.

$$M_{Ed} = M_{0Ed}\left[1 + \frac{\beta}{(N_B/N_{Ed}) - 1}\right] \tag{5}$$

where M_{0Ed} is the first order moment, N_{Ed} is the design value of the axial load, N_B is the critical buckling load based on nominal stiffness and $\beta = \pi^2/c_0$ is a factor accounting for the curvature distribution along the member, assuming that the second order moments have a sinusoidal distribution. The c_0 factor depends on the distribution of the first order moments and, according to EN 1992-1-1 [14], can be approximated as $c_0 = 8$ for a constant distribution, $c_0 = 9.6$ for a parabolic distribution, $c_0 = 12$ for a symmetric triangular distribution.

Parme [34] has suggested simplifying Eqs. (5) and (6), this form of expressing the second order effects being currently adopted in the European norm EN 1992-1-1 [14].

$$M_{Ed} = \frac{M_{0Ed}}{1 - N_{Ed}/N_B} \tag{6}$$

Robinson et al. [17] concluded that the equivalent column procedure should not be used to design RC walls with steel reinforcement ratios lower than 1%, or those with central reinforcements regardless of the reinforcement ratio (as observed in [15]). This is because in these cases the axial capacity depends mainly on the un-cracked wall section stiffness and the tensile strength of the concrete in flexure [17].

While the above method explicitly accounts for parameters such as eccentricity, slenderness and creep, it tends to not be used in practice because of its generalized form and complexity. Instead, numerous models have been derived empirically that are simpler but less accurate. Some of these models have been implemented in design codes, and the details of these models are presented in the following section.

3.1. Design models in codes

Currently the practical design of RC walls, described in standards such as ACI318 [11], AS3600 [12] or CAN/CSA-A23.3 [13] is based on empirical models whereas EN 1992-1-1 [14] is based on calibration against the results of non-linear analysis. The design equation of ACI318 [11] was developed over the time with contributions from several studies [15,35–38]. Its current form was first proposed by Kripanarayanan [35], and adopted by ACI Committee 318 [39]. Despite the subsequent completion of numerous studies, no modifications to this formula have been implemented. The design equation found in CAN/CSA-A23.3 [13] is similar to that of [11], the only differences being in the design factors. Doh [40] suggested that the simplified design method found in AS3600 [12] is based on the complementary moment method recommended in the British Concrete standard [41].

According to Hegger et al. [42] the EN 1992-1-1 [14] approach was adapted from the work of Haller [43], a method that was originally developed for masonry elements.

The empirical method is based on the following assumptions: (1) the steel reinforcement will not bring any contribution to the load capacity; (2) the tensile strength of concrete is disregarded; (3) the wall is loaded with an eccentricity applied only at the top. The most important differences between the design models discussed above will now be highlighted.

Differences exist between design codes regarding how they deal with the following parameters: variation of the compressive forces within the stress block, eccentricities, slenderness and creep. The first important difference in development occurs in the assumptions made on the distribution of stresses within the compressed concrete block. ACI318 [11], AS3600 [12], CAN/CSA-A23.3 [13] define a linear stress distribution, as shown in Fig. 5a, whereas EN 1992-1-1 [14] assume a rectangular stress distribution (Fig. 5b). The ultimate capacity is then defined as the resultant force of the stress distribution, where σ_c is the allowable compressive stress and x is the un-cracked depth of the concrete section.

Furthermore, the initial eccentricity caused by the applied loads, e_i, is further increased by an additional one, e_a, due to the lateral deflection of the wall. This factor accounts for the effect of slenderness, known also as second order effects (or P–Δ effects). The procedure described in [11–13] to find the maximum deflection at the critical wall section uses a sinusoidal curvature (Fig. 5a), using deflections obtained from the bending-moment theory [44]. Conversely a triangular curvature is assumed in [14], a consequence of a concentrated horizontal force at the critical point of the wall (Fig. 5b). This approach results in a linear, rather than parabolic, deformation, which acts to reduce the predicted ultimate capacity of slender walls [45]. For the sake of brevity the derivations of these models are not presented in this paper, and can be found in [40].

Most of the experimental studies involved short-term tests and so their results are not very relevant to real walls, which are always subject to a relatively high sustained load. Macgregor et al. [46] showed that sustained loads tend to weaken the performance of slender columns by increasing their deflections. The creep due to sustained loads may also decrease the column's ultimate capacity. Consequently, the effects of creep should always be considered for safety reasons. As shown by Doh [40], the AS3600 [12] standard accounts for the effects of creep by increasing the first-order eccentricity by 20%. Similarly, the EN 1992-1-1 [14] standard states that the normal effects of creep are included in its underlying model. However, Westerberg [47] has demonstrated that the effects of creep are not properly described in the EC model because it produces results that are inconsistent with those obtained using a general method that explicitly accounts for creep effects.

In order to facilitate their comparison, the wall design formulas presented in the design codes [9–12] have been rearranged into similar forms. For codes [9–11] the original equations are derived using an eccentricity of $t/6$, this assumption being used to further rearrange the equations given below. It is unclear how the European norm accounts for a maximum limit of the eccentricity.

ACI318-11 [11]

$$N_u = 0.55\phi\left[1 - \left(\frac{k\lambda}{32}\right)^2\right]f_c Lt \tag{7}$$

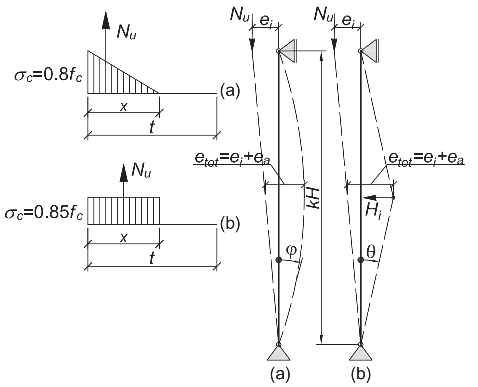

Fig. 5. Slender elements subjected to axial load and their corresponding stress distribution: (a) EN 1992-1-1 [14]; (b) ACI318 [11], AS3600 [12], CAN/CSA-A23.3 [13].

AS3600-09 [12]

$$N_u = 0.48\phi\left(1-\left(\frac{k\lambda}{31.6}\right)^2\right)f_cLt \tag{8}$$

CSA-04 [13]

$$N_u = 0.45\phi\left[1-\left(\frac{k\lambda}{32}\right)^2\right]f_cLt \tag{9}$$

EN 1992-1-1 [14]

$$N_u = \Phi\frac{1}{\gamma_c}f_cLt \text{ where } \Phi = 0.76 - 0.0257k\lambda \leqslant 0.67 - \frac{k\lambda}{200} \tag{10}$$

The term φ in Eqs. 7–9 represents the strength reduction factor corresponding to compression-controlled sections. Its value ranges from 0.6 for AS3600 [12] to 0.65 for both ACI318 [11] and CAN/CSA-A23.3 [13], while for EN 1992-1-1 [14] an equivalent value would be $1/\gamma_c$, equal to 0.67.

Values for the effective height factor k are given for the most commonly encountered restraints. The American and Canadian codes [11,13] only take into consideration restraints applied at the top and bottom of the wall, i.e. OW walls.

For OW walls, restrained against rotation provided at both ends, k, takes different values for different codes, i.e. $k = 0.75$ [12], $k = 0.8$ [11,13], $k = 0.85$ [14]. Unless no restraint against rotation is provided at one or both ends, the slenderness factor k equals 1.

Both Australian [12] and European [14] design codes include the effect of the side restraints, applied to TW walls, through the effective height factor k (Eqs. (11) and (12)). This factor is dependent on the aspect ratio of the wall and is given by Eq. (11) for walls restrained on three sides and Eq. (12) for walls restrained on all four sides.

$$k = 1/(1+\delta^2/9) \tag{11}$$

$$\begin{cases} k = 1/(1+\delta^2) & \text{if } \delta \leqslant 1 \\ k = 1/2\delta & \text{if } \delta > 1 \end{cases} \tag{12}$$

3.2. Other models proposed by researchers

Numerous studies have attempted to further improve the design models. Their proposed models incorporate the effects of the slenderness, aspect and thickness ratios, boundary conditions and steel reinforcement. The early studies that modelled RC walls as compression members were performed by [2,15,21,35,37,38], and subsequently reviewed by [48]. In this section only the most recently developed models are presented, although the results obtained from the earlier studies are included in the database and used for the performance assessment of the current models.

In the next section, the models proposed by recent studies will be given in chronological order. All models are abbreviated as OWM – one-way model for solid walls, TWM – two-way model for solid walls and OM – model for walls with openings.

3.2.1. Design equations for solid walls

3.2.1.1. Saheb and Desayi model (OWM1) [22]. To the best of the author's knowledge the first systematic study of solid concrete walls tested under both OW and TW actions was reported by Saheb and Desayi [22]. The influence of the aspect, thickness and slenderness ratios, as well as the vertical and horizontal steel reinforcement ratios, on the ultimate load was studied. Based on their own experimental results and those reported in [15,37,38], an empirical equation was proposed (Eq. (13)), valid for OW walls. In the assessment chapter (Section 4) this model is abbreviated as OWM1.

$$N_u = 0.55\phi[f_cLt + (f_y - f_c)A_{sv}]\left[1-\left(\frac{\lambda}{32}\right)^2\right]\left(1.20 - \frac{\delta}{10}\right) \tag{13}$$

where A_{sv} is the area of vertical steel reinforcement.

When compared to Eq. (7) this model additionally takes into account both the effect of the steel reinforcement and that of the aspect ratio. However, for walls with an aspect ratio higher than 2, the effect of the aspect ratio is not accounted for (i.e. the term $(1.20 - \delta/10) = 1$). This model has been validated for axially loaded walls with an eccentricity of $t/6$ and a slenderness of up to 27. Another important assumption was that the minimum amount of steel reinforcement placed in two layers yields at ultimate load. Therefore, this model may not be suitable for walls that are centrally reinforced, or when the eccentricity is less than $t/6$.

3.2.1.2. Saheb and Desayi model (TWM1 & TWM1) [19].* In the same way as the authors did for OW panels, the influence of the aspect, thickness and slenderness ratios, as well as the vertical and horizontal steel reinforcement ratios, on the ultimate load was studied for TW action panels. It was found that the ultimate load increased as the percentage of vertical steel increased, this was due to the reinforcement being placed in two layers. From their results it can also be concluded that the steel ratio has a more pronounced effect on the ultimate capacity when the panels have a high slenderness.

Before the Saheb and Desayi study there were no equations for predicting the ultimate strength of TW wall panels, because of this the authors proposed both an empirical and a semi-empirical model. The first one (*TWM1*) is an empirical formulation that was validated using their own experimental data and that published by Swartz et al. [21]. Shown in Eq. (14), it is limited to those panels whose aspect ratio is between 0.5 and 2, and the maximum limit of the thickness ratio is 60.

$$N_u = 0.67\phi\left[1-\left(\frac{\eta}{120}\right)^2\right](1+0.12\delta)f_cLt \tag{14}$$

The second proposal (*TWM1**) is a semi-empirical method (Eq. (15)), developed from a modification of the buckling strength theory of thin rectangular metal sheets, proposed by Timoshenko and Gere [49]. The original formulation of Timoshenko and Gere [49] was modified by substituting the yield strength of the metal plate with the compressive strength of the concrete wall.

$$N_u = \phi cR \tag{15}$$

with, $R = \dfrac{f_cLt + A_{sv}f_{yv}\left(1+\frac{A_{sh}f_{yh}}{A_{sv}f_{yv}}\right)}{\eta}$ and $c = 0.8352\eta - 0.0052\eta^2$, where A_{sv}, A_{sh} are the areas of vertical and horizontal steel reinforcement, respectively.

Unlike the model for OW panels, the effect of the steel reinforcement could not be directly accounted for because of limited available data; however, it was included indirectly through the term R.

3.2.1.3. Aghayere and MacGregor model [50]. A procedure for obtaining the maximum eccentricity, e_y, for a given set of loads, N_x and N_y, was proposed by Aghayere and MacGregor [50]. By obtaining the M–N–φ relationship for sections of unit length at the centre of the plate, one can determine the internal resisting moments per unit length M_{xi} and M_{yi}, corresponding to the maximum curvatures φ_{xo} and φ_{yo}, respectively. Different eccentricities can be obtained for various load levels, and through interpolation the maximum in-plane load for a given eccentricity can be obtained [50].

$$N_y e_y = \delta^2 \left(M_{xi} - \frac{N_x L^2 \phi_{xo}}{\pi^2} - N_x e_x \right) + \left(M_{yi} - \frac{N_y H^2 \phi_{yo}}{\pi^2} \right) + \delta \sqrt{M_{xi} M_{yi}} \quad (16)$$

where e_x and e_y give the eccentricity of the in-plane load in the x and y directions, respectively, N_x and N_y are compressive forces per unit length in the x and y directions, respectively, M_{xi} and M_{yi} are the internal resisting moments per unit length in the x and y directions, respectively, and φ_{xo} and φ_{yo} give the maximum curvature in the x and y directions, respectively.

The model proposed by Aghayere and MacGregor [50] takes into account material nonlinearities including tension-stiffening effects. Owing to its complexity and the limited information reported in previous experimental tests, however, this model was not included in the assessment.

3.2.1.4. Fragomeni and Mendis model (OWM2) [51]. The experimental programme undertaken by Fragomeni [52] focused on investigating the axial load capacity of normal and high-strength concrete OW walls. It was found that the ultimate load capacity is not influenced by the minimum amount of steel reinforcement when this reinforcement is placed centrally in one layer. It was also found that the ultimate load capacity did increase for aspect ratios higher than 2, in contradiction to the results reported in [22]. Significant differences exist, however, between these two studies, for instance the concrete compressive strength and steel ratio are both higher for the specimens tested in [52].

The proposed model [51], that suggests modifications to the Australian code, accounts for the high strength concrete contribution through Eqs. (17a) and (17b).

$$N_u = 0.6 \left[t_w - 1.2e - 2 \left(\frac{k^2 \lambda H}{2500} \right) \right] f_c L \quad \text{for } f_c < 50\text{ MPa} \quad (17a)$$

$$N_u = \left[t_w - 1.2e - 2 \left(\frac{k^2 \lambda H}{2500} \right) \right] 30 \left[1 + \frac{(f_c - 50)}{80} \right] L \quad \text{for } f_c > 50\text{ MPa} \quad (17b)$$

3.2.1.5. Doh and Fragomeni model (OWM3) [20]. Following the suggestions of Fragomeni [52], who took high concrete strength values into account to increase the wall strength, Doh [40] attempted to refine the existing equation through an extensive experimental study on OW concrete walls. The design equation that this research produced, shown in Eq. (18), applies to walls with larger slenderness ratios and a variety of concrete strengths.

$$N_u = \phi \left[t - 1.2e - 2 \left(\frac{k^2 \lambda H}{2500} \right) \right] 2.0 f_c^{0.7} L \quad (18)$$

where the effective length factor k *is* $k = 1$ for $\lambda < 27$ and $k = 18/\lambda^{0.88}$ for $\lambda \geqslant 27$.

This model omits the centrally placed reinforcement and the aspect ratio effects.

3.2.1.6. Doh and Fragomeni model (TWM2) [20]. In addition to the above tests performed on OW wall panels, Doh [40] tested walls in TW action in order to extend the applicability of their design equation. In this way they were able to extend Eq. (18) to include the effects of side restraints, through the effective length factor k.

$$k = \begin{cases} \alpha/(1+\delta^2) & \text{for } \delta \leqslant 1 \\ \alpha/2\delta & \text{for } \delta > 1 \end{cases} \quad (19)$$

where α is an eccentricity parameter equal to,

$$\alpha = \begin{cases} 1/(1-e/t) & \text{for } \lambda < 27 \\ 18/[(1-e/t)\cdot\lambda^{0.88}] & \text{for } \lambda \geqslant 27 \end{cases} \quad (20)$$

3.2.1.7. Hegger et al. model (OWM4) [42]. Hegger et al. [42] have proposed a new model valid for OW walls, based on the methodology presented in [43]. Their model is similar to [14] and, by taking into account the concrete tensile strength and material nonlinearity, predicts an increase in ultimate capacity. This increase is more pronounced when considering specimens of high slenderness and eccentricity. Chen and Atsuta [53] suggested that the tensile strength of normal concrete has a significant effect on the wall strength, and should therefore be taken into account when computing ultimate strengths.

In the study Hegger et al. [42] proposed two functions for the purposes described above, one to describe the nonlinear behaviour of concrete material, Eq. (21), and the other to describe the linear-elastic behaviour, Eq. (22). Eq. (21) is in accordance with the paper of Kirtschig and Anstötz [54], and is valid only for normal strength concrete. Eq. (22) was first proposed by Glock [55], who showed that the formulation is valid only for high slenderness and eccentricity values, i.e. $e \geqslant 0.2t$.

$$\Phi_{non\,lin} = (1 - 2e/t) \exp\left\{ -\left[\frac{k\lambda\sqrt{\varepsilon_{c2}}}{A(1-2e/t)} \right]^B \Big/ 2 \right\} \quad (21)$$

with $\varepsilon_{c2} = 2f_{cd}/E_{c0d}$, $A = 1.25$ and $B = 1.70$. Here ε_{c2} is the strain in the concrete at the peak stress f_{cd} and E_{c0d} is the design value of the modulus of elasticity of concrete.

$$\Phi_{lin-el} = -\frac{1}{2}\frac{f_{ctd}}{f_{cd}} + \frac{\pi^2 E_{c0d}}{24(k\lambda)^2 f_{cd}} \times \left[1 - 6e/t + \sqrt{\left(\frac{1-6e}{h - 12((k\lambda)^2/\pi^2 E_{c0d}) f_{ctd}} \right)^2 + 48\frac{(k\lambda)^2}{\pi^2 E_{c0d}} f_{ctd}} \right] \quad (22)$$

The maximum value between $\Phi_{non\ lin}$ and $\Phi_{lin\text{-}el}$ has to be used in connection with Eq. (23) with a minimum eccentricity of $e = 0.2t$, suggesting that the formula would be suitable for higher eccentricities as well.

$$N_u = \Phi f_{cd} L t \quad (23)$$

This model requires specific material characteristics, namely the tensile strength and modulus of elasticity of concrete, and as such information is limited in the experimental test reports it is difficult to test the model precisely. Instead the required characteristics where estimated using the equations proposed in fib Model Code 2010 [56].

3.2.1.8. Ganesan et al. model (OWM5) [23]. In two recent studies, Ganesan et al. [23,24] tested wall panels under OW action to study the axial strength of steel fiber reinforced concrete and geopolymer concrete. The authors reported that if the slenderness is kept constant, the ultimate strength of the concrete panels decreases as the aspect ratio increases. Their proposed model is similar to the one developed by Saheb and Desayi [22], including both the effect of the steel reinforcement and that of the aspect ratio. The specimens used to derive the model, however, had aspect ratios lower than 2, meaning that for higher values the model may not be valid.

$$N_u = 0.56\phi[f_c L t + (f_y - f_c)A_{sv}] \left[1 + \left(\frac{\lambda}{29} \right) - \left(\frac{\lambda}{26} \right)^2 \right] \left[1 - \left(\frac{\delta}{11} \right) \right] \quad (24)$$

Furthermore, due to the differences between the material characteristics of the concrete, the authors suggested new modifications to Eq. (24). Eq. (25) is suitable for reinforced geopolymer concrete walls under OW action.

$$N_u = 0.585\phi[f_c Lt + (f_y - f_c)A_{sv}]\left[1 + \left(\frac{\lambda}{40}\right) - \left(\frac{\lambda}{30}\right)^2\right]\left[1 - \left(\frac{\delta}{18}\right)\right] \quad (25)$$

3.2.1.9. Robinson et al. model (OWM6) [17]. From experimental results obtained in a series of tests performed on slender OW wall panels Robinson et al. [17] found that current design methodologies are considerably conservative. The authors devised a new model using the semi-empirical semi-probabilistic DAT (Design Assisted by Testing) methodology [57], based on the "lumped plasticity" concept. This concept allows the entire inelasticity of the element to be concentrated at the critical section, using a "non-linear" fibre hinge [17].

The model (Eq. (26)) has been validated using their experimental data, and was calibrated using statistical techniques.

$$N_u = \frac{1}{2}\left(\frac{10}{e} - \frac{\lambda}{100e} - 4 \cdot 10^{-4} \cdot \lambda^2\right) \cdot f_c Lt \quad (26)$$

3.2.2. Design equations for walls with openings

The design codes that have been reviewed above [11–14] do not provide design equations to evaluate the axial strength of a concrete wall that contains openings. There is very little information in the research literature, therefore, probably due to the complex failure mechanisms of such elements. Some guidelines are provided, such as in AS3600 [12] and EN 1992-1-1 [14]. These state that if the walls are restrained on all sides, and enclose an opening with an area less than 1/10 of the total, the effects of this opening on the axial strength can be neglected. The height of the opening should also be less than 1/3 of the wall height. If these conditions are not accomplished, the portion between restraining member and opening has to be treated as being supported on three sides, and the area between the openings (if more than one) has to be treated as being supported on two sides. This approach is only valid if the openings are included at the early stages of the design, as special reinforcement bars have to be placed around openings to avoid premature failure. No recommendations are given, therefore, if the openings are created in an existing wall.

3.2.2.1. Saheb and Desayi model (OM1) [18]. The effect of one or two openings, placed either symmetrically or asymmetrically, and combinations of door or window openings, have been studied by Saheb and Desayi [18]. To extend the usefulness of their empirical method to account for the presence, size and location of an opening, the authors proposed a new equation that is given below.

$$N_{uo} = (k_1 - k_2\alpha_x)N_u \quad (27)$$

where N_u is the ultimate load of an identical panel without openings under OW (Eq. (13)) or TW action (Eq. (14)). The constants k_1 and k_2 were obtained using curve-fitting techniques. Under OW action this procedure yields $k_1 = 1.25$ and $k_2 = 1.22$, while under TW action $k_1 = 1.02$ and $k_2 = 1.00$. The effect of the size and location of the opening in the wall is taken into account through a dimensionless parameter, α_x, defined as,

$$\alpha_x = \frac{A_{0x}}{A_x} + \frac{a}{L} \quad (28)$$

where A_{0x} and A_x represent the horizontal wall cross-sectional area of the opening (i.e. $A_{0x} = L_0 t$) and of the solid wall (i.e. $A_x = Lt$), respectively. All parameters involved in Eq. (28) can be easily determined from Fig. 1, however, for simplicity the term $\bar{a}$ is calculated according to Eq. (29).

$$\bar{a} = \frac{L^2 t/2 - L_0 t a_0}{Lt - L_0 t} \quad (29)$$

3.2.2.2. Doh and Fragomeni model (OM2) [27]. Based on a new series of tests on walls with openings under both OW and TW actions, Doh and Fragomeni [27] proposed a new set of constants for Eq. (27). The only differences between this model and the Saheb and Desayi model (OM1) are:

- Provide different values for the constants, based on a new set of experimental tests.
- The ultimate load of the solid wall is calculated according to Eq. (18).

Again, the constants k_1 and k_2 were obtained using curve-fitting techniques, this time through a larger number of tests. For OW panels this yielded $k_1 = 1.175$ and $k_2 = 1.188$, while for TW panels $k_1 = 1.004$ and $k_2 = 0.933$.

While the differences between these constants are not large, the main contributor to the ultimate load comes from the load capacity of the solid wall, which is calculated in a different way. Both models take into account the size and position of an opening through the parameter α_x, allowing a reduction in the ultimate capacity.

Fragomeni et al. [28] found that this model gives results in good agreement with the test results from another experimental study [58].

3.2.2.3. Guan et al. model (OM3) [59]. Guan et al. [59] found that increasing both the length and the height of an opening has the most significant effect on the capacity, and proposed a new model to account for this effect. Having established a benchmark model, the authors performed a parametric study by varying the parameters that the capacity was most sensitive to. Their analysis proceeded through a nonlinear finite element method. In the model a three-dimensional stress state was used with elastic brittle fracture behaviour for concrete in tension, and a strain hardening plasticity approach was assumed for concrete in compression. Their model is nearly identical to that proposed by Doh and Fragomeni (OM2), the only difference being that α_x was changed to α_{xy} to account for the opening height.

$$\alpha_{xy} = \frac{\alpha_x + \gamma\alpha_y}{1 + \gamma} \quad (30)$$

where

$$\alpha_y = \frac{A_{0y}}{A_y} + \frac{d}{H} \quad (31)$$

in which A_{0y} represents the vertical cross-sectional area of the opening (i.e. $A_{0y} = H_0 t$), A_y represents the vertical cross-sectional area of the solid wall (i.e. $A_y = Ht$) and d represents the distance between centres of gravity (G_1 and G_3) of the wall with and without the opening, in the vertical direction (Fig. 1). In Eq. (30), γ represents "the weighting ratio indicating the percentage of α_y in relation to α_x". Using regression analysis, a new set of constants was determined; $\gamma = 0.21$, $k_1 = 1.361$ and $k_2 = 1.952$ for OW walls and $\gamma = 0.40$, $k_1 = 1.358$ and $k_2 = 1.795$ for TW walls. It should be noted that this model was derived from walls with a fixed slenderness ratio (i.e. $\lambda = 30$) and an aspect ratio of unity.

3.2.2.4. Mohammed et al. model [4]. In a more recent study, Mohammed et al. [4] tested OW walls with cut-out openings. The size of the openings was varied from 5% to 30% of the solid wall. It was found that the presence of a cut-out opening in a solid OW wall led to the formation of disturbance zones. Discontinuities in these disturbance zones cause high stresses in the concrete, and cracks will form at the corners of the opening if improperly reinforced.

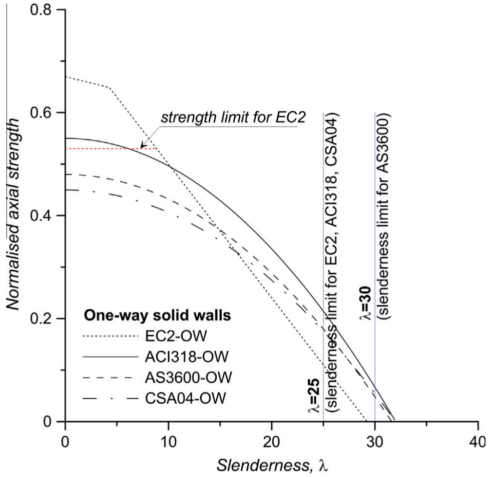

Fig. 6. Comparison of different design models in the investigated codes [11–14] for OW solid walls.

For this case, Mohammed et al. [4] suggested a new set of constants to be used in Eq. (27). The authors tested one-way panels only, obtaining $k_1 = 1.281$ and $k_2 = 0.737$. It should be noted that Eq. (27), proposed by Saheb and Desayi [19], considers steel reinforcement placed in two layers that yields at ultimate, whereas the experimental programme presented in [4] consisted only of centrally reinforced panels.

Since the model was calibrated on walls with cut-out openings (i.e. no diagonal bars around corners) it cannot be assessed through the current database. However, the results of the experiments by Mohammed et al. [4] were incorporated into the current database and used in the assessment of other models (i.e. OM1, OM2, and OM3).

4. Assessment of existing design models

The empirical design models reviewed above were derived using a limited number of either experimental tests or numerical simulations. Some models were developed solely from tests performed by the researchers themselves, while others additionally used tests from other sources, therefore the predictions of the latter may give more reasonable outcomes by covering a broader spectrum of designs. The studies focussed on either the variation of geometric characteristics (i.e. slenderness, aspect ratio, size and position of the opening) or the variation of material properties (i.e. concrete strength, influence of steel reinforcement). If one has to design a compression member under conditions that were not specifically covered by any of the available design models, then it remains unclear how accurate the models will be. In order to quantify this a statistical analysis was performed on each model in turn, using all of the experimental results available (these are included in Appendices A1–A3), unless the model explicitly specifies its limiting parameters.

The accuracy of the models was evaluated using the following statistical indicators; the average (Avg), the standard deviation (St Dev) which measures the amount of variation from the average, the coefficient of variation (CoV) which shows the extent of variation and the coefficient of determination (R^2) that indicates how well the data fit a model within a 95% confidence interval.

The analysis was conducted separately for solid OW action, solid TW action and for walls with openings. For all models, the material strength reduction factor, φ, was set to 1.0.

Table 1
Statistical summary for OW models of the solid walls.

Model	One-way solid walls			
	Avg	St Dev	CoV (%)	R^2
ACI318 [11]	0.69	0.25	36	0.91
AS3600 [12]	0.59	0.22	38	0.90
CSA-04 [13]	0.57	0.20	36	0.91
EC2 [14]	0.62	0.24	39	0.87
OWM1 [22]	0.77	0.28	37	0.90
OWM2 [51]	0.59	0.25	37	0.90
OWM3 [20]	0.74	0.20	27	0.94
OWM4 [42]	0.89	0.17	19	0.98
OWM5 [23]	1.10	0.35	32	0.92
OWM6 [17]	1.24	0.68	55	0.68
OWM6* [17]	1.10	0.41	37	0.82

4.1. Assessment of predicted values for OW solid walls

Fig. 6 shows the normalized strength versus slenderness, as predicted by the investigated design codes for a typical wall that is assumed to be loaded axially with an eccentricity of $t/6$ and has a strength reduction factor $\varphi = 1$. ACI318 [11] model provides higher loads for slenderness values above 10 when compared to EN 1992-1-1 [14].

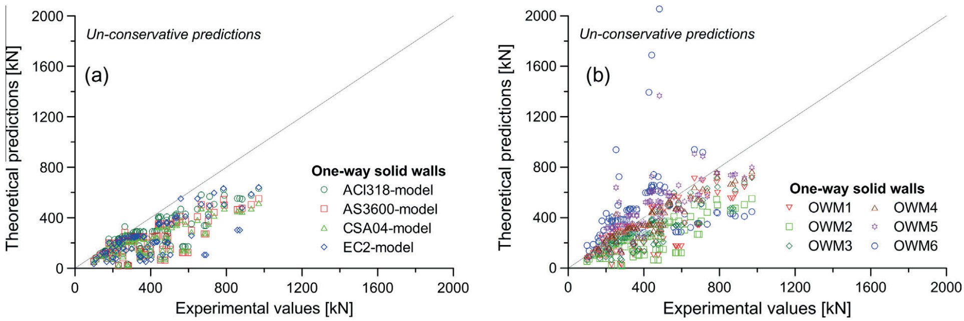

Fig. 7. Assessment of the current design models of one-way solid walls: (a) design codes; (b) design equation from different studies.

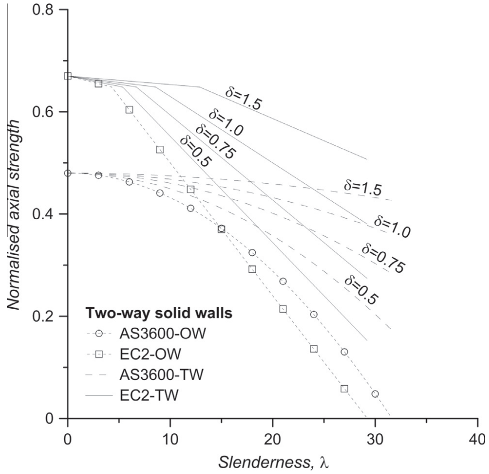

Fig. 8. Comparison of different design models in the investigated codes [12,14] for TW solid walls.

The AS3600 [12] and CAN/CSA-A23.3 [13] models predict the lowest load values for slenderness values lower than 15, above this value the load value predictions increase above those of EN 1992-1-1 [14], while remaining lower than ACI318 [11].

The limits of the slenderness values given in the codes are also plotted in Fig. 6. Beyond these limits, presumably imposed by the data available at the time of development, the models are not accurately calibrated and can yield negative values for the normalized strength. Recent studies have shown that the slenderness limit can be increased with confidence [15,17,23,40], however, suggesting that there is a need to update the current design codes.

How these models perform when assessed using experimental tests from the database is shown in Fig. 7a and b. While code models [11–14] present a natural degree of conservationism, due to statistical calibration, the trend is opposite for the models presented in the literature [17,20,22,23,51] (see Fig. 7b). A statistical summary for these models is presented in Table 1. Overall, the most conservative model is that proposed by CAN/CSA-A23.3 [13], with an average ratio between theoretically and experimentally determined capacity of 0.57 and a standard deviation of 0.20. The least conservative model is OWM6 [17], with an average ratio between theoretically and experimentally determined capacities of 1.24 and a standard deviation of 0.68. However, most of the extreme non-conservative results for the later model come from walls made of high-strength concrete. Since this aspect was not discussed in [17], the authors assumed that using the OWM6 model for normal strength concrete would provide better results. The new results obtained excluding high-strength concrete values are abbreviated as OWM6* and are listed in Table 1. The model proposed by Hegger et al. [42] (OWM4) is the most statistically accurate, with an average ratio between the theoretically and experimentally determined capacities of 0.89 and a standard deviation of 0.17.

4.2. Assessment of predicted values for TW solid walls

In the case of TW walls, EC2 and AS3600 are the only major codes that provide a methodology to account for a higher capacity due to restraints on all sides. It remains unclear whether the limitations placed on the slenderness values in these models ($\lambda = 25$ [14] and $\lambda = 30$ [12]) apply only to OW walls or to both OW and TW walls. By plotting both models with aspect ratios usually encountered in practice, one can observe that such limitations would be highly restrictive. The way that these codes account for lateral restraints is by using a subunitary coefficient (k), based on the end-restraint of the wall and its aspect ratio (Eqs. (11) and (12)). Significant increases in strength can be achieved by restraining the walls on all their sides, as can be observed in Fig. 8.

Fewer testes were carried out on walls restrained on all sides; correspondingly less models are also available. The performances of these models are shown in Fig. 9a for design codes and Fig. 9b for models found in the literature.

The outliers in Fig. 9a (EC2 and AS3600) and Fig. 9b (TWM1 and TWM1*), enclosed by the ellipsoids, originated from walls made of high-strength concrete. In addition, the tests were performed in a horizontal position with the eccentricity acting in favour of the strength, due to effect of gravity, and are consequently extremely non-conservative. A statistical summary for these models is presented in Table 2. The most conservative model is that proposed by AS3600 [12], with an average ratio between the theoretically and experimentally determined capacities of 0.71 and a standard deviation of 0.40. The least conservative model is TWM1* [19], with an average ratio between the theoretically and experimentally determined capacities of 1.44 and a standard deviation of 0.87. The most accurate model in terms of average ratio is TWM2 [20], however, a relatively high standard deviation of 0.30 weakens its precision.

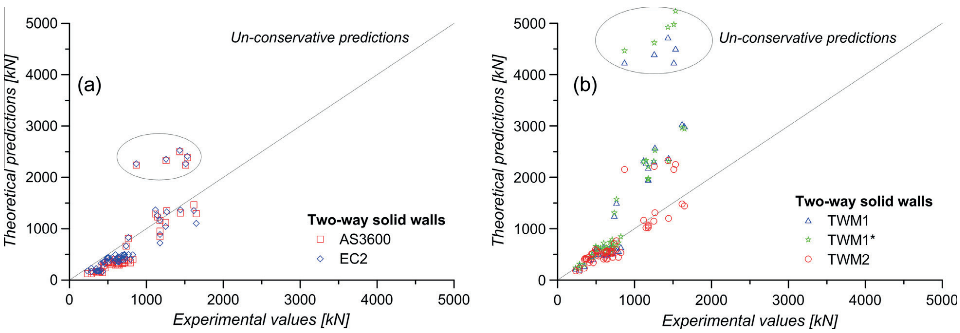

Fig. 9. Assessment of the current design models of two-way solid walls: (a) design codes; (b) design equation from different studies.

Table 2
Statistical summary for TW models of the solid walls.

Model	Two-way solid walls			
	Avg	St Dev	CoV (%)	R^2
AS3600 [12]	0.71	0.40	56	0.81
EC2 [14]	0.80	0.38	47	0.83
TWM1 [19]	1.35	0.84	62	0.80
TWM1* [19]	1.44	0.87	61	0.79
TWM2 [20]	0.95	0.30	32	0.89

4.3. Assessment of predicted values for walls with openings

The first model to include the effect of the openings, OM1 [18], was derived using six OW and six TW specimens, while model OM2 [27] was derived using ten OW and ten TW specimens. The model OM3 [59] was calibrated on thirty-six OW and thirty-seven TW specimens. The number of tests used to calibrate these models, therefore, is rather limited. This means that their predictive value may not extend to the design of openings in walls with different material and geometric characteristics.

4.3.1. OW walls with openings

The OM1 model provides the most conservative results, with the smallest value of the average ratio between the theoretically and experimentally determined capacities of 0.77 and a standard deviation of 0.16, while the best model in terms of average is OM2, i.e. 0.95 with a standard deviation of 0.19. The performances of these models are shown in Fig. 10 and the statistical summary is presented in Table 3.

4.3.2. TW walls with openings

Owing to its limited number of tests, OM1 model shows a large scatter from the bisector for those walls restrained on all their sides. A significantly more accurate model is OM2, with an average of 0.90 and a standard deviation of 0.13, proposed by Doh and Fragomeni [27].

5. FRP – based strengthening

The successful application of FRP to strengthen solid concrete walls has been achieved in several studies [60–62]. All of them performed a rehabilitation of structural walls using externally bonded FRPs to increase the flexural and/or shear strength, stiffness and energy dissipation. The creation of large openings in walls removes a significant quantity of concrete and steel reinforcement, necessarily reducing the load capacity of the wall. FRPs are able to strengthen such walls by redistributing the stresses, allowing the wall to recover almost its full capacity before the opening was created, if not more [3,4,63,64].

As the size of the opening increases, the global behaviour of the wall will change to that of a frame, and consequently new failure modes may arise. This has an influence on the optimal strengthening configuration. The research conducted so far on strengthening structural members with openings, such as slabs, walls or beams, using FRPs is promising [3,4,63,65–67]. The alignment of the fibres was based on observations of the failure modes of the un-strengthened elements. Usually the FRP material is placed around openings in a vertical, horizontal or inclined alignment, or a combination of these. In some cases the side strips were fully or partially wrapped to provide confinement. In general, the amount of FRPs were chosen intuitively, or by converting the amount of steel reinforcement

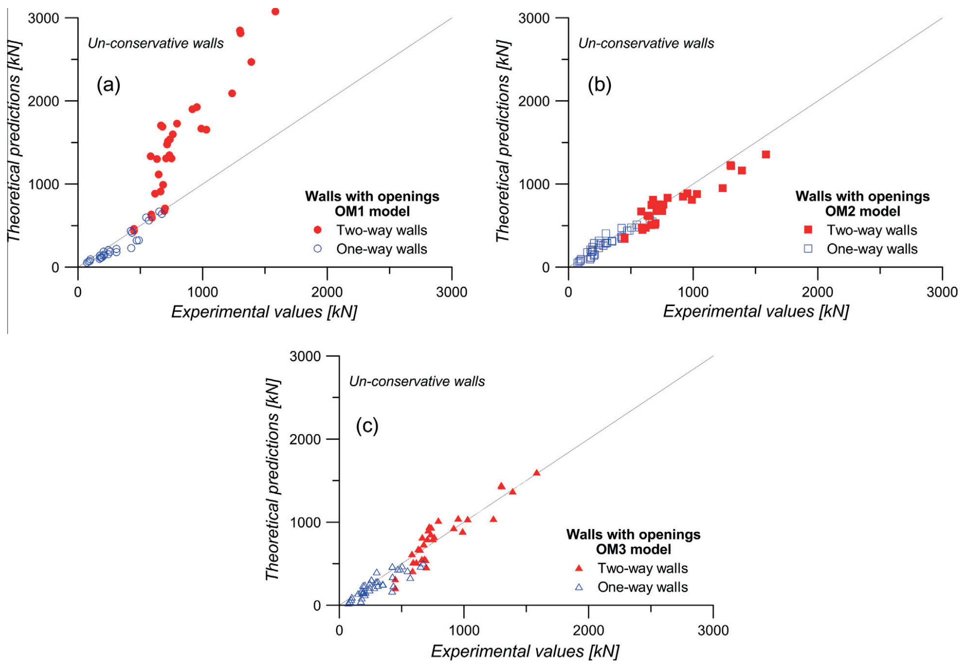

Fig. 10. Assessment of design equations for one-way and two-way walls with openings. (a) OM1 model; (b) OM2 model; (c) OM3 model.

Table 3
Statistical summary for OW & TW walls with openings.

Model	One-way action			
	Avg	St Dev	CoV (%)	R^2
OM1 [18]	0.77	0.16	21	0.96
OM2 [27]	0.95	0.19	20	0.98
OM3 [59]	0.83	0.24	29	0.98
	Two-way action			
	Avg	St Dev	CoV (%)	R^2
OM1 [18]	1.76	0.42	26	0.96
OM2 [27]	0.90	0.13	14	0.98
OM3 [59]	0.99	0.20	20	0.98

removed into FRP material. Li and Qian [63] have demonstrated that the optimization of the direction, width, and number of layers of the FRP strips by using a strut-and-tie model can provide rigorous results.

Mohammed et al. [4] tested 1/3-scale one-way RC walls with cut out openings, these openings having areas varying from 5% to 30% of the total wall area. The specimens were tested with a uniformly distributed axial load applied with an eccentricity of $t/6$. The introduction of small openings (5% area) reduced the axial capacity by 9%, while large openings (30% area) reduced the capacity by nearly 33%. While keeping the same geometric characteristics and applying two different CFRP patterns (see Fig. 11), the capacity was increased as the principal stresses on the opening corners were reduced. When applied to small openings the first pattern, in which the CFRP was applied around the corners, increased the axial strength by 49.9%. The second pattern, with CFRP placed at the corners, performed better on small openings, causing an increase in axial strength of 75.4%. When applied to large openings, however, the efficiency of these reinforcements was significantly reduced, with 11.3% and 15.1% increases for the first and second patterns, respectively. This confirms the aforementioned claim that different sized openings lead to different failure modes, and consequently require different strengthening patterns. A configuration that may yield better results for large openings would be to fully wrap the side chords, as their thickness ratio was slightly above 2. EN 1992-1-1 [14] emphasizes that elements with a thickness ratio below 4 should be considered as columns rather than walls.

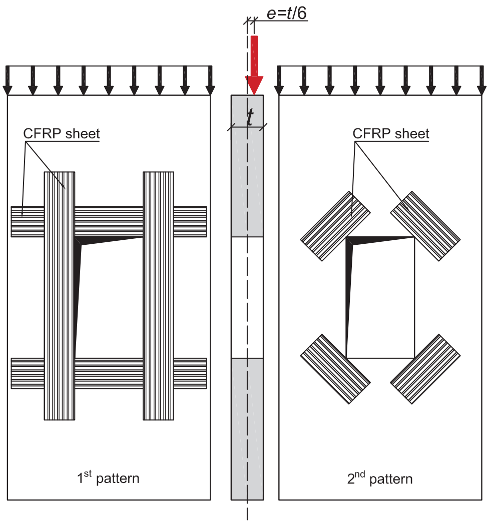

Fig. 11. CFRP patterns used to strengthen axially loaded RC walls with openings (adapted from [4]).

The research conducted so far on the rehabilitation of walls using FRPs was promising, however, the repaired walls were loaded principally in the horizontal direction to simulate the effects of earthquakes. The proposed strengthening schemes, therefore, may not be suitable for the repair of gravitationally loaded walls, and more research is required with the loads applied vertically.

Just one study was found in the literature that focused on using FRPs to strengthen axially loaded RC walls with cut-out openings [4]. In order to better understand the structural behaviour of such a configuration, therefore, more studies are required. To this end a research programme at the Luleå University of Technology is currently underway. This study will test a number of concrete walls with different parameters, such as size opening and strengthening configurations, under TW action. The results are expected to be published upon completion of the study.

6. Conclusions and future directions

Through the statistical analysis of existing experimental studies this study indicated areas where further testing is required in order to enhance the reliability of current design models. It was found that most experimental studies have focussed on testing RC walls under OW action, with a fixed eccentricity of $t/6$. Fewer tests exist on walls under TW action, walls with openings or different eccentricities, and more tests are required in these experimental regimes to facilitate the development of appropriate design models. The current database is useful because it highlights areas where the current literature is lacking, and where systematic studies could provide important insights into the behaviour of wall types that are poorly understood (e.g. walls with eccentricities above $t/6$ or OW solid walls with high slenderness ratios) or the effects of parameters that are not well covered by existing design provisions (e.g. the presence of an opening or the influence of steel reinforcement).

The design of the experimental programme has a significant role in determining the accuracy of the regression-based models derived. Although the design is carried out assuming a perfect hinge, laboratory evidence shows that neither a perfect hinge nor a full rotation restraint could be achieved in the laboratory environment, much less in practice. All design models empirically derived from such tests, therefore, will necessarily contain a certain level of inaccuracy.

Since the simplified methods assume that the walls are unreinforced elements, the contribution of any steel reinforcement is disregarded. This occurs regardless of the location of the steel mesh layer, or if the reinforcement is placed in one or two layers. For centrally reinforced walls this seems to be valid, although in some cases it may bring some ductility at higher loads. For double-reinforced walls, however, the enhanced capacity should be accounted for, even when the steel ratio is at a minimum level.

The design models found in established design codes provide the most conservative results, while those proposed in other studies showed a certain level of non-conservatism. However, all design models were plotted using $\varphi = 1$, while a carefully chosen safety factor should be used in practice.

FRPs have been recognised as a viable alternative for the strengthening of concrete structures. The potential applications of FRPs in strengthening walls that have been weakened by new openings need to be further studied. There are only a few research studies in the literature on the FRP strengthening of walls with openings, and almost all the experimental tests involved wall openings that were initially planned. The case of RC walls with cut-out openings is still largely unexplored, with just one research study focussing on this problem [4]. Currently there are no design philosophies or reliable theoretical guidelines for calculating the capacity of strengthened walls in the literature. Safe and clear design procedures for strengthening walls with openings are needed. In the bullet points listed below the main gaps in the research literature, that require further study, are presented.

1. Openings can be of different sizes and may have different positions with respect to a reference point of the RC wall. Therefore, it is natural to ask: How do these parameters influence the FRP contribution to the overall capacity of the wall?
2. What are the efficiencies of different FRP strengthening configurations and systems (sheets, plates or bars) when strengthening RC walls with openings?
3. How does the failure mechanism of an RC wall with an opening change after strengthening with FRP?
4. When designing RC walls with openings, engineers tend to adopt a simplified method by dividing the wall openings into isolated columns connected by beams. While this method provides acceptable results it is overly conservative, and it would be beneficial to know how to delineate small and large openings in walls, and where the transition from RC walls to RC frames should occur in the design of structural elements.

Acknowledgements

The authors would like to acknowledge The Research Council of Norway (RFF) and Development Fund of the Swedish Construction Industry (SBUF) for financing their work within this project. The authors also like to thank Dr. Bo Westerberg for his contribution in reviewing the paper.

Appendix A

See Tables A1–A3.

Table A1

Refs.	Designation	Geometrical dimensions								Material properties					Capacity
		H (mm)	t (mm)	L (mm)	δ	λ	η	e	n	ρ_v (%)	f_{yv} (MPa)	ρ_h (%)	f_{yh} (MPa)	f_c (MPa)	N_u (kN)
Pillai and Parthasarathy [15]	A1	1200	40	400	3	30	10	$t/6$	1	0.156	273	0.250	273	25.0	229
	A2	1200	48	500	2.4	25	10.4	$t/6$	1	0.150	233	0.241	233	25.0	367
	A3	1200	60	550	2.2	20	9.2	$t/6$	1	0.153	233	0.244	233	20.8	382
	A5	800	80	700	1.1	10	8.8	$t/6$	1	0.150	347	0.241	347	20.8	932
	A6	400	80	700	0.6	5	8.8	$t/6$	1	0.150	347	0.250	347	15.6	647
	B1	1200	40	400	3	30	10	$t/6$	1	0.300	233	0.500	233	24.3	282
	B2	1200	48	500	2.4	25	10.4	$t/6$	1	0.300	233	0.500	233	24.3	402
	B3	1200	60	560	2.1	20	9.3	$t/6$	1	0.301	233	0.500	233	31.1	616
	B4	1200	80	700	1.7	15	8.8	$t/6$	1	0.300	347	0.500	347	22.8	883
	B5	800	80	700	1.1	10	8.8	$t/6$	1	0.300	347	0.500	347	22.8	971
	B6	400	80	700	0.6	5	8.8	$t/6$	1	0.300	347	0.500	347	15.6	559
	C1	1200	40	400	3	30	10	$t/6$	1	0	0	0	0	31.0	277
	C2	1200	48	500	2.4	25	10.4	$t/6$	1	0	0	0	0	20.6	343
	C3	1200	60	560	2.1	20	9.3	$t/6$	1	0	0	0	0	24.0	490
	C4	1200	80	700	1.7	15	8.8	$t/6$	1	0	0	0	0	24.0	789
	C5	800	80	700	1.1	10	8.8	$t/6$	1	0	0	0	0	22.5	785
	C6	400	80	700	0.6	5	8.8	$t/6$	1	0	0	0	0	16.9	735
Saheb and Desayi [22]	WAR-1	600	50	900	0.7	12	18	$t/6$	2	0.2	297	0.199	286	17.9	484
	WAR-2	600	50	600	1	12	12	$t/6$	2	0.173	297	0.199	286	17.9	315
	WAR-3	600	50	400	1.5	12	8	$t/6$	2	0.173	297	0.199	286	17.9	198
	WAR-4	600	50	300	2	12	6	$t/6$	2	0.173	297	0.199	286	17.9	147
	WSR-1	450	50	300	1.5	9	6	$t/6$	2	0.165	297	0.199	286	17.3	214
	WSR-2	600	50	400	1.5	12	8	$t/6$	2	0.165	297	0.199	286	17.3	254
	WSR-3	900	50	600	1.5	18	8	$t/6$	2	0.165	297	0.199	286	17.3	299
	WSR-4	1350	50	900	1.5	27	18	$t/6$	2	0.165	297	0.199	286	17.3	374
	WSTV-2	600	50	900	0.7	12	18	$t/6$	2	0.331	286	0.199	286	20.1	535
	WSTV-3	600	50	900	0.7	12	18	$t/6$	2	0.528	581	0.199	286	20.1	584
	WSTV-4	600	50	900	0.7	12	18	$t/6$	2	0.845	570	0.199	286	20.1	704
	WSTV-5	1200	50	800	1.5	24	16	$t/6$	2	0.177	297	0.199	286	18.3	339
	WSTV-6	1200	50	800	1.5	24	16	$t/6$	2	0.335	286	0.199	286	18.3	399
	WSTV-7	1200	50	800	1.5	24	16	$t/6$	2	0.528	581	0.199	286	18.3	463
	WSTV-8	1200	50	800	1.5	24	16	$t/6$	2	0.856	570	0.199	286	18.3	503
	WSTH-2	600	50	900	0.7	12	18	$t/6$	2	0.173	297	0.352	581	19.6	538
	WSTH-3	600	50	900	0.7	12	18	$t/6$	2	0.173	297	0.440	581	19.6	528
	WSTH-4	600	50	900	0.7	12	18	$t/6$	2	0.173	297	0.507	570	19.6	528
	WSTH-6	1200	50	800	1.5	24	16	$t/6$	2	0.176	297	0.352	581	16.1	349
	WSTH-7	1200	50	800	1.5	24	16	$t/6$	2	0.176	297	0.440	581	16.1	344
	WSTH-8	1200	50	800	1.5	24	16	$t/6$	2	0.176	297	0.507	570	16.1	349
Fragomeni [52]	1a	1000	50	200	5	20	4	$t/6$	1	0.250	450	0.250	450	40.7	162
	1b	1000	50	200	5	20	4	$t/6$	1	0.250	450	0.250	450	58.9	187
	2a	1000	50	300	3.3	20	6	$t/6$	1	0.250	450	0.250	450	42.4	232
	2b	1000	50	300	3.3	20	6	$t/6$	1	0.250	450	0.250	450	65.4	264
	3a	1000	40	200	5	25	5	$t/6$	1	0.310	450	0.280	450	37.1	100
	3b	1000	40	200	5	25	5	$t/6$	1	0.310	450	0.280	450	54.0	168

(continued on next page)

Table A1 (*continued*)

Refs.	Designation	Geometrical dimensions								Material properties					Capacity
		H (mm)	t (mm)	L (mm)	δ	λ	η	e	n	ρ_v (%)	f_{yv} (MPa)	ρ_h (%)	f_{yh} (MPa)	f_c (MPa)	N_u (kN)
	4a	1000	40	300	3.3	25	7.5	$t/6$	1	0.210	450	0.280	450	35.7	199
	4b	1000	40	300	3.3	25	7.5	$t/6$	1	0.210	450	0.280	450	54.0	217
	5a	1000	40	500	2	25	12.5	$t/6$	1	0.250	450	0.280	450	35.7	201
	5b	1000	40	500	2	25	12.5	$t/6$	1	0.250	450	0.280	450	59.7	269
	6a	600	40	200	3	15	5	$t/6$	1	0.310	450	0.260	450	38.3	163
	6b	600	40	200	3	15	5	$t/6$	1	0.310	450	0.260	450	67.4	178
	7a	600	40	150	4	15	3.8	$t/6$	1	0.260	450	0.260	450	32.9	111
	7b	600	40	150	4	15	3.8	$t/6$	1	0.260	450	0.260	450	45.1	132
	8a	420	35	210	2	12	6	$t/6$	1	0.320	450	0.260	450	39.6	158
	8b	420	35	210	2	12	6	$t/6$	1	0.320	450	0.260	450	67.4	233
Doh [40]	OWNS2	1200	40	1200	1	30	30	$t/6$	1	0.310	500	0.310	500	35.7	253
	OWNS3	1400	40	1400	1	35	35	$t/6$	1	0.310	500	0.310	500	52.0	427
	OWNS4	1600	40	1600	1	40	40	$t/6$	1	0.310	500	0.310	500	51.0	442
	OWHS2	1200	40	1200	1	30	30	$t/6$	1	0.310	500	0.310	500	78.2	483
	OWHS3	1400	40	1400	1	35	35	$t/6$	1	0.310	500	0.310	500	63.0	442
	OWHS4	1600	40	1600	1	40	40	$t/6$	1	0.310	500	0.310	500	75.9	456
Ganesan et al. [23]	OWSFN-1	480	40	320	1.5	12	8	$t/6$	1	0.880	445	0.740	445	42.3	299
	OWSFN-2	600	40	400	1.5	15	10	$t/6$	1	0.880	445	0.740	445	42.3	323
	OWSFN-3	840	40	560	1.5	21	14	$t/6$	1	0.880	445	0.740	445	42.3	476
	OWSFN-4	1200	40	800	1.5	30	20	$t/6$	1	0.880	445	0.740	445	42.3	451
	OWAFN-1	600	40	320	1.9	15	8	$t/6$	1	0.880	445	0.740	445	42.3	235
	OWAFN-2	600	40	400	1.5	15	10	$t/6$	1	0.880	445	0.740	445	42.3	343
	OWAFN-3	600	40	560	1.1	15	14	$t/6$	1	0.880	445	0.740	445	42.3	486
	OWAFN-4	600	40	800	0.8	15	20	$t/6$	1	0.880	445	0.740	445	42.3	667
	OWSFS-1	480	40	320	1.5	12	8	$t/6$	1	0.880	445	0.740	445	42.3	309
	OWSFS-2	600	40	400	1.5	15	10	$t/6$	1	0.880	445	0.740	445	42.3	363
	OWSFS-3	840	40	560	1.5	21	14	$t/6$	1	0.880	445	0.740	445	41.3	491
	OWSFS-4	1200	40	800	1.5	30	20	$t/6$	1	0.880	445	0.740	445	41.3	476
	OWAFS-1	600	40	320	1.9	15	8	$t/6$	1	0.880	445	0.740	445	41.3	250
	OWAFS-2	600	40	400	1.5	15	10	$t/6$	1	0.880	445	0.740	445	41.3	363
	OWAFS-3	600	40	560	1.1	15	14	$t/6$	1	0.880	445	0.740	445	41.3	510
	OWAFS-4	600	40	800	0.8	15	20	$t/6$	1	0.880	445	0.740	445	41.3	711
Ganesan et al. [24]	OPCSR-1	480	40	320	1.5	12	8	$t/6$	1	0.880	445	0.740	445	42.3	279
	OPCSR-1	480	40	320	1.5	12	8	$t/6$	1	0.880	445	0.740	445	42.3	290
	OPCSR-2	600	40	400	1.5	15	10	$t/6$	1	0.880	445	0.740	445	42.3	330
	OPCSR-2	600	40	400	1.5	15	10	$t/6$	1	0.880	445	0.740	445	42.3	328
	OPCSR-3	840	40	560	1.5	21	14	$t/6$	1	0.880	445	0.740	445	42.3	435
	OPCSR-3	840	40	560	1.5	21	14	$t/6$	1	0.880	445	0.740	445	42.3	429
	OPCAR-1	600	40	320	1.9	15	8	$t/6$	1	0.880	445	0.740	445	42.3	228
	OPCAR-1	600	40	320	1.9	15	8	$t/6$	1	0.880	445	0.740	445	42.3	233
	OPCAR-2	600	40	560	1.1	15	14	$t/6$	1	0.880	445	0.740	445	42.3	441
	OPCAR-2	600	40	560	1.1	15	14	$t/6$	1	0.880	445	0.740	445	42.3	451
	GPCSR-1	480	40	320	1.5	12	8	$t/6$	1	0.880	445	0.740	445	41.3	261
	GPCSR-1	480	40	320	1.5	12	8	$t/6$	1	0.880	445	0.740	445	41.3	251
	GPCSR-2	600	40	400	1.5	15	10	$t/6$	1	0.880	445	0.740	445	41.3	310
	GPCSR-2	600	40	400	1.5	15	10	$t/6$	1	0.880	445	0.740	445	41.3	319
	GPCSR-3	840	40	560	1.5	21	14	$t/6$	1	0.880	445	0.740	445	41.3	420
	GPCSR-3	840	40	560	1.5	21	14	$t/6$	1	0.880	445	0.740	445	41.3	409
	GPCAR-1	600	40	320	1.9	15	8	$t/6$	1	0.880	445	0.740	445	41.3	232
	GPCAR-1	600	40	320	1.9	15	8	$t/6$	1	0.880	445	0.740	445	41.3	210
	GPCAR-2	600	40	560	1.1	15	14	$t/6$	1	0.880	445	0.740	445	41.3	445
	GPCAR-2	600	40	560	1.1	15	14	$t/6$	1	0.880	445	0.740	445	41.3	440
Robinson et al. [17]	7	2500	100	500	5	25	5	$t/6$	1	–	–	–	–	51.5	871
	8	2500	100	500	5	25	5	$t/6$	1	–	–	–	–	51.5	858
	9	2800	100	500	5.6	28	5	$t/6$	1	–	–	–	–	52.4	692
	10	2800	100	500	5.6	28	5	$t/6$	1	–	–	–	–	52.4	683
	11	3000	100	500	6	30	5	$t/6$	1	–	–	–	–	51.6	582
	12	3000	100	500	6	30	5	$t/6$	1	–	–	–	–	51.6	597
	13	3000	100	500	6	30	5	$t/6$	1	–	–	–	–	51.6	572
	14	3000	100	500	6	30	5	$t/6$	1	–	–	–	–	51.6	568

Table A2

Refs.	Designation	Geometrical dimensions								Material properties					Capacity
		H (mm)	t (mm)	L (mm)	δ	λ	η	e	n	ρ_v (%)	f_{yv} (MPa)	ρ_h (%)	f_{yh} (MPa)	f_c (MPa)	N_u (kN)
Sanjayan and Maheswaran [16]	2	2000	50	1500	1.3	40	30	$t/6$	1	0.850	513	0.850	513	80.5	1256.0
	3	2000	50	1500	1.3	40	30	$t/6$	1	0.850	513	0.850	513	86.5	1435.0
	5	2000	50	1500	1.3	40	30	$t/6$	1	0.850	513	0.850	513	77.5	871.0
	6	2000	50	1500	1.3	40	30	$t/6$	1	1.690	513	1.690	513	77.5	1510.0
	8	2000	50	1500	1.3	40	30	$t/6$	1	1.690	513	1.690	513	82.5	1533.0
Swartz et al. [21]	1	2438	25.4	1219	2	96	48	0	1	0.200	530	0.200	530	26.9	490.2
	2	2438	25.4	1219	2	96	48	0	1	0.200	530	0.200	530	26.2	506.7
	3	2438	25.4	1219	2	96	48	0	2	0.500	530	0.200	530	21.8	444.4
	4	2438	25.4	1219	2	96	48	0	2	0.500	530	0.200	530	23.7	534.2
	5	2438	25.4	1219	2	96	48	0	2	0.750	530	0.200	530	22.7	623.6
	6	2438	25.4	1219	2	96	48	0	2	0.750	530	0.200	530	24.5	691.7
	7	2438	25.4	1219	2	96	48	0	2	1.000	530	0.200	530	25.4	640.1
	8	2438	25.4	1219	2	96	48	0	2	1.000	530	0.200	530	22.1	455.1
	9	2438	31.8	1219	2	77	38	0	1	0.200	530	0.200	530	17.7	625.9
	10	2438	31.8	1219	2	77	38	0	1	0.200	530	0.200	530	18.3	696.2
	11	2438	31.8	1219	2	77	38	0	2	0.500	530	0.200	530	16.6	636.5
	12	2438	31.8	1219	2	77	38	0	2	0.500	530	0.200	530	17.9	639.7
	13	2438	31.8	1219	2	77	38	0	2	0.750	530	0.200	530	17.6	512.0
	14	2438	31.8	1219	2	77	38	0	2	0.750	530	0.200	530	19.8	716.2
	15	2438	31.8	1219	2	77	38	0	2	1.000	530	0.200	530	19.9	766.4
	16	2438	31.8	1219	2	77	38	0	2	1.000	530	0.200	530	17.9	722.0
	17	2438	19	1219	2	128	64	0	1	0.200	530	0.200	530	22.6	429.3
	18	2438	19	1219	2	128	64	0	1	0.200	530	0.200	530	23.3	396.3
	19	2438	19	1219	2	128	64	0	1	0.500	530	0.200	530	23.8	377.7
	20	2438	19	1219	2	128	64	0	1	0.500	530	0.200	530	24.5	372.8
	21	2438	19	1219	2	128	64	0	1	0.750	530	0.200	530	25.0	368.3
	22	2438	19	1219	2	128	64	0	1	0.750	530	0.200	530	24.8	355.9
	23	2438	19	1219	2	128	64	0	1	1.000	530	0.200	530	23.4	347.0
	24	2438	19	1219	2	128	64	0	1	1.000	530	0.200	530	27.0	400.3
Saheb and Desayi [19]	WAR-1(P)	600	50	900	0.7	12	18	$t/6$	2	0.173	297	0.199	286	17.9	556.0
	WAR-2(P)	600	50	600	1	12	12	$t/6$	2	0.173	297	0.199	286	17.9	413.5
	WAR-3(P)	600	50	400	1.5	12	8	$t/6$	2	0.173	297	0.199	286	17.9	284.9
	WAR-4(P)	600	50	300	2	12	6	$t/6$	2	0.173	297	0.199	286	17.9	235.2
	WSR-1(P)	450	50	300	1.5	9	6	$t/6$	2	0.165	297	0.199	286	17.3	283.9
	WSR-2(P)	600	50	400	1.5	12	8	$t/6$	2	0.165	297	0.199	286	17.3	346.7
	WSR-3(P)	900	50	600	1.5	18	12	$t/6$	2	0.165	297	0.199	286	17.3	463.3
	WSR-4(P)	1350	50	900	1.5	27	18	$t/6$	2	0.165	297	0.199	286	17.3	534.0
	WSTV-2(P)	600	50	900	0.7	12	18	$t/6$	2	0.331	297	0.199	286	20.1	597.8
	WSTV-3(P)	600	50	900	0.7	12	18	$t/6$	2	0.528	581	0.199	286	20.1	709.4
	WSTV-4(P)	600	50	900	0.7	12	18	$t/6$	2	0.845	570	0.199	286	20.1	823.0
	WSTV-5(P)	1200	50	900	1.3	24	18	$t/6$	2	0.177	297	0.199	286	18.3	498.2
	WSTV-6(P)	1200	50	800	1.5	24	16	$t/6$	2	0.335	286	0.199	286	18.3	612.7
	WSTV-7(P)	1200	50	800	1.5	24	16	$t/6$	2	0.528	581	0.199	286	18.3	717.4
	WSTV-8(P)	1200	50	800	1.5	24	16	$t/6$	2	0.856	570	0.199	286	18.3	790.1
	WSTH-2(P)	600	50	900	0.7	12	18	$t/6$	2	0.173	297	0.352	581	19.6	712.4
	WSTH-3(P)	600	50	900	0.7	12	18	$t/6$	2	0.173	297	0.440	581	19.6	712.4
	WSTH-4(P)	600	50	900	0.7	12	18	$t/6$	2	0.173	297	0.507	570	19.6	682.6
	WSTH-6(P)	1200	50	800	1.5	24	16	$t/6$	2	0.176	297	0.352	581	16.1	597.8
	WSTH-7(P)	1200	50	800	1.5	24	16	$t/6$	2	0.176	297	0.440	581	16.1	647.7
	WSTH-8(P)	1200	50	800	1.5	24	16	$t/6$	2	0.176	297	0.507	570	16.1	632.7
Doh [40]	TWNS1	1000	40	1200	0.8	25	30	$t/6$	1	0.310	500	0.310	500	45.4	765.8
	TWNS2	1200	40	1200	1	30	30	$t/6$	1	0.310	500	0.310	500	37.0	735.8
	TWNS3	1400	40	1400	1	35	35	$t/6$	1	0.310	500	0.310	500	51.0	1177.2
	TWNS4	1600	40	1600	1	40	40	$t/6$	1	0.310	500	0.310	500	45.8	1177.2
	TWHS1	1000	40	1200	0.8	25	30	$t/6$	1	0.310	500	0.310	500	68.7	1147.8
	TWHS2	1200	40	1200	1	30	30	$t/6$	1	0.310	500	0.310	500	64.8	1177.2
	TWHS3	1400	40	1400	1	35	35	$t/6$	1	0.310	500	0.310	500	60.1	1250.8
	TWHS4	1600	40	1600	1	40	40	$t/6$	1	0.310	500	0.310	500	70.2	1648.1
	TAHS1	1600	40	1400	1.1	40	35	$t/6$	1	0.310	500	0.310	500	77.8	1618.7
	TAHS2	1400	40	1000	1.4	35	25	$t/6$	1	0.310	500	0.310	500	77.8	1118.3
	TAHS3	1600	40	1200	1.3	40	30	$t/6$	1	0.310	500	0.310	500	73.8	1265.5
	TAHS4	1600	40	1000	1.6	40	25	$t/6$	1	0.310	500	0.310	500	77.8	1442.1

Table A3

Refs.		Designation	Geometrical dimensions																Material properties					Capacity
			H	t	L	δ	λ	η	1st Opening				2nd Opening				e	n	ρ_v	f_{yv}	ρ_h	f_{yh}	f_c	N_u
			(mm)	(mm)	(mm)				H_0 (mm)	L_0 (mm)	X_{G1} (mm)	y_{G1} (mm)	H_0 (mm)	L_0 (mm)	x_{G2} (mm)	y_{G2} (mm)			(%)	(MPa)	(%)	(MPa)	(MPa)	(kN)
Saheb and Desayi [18]	OW	WWO-1	600	50	900	0.7	12	18	240	240	0	0	0	0	0	0	$t/6$	2	0.173	297	0.236	297	28.2	672.6
		WWO-2	600	50	900	0.7	12	18	240	240	−230	0	0	0	0	0	$t/6$	2	0.173	297	0.236	297	28.2	568.9
		WWO-3	600	50	900	0.7	12	18	240	240	−230	0	240	240	230	0	$t/6$	2	0.173	297	0.236	297	28.2	433.5
		WWO-4	600	50	900	0.7	12	18	420	210	0	−90	0	0	0	0	$t/6$	2	0.173	297	0.236	297	28.2	652.7
		WWO-5	600	50	900	0.7	12	18	420	210	−245	−90	0	0	0	0	$t/6$	2	0.173	297	0.236	297	28.2	548.0
		WWO-6	600	50	900	0.7	12	18	420	210	−245	−90	240	240	230	0	$t/6$	2	0.173	297	0.236	297	28.2	423.5
	TW	WWO-1(P)	600	50	900	0.7	12	18	240	240	0	0	0	0	0	0	$t/6$	2	0.173	297	0.236	297	28.2	692.5
		WWO-2(P)	600	50	900	0.7	12	18	240	240	−230	0	0	0	0	0	$t/6$	2	0.173	297	0.236	297	28.2	592.8
		WWO-3(P)	600	50	900	0.7	12	18	240	240	−230	0	240	240	230	0	$t/6$	2	0.173	297	0.236	297	28.2	448.4
		WWO-4(P)	600	50	900	0.7	12	18	420	210	0	−90	0	0	0	0	$t/6$	2	0.173	297	0.236	297	28.2	697.5
		WWO-5(P)	600	50	900	0.7	12	18	420	210	−245	−90	0	0	0	0	$t/6$	2	0.173	297	0.236	297	28.2	587.8
		WWO-6(P)	600	50	900	0.7	12	18	420	210	−245	−90	240	240	230	0	$t/6$	2	0.173	297	0.236	297	28.2	448.4
Doh and Fragomeni [27]	OW	OW11	1200	40	1200	1	30	30	300	300	0	0	0	0	0	0	$t/6$	1	0.310	500	0.310	500	53	309.0
		OW12	1600	40	1600	1	40	40	400	400	0	0	0	0	0	0	$t/6$	1	0.310	500	0.310	500	47	294.3
		OW21	1200	40	1200	1	30	30	300	300	−250	0	300	300	250	0	$t/6$	1	0.310	500	0.310	500	50	185.4
		OW22	1600	40	1600	1	40	40	400	400	−333	0	400	400	333	0	$t/6$	1	0.310	500	0.310	500	51.1	195.7
	TW	TW11	1200	40	1200	1	30	30	300	300	0	0	0	0	0	0	$t/6$	1	0.310	500	0.310	500	50.3	750.5
		TW12	1600	40	1600	1	40	40	400	400	0	0	0	0	0	0	$t/6$	1	0.310	500	0.310	500	50.3	1030.1
		TW21	1200	40	1200	1	30	30	300	300	−250	0	300	300	250	0	$t/6$	1	0.310	500	0.310	500	50.3	618.0
		TW22	1600	40	1600	1	40	40	400	400	−333	0	400	400	333	0	$t/6$	1	0.310	500	0.310	500	50.3	647.5
Lee [58]	OW	O50W1C1.2	1200	40	1200	1	30	30	300	300	0	0	0	0	0	0	$t/6$	1	0.310	500	0.310	500	53	309
		O70W1C1.2	1200	40	1200	1	30	30	300	300	0	0	0	0	0	0	$t/6$	1	0.310	500	0.310	500	67.7	426.7
		O90W1C1.2	1200	40	1200	1	30	30	300	300	0	0	0	0	0	0	$t/6$	1	0.310	500	0.310	500	95.1	470.9
		O95W1C1.2	1200	40	1200	1	30	30	300	300	0	0	0	0	0	0	$t/6$	1	0.310	500	0.310	500	96.2	488.5
		O45W1C1.4	1400	40	1400	1	35	35	350	350	0	0	0	0	0	0	$t/6$	1	0.310	500	0.310	500	38	191.3
		O90W1C1.4	1400	40	1400	1	35	35	350	350	0	0	0	0	0	0	$t/6$	1	0.310	500	0.310	500	80	300.2
		O95W1C1.4	1400	40	1400	1	35	35	350	350	0	0	0	0	0	0	$t/6$	1	0.310	500	0.310	500	99.3	426.1
		O50W1C1.6	1600	40	1600	1	40	40	400	400	0	0	0	0	0	0	$t/6$	1	0.310	500	0.310	500	47	294.3
		O90W1C1.6	1600	40	1600	1	40	40	400	400	0	0	0	0	0	0	$t/6$	1	0.310	500	0.310	500	97.1	503.3
		O50W2C1.2	1200	40	1200	1	30	30	300	300	−250	0	300	300	250	0	$t/6$	1	0.310	500	0.310	500	50.3	191.3
		O70W2C1.2	1200	40	1200	1	30	30	300	300	−250	0	300	300	250	0	$t/6$	1	0.310	500	0.310	500	67.7	242.8
		O95W2C1.2	1200	40	1200	1	30	30	300	300	−250	0	300	300	250	0	$t/6$	1	0.310	500	0.310	500	96.2	308.1
		O45W2C1.4	1400	40	1400	1	35	35	350	350	−292	0	350	350	292	0	$t/6$	1	0.310	500	0.310	500	44.5	150.7
		O90W2C1.4	1400	40	1400	1	35	35	350	350	−292	0	350	350	292	0	$t/6$	1	0.310	500	0.310	500	80	244.3
		O95W2C1.4	1400	40	1400	1	35	35	350	350	−292	0	350	350	292	0	$t/6$	1	0.310	500	0.310	500	99.3	350.8
		O50W2C1.6	1600	40	1600	1	40	40	400	400	−333	0	400	400	333	0	$t/6$	1	0.310	500	0.310	500	51.1	195.7
		O70W2C1.6	1600	40	1600	1	40	40	400	400	−333	0	400	400	333	0	$t/6$	1	0.310	500	0.310	500	74.1	279
		O90W2C1.6	1600	40	1600	1	40	40	400	400	−333	0	400	400	333	0	$t/6$	1	0.310	500	0.310	500	97.1	347.3
		O65W1W1.2	1200	40	1200	1	30	30	300	600	0	0	0	0	0	0	$t/6$	1	0.310	500	0.310	500	60.3	176
		O65W1L1.2	1200	40	1200	1	30	30	300	300	−250	0	0	0	0	0	$t/6$	1	0.310	500	0.310	500	60.3	258.4
		O65W1U1.2	1200	40	1200	1	30	30	300	300	−250	150	0	0	0	0	$t/6$	1	0.310	500	0.310	500	60.3	257.8
		O65D1C1.2	1200	40	1200	1	30	30	750	300	0	−225	0	0	0	0	$t/6$	1	0.310	500	0.310	500	60.3	243.7
		O65D1L1.2	1200	40	1200	1	30	30	750	300	−250	−225	0	0	0	0	$t/6$	1	0.310	500	0.310	500	60.3	206
	TW	T50W1C1.2	1200	40	1200	1	30	30	300	300	0	0	0	0	0	0	$t/6$	1	0.310	500	0.310	500	50.3	706.3
		T70W1C1.2	1200	40	1200	1	30	30	300	300	0	0	0	0	0	0	$t/6$	1	0.310	500	0.310	500	74.1	953.5
		T45W1C1.4	1400	40	1400	1	35	35	350	350	0	0	0	0	0	0	$t/6$	1	0.310	500	0.310	500	45.5	732.8
		T90W1C1.4	1400	40	1400	1	35	35	350	350	0	0	0	0	0	0	$t/6$	1	0.310	500	0.310	500	95.1	1303.7
		T95W1C1.4	1400	40	1400	1	35	35	350	350	0	0	0	0	0	0	$t/6$	1	0.310	500	0.310	500	96.2	1298.4
		T50W1C1.6	1600	40	1600	1	40	40	400	400	0	0	0	0	0	0	$t/6$	1	0.310	500	0.310	500	50.3	1030.1
		T70W1C1.6	1600	40	1600	1	40	40	400	400	0	0	0	0	0	0	$t/6$	1	0.310	500	0.310	500	75.1	1390.6

		T90W1C1.6	1600	40	1600	1	40	40	400	400	0	0	0	0	0	0	*t*/6	1	0.310	500	0.310	500	93.6	1583.3
		T50W2C1.2	1200	40	1200	1	30	30	300	300	−250	0	300	300	250	0	*t*/6	1	0.310	500	0.310	500	50.3	618
		T70W2C1.2	1200	40	1200	1	30	30	300	300	−250	0	300	300	250	0	*t*/6	1	0.310	500	0.310	500	74.1	633.4
		T90W2C1.2	1200	40	1200	1	30	30	300	300	−250	0	300	300	250	0	*t*/6	1	0.310	500	0.310	500	97.1	665.1
		T45W2C1.4	1400	40	1400	1	35	35	350	350	−292	0	350	350	292	0	*t*/6	1	0.310	500	0.310	500	45.5	662.2
		T90W2C1.4	1400	40	1400	1	35	35	350	350	−292	0	350	350	292	0	*t*/6	1	0.310	500	0.310	500	95.1	918.2
		T95W2C1.4	1400	40	1400	1	35	35	350	350	−292	0	350	350	292	0	*t*/6	1	0.310	500	0.310	500	80	759.9
		T50W2C1.6	1600	40	1600	1	40	40	400	400	−333	0	400	400	333	0	*t*/6	1	0.310	500	0.310	500	50.3	647.5
		T70W2C1.6	1600	40	1600	1	40	40	400	400	−333	0	400	400	333	0	*t*/6	1	0.310	500	0.310	500	75.1	988.8
		T90W2C1.6	1600	40	1600	1	40	40	400	400	−333	0	400	400	333	0	*t*/6	1	0.310	500	0.310	500	94.2	1236.1
		T65W1W1.2	1200	40	1200	1	30	30	300	600	0	0	0	0	0	0	*t*/6	1	0.310	500	0.310	500	56.4	682.2
		T65W1L1.2	1200	40	1200	1	30	30	300	300	−250	0	0	0	0	0	*t*/6	1	0.310	500	0.310	500	65	737.5
		T65W1U1.2	1200	40	1200	1	30	30	300	300	−250	150	0	0	0	0	*t*/6	1	0.310	500	0.310	500	62.4	715.7
		T65D1C1.2	1200	40	1200	1	30	30	750	300	0	−225	0	0	0	0	*t*/6	1	0.310	500	0.310	500	65	676.9
		T65D1L1.2	1200	40	1200	1	30	30	750	300	−250	−225	0	0	0	0	*t*/6	1	0.310	500	0.310	500	56.4	582.7
		T65W1SB1.2	1200	40	1200	1	30	30	240	240	0	−120	0	0	0	0	*t*/6	1	0.310	500	0.310	500	62.4	794.6
		T65W1SL1.2	1200	40	1200	1	30	30	240	240	120	0	0	0	0	0	*t*/6	1	0.310	500	0.310	500	56.4	721
Mohammed et al. [4]	OW	WO1	800	50	400	2	16	8	170	95	0	0	0	0	0	0	*t*/6	1	0.400	478	0.700	478	16.9	210
		WO2	800	50	400	2	16	8	240	135	0	0	0	0	0	0	*t*/6	1	0.400	478	0.700	478	17.7	203.8
		WO3	800	50	400	2	16	8	340	185	0	0	0	0	0	0	*t*/6	1	0.400	478	0.700	478	18.4	179.8
		WO4	800	50	400	2	16	8	420	230	0	0	0	0	0	0	*t*/6	1	0.400	478	0.700	478	19.8	172.8
		WO1a	800	40	400	2	20	10	170	95	0	0	0	0	0	0	*t*/6	1	0.500	478	0.900	478	16	100
		WO2a	800	40	400	2	20	10	240	135	0	0	0	0	0	0	*t*/6	1	0.500	478	0.900	478	13.9	95.3
		WO3a	800	40	400	2	20	10	340	185	0	0	0	0	0	0	*t*/6	1	0.500	478	0.900	478	15.6	85
		WO4a	800	40	400	2	20	10	420	230	0	0	0	0	0	0	*t*/6	1	0.500	478	0.900	478	15.8	73.7

References

[1] Dol K, Haffner M. Housing Statistics in the European Union 2010. Delft University of Technology, Netherlands: OTB Research Institute for the Built Environment; 2010.
[2] Seddon AE. The strength of concrete walls under axial and eccentric loads. In: Andrew RP, editor. Symposium on the strength of concrete structures. London, UK: Cement and Concrete Association; 1956. p. 445–86.
[3] Demeter I. Seismic retrofit of precast RC walls by externally bonded CFRP composites. Romania: PhD Thesis, Politehnica University of Timisoara; 2011.
[4] Mohammed B, Ean LW, Malek MA. One way RC wall panels with openings strengthened with CFRP. Constr Build Mater 2013;40:575–83.
[5] Engel P. General rehabilitation techniques using steel. <http://www.constructalia.com/english/renovation_with_steel/ii_general_rehabilitation_techniques_using_steel#.VMPsNP6G9Wg> [accessed 01.23.15]
[6] Delatte N. Failure, distress and repair of concrete structures. Woodhead Publishing; 2009.
[7] Bakis CE, Bank LC, Brown VL, Cosenza E, Davalos JF, Lesko JJ, et al. Fiber-reinforced polymer composites for construction – state-of-the-art review. J Compos Constr 2002;6:73–87.
[8] Van Den Einde L, Zhao L, Seible F. Use of FRP composites in civil structural applications. Constr Build Mater 2003;17:389–403.
[9] Hollaway LC, Hollaway LC. A review of the present and future utilisation of FRP composites in the civil infrastructure with reference to their important in-service properties. Constr Build Mater 2010;24:2419–45.
[10] Täljsten B, Blanksvärd Thomas, Sas G. FRP strengthening of existing concrete structures. Design guideline (in Swedish). Luleå, Sweden: Luleå University of Technology, Division of Structural Engineering; 2012.
[11] ACI318. Building code requirements for structural concrete and commentary (ACI 318–11). Farmington Hills: AMERICAN CONCRETE INSTITUTE; 2011. p. 503.
[12] AS3600. Concrete structures. Sydney, Australia: Standards Australia; 2009.
[13] CAN/CSA-A23.3. Design of concrete structures. Mississauga, Ontario: CANADIAN STANDARDS ASSOCIATION; 2004.
[14] EN 1992-1-1. Eurocode 2: design of concrete structures – Part 1–1: General rules and rules for buildings. Brussels: COMITÉ EUROPÉEN DE NORMALISATION; 2004.
[15] Pillai SU, Parthasarathy CV. Ultimate strength and design of concrete walls. Build Environ 1977;12:25–9.
[16] Sanjayan JG, Maheswaran T. Load capacity of slender high-strength concrete walls with side supports. ACI Struct J 1999;96:571–6.
[17] Robinson G, Palmeri A, Austin S. Design methodologies for one way spanning eccentrically loaded minimally or centrally reinforced pre-cast RC panels. Eng Struct 2013;56:1945–56.
[18] Saheb SM, Desayi P. Ultimate strength of RC wall panels with openings. J Struct Eng-Asce 1990;116:1565–78.
[19] Saheb SM, Desayi P. Ultimate strength of R.C. wall panels in two-way in-plane action. J Struct Eng-Asce 1990;116:1384–402.
[20] Doh JH, Fragomeni S. Evaluation of experimental work on concrete walls in one-way and two-way action. Aust J Struct Eng 2005;6:37–52.
[21] Swartz SE, Rosebraugh VH, Rogacki SA. A method for determining the buckling strength of concrete panels. Exp Mech 1974;14:138–44.
[22] Saheb SM, Desayi P. Ultimate strength of RC wall panels in one-way in-plane action. J Struct Eng-Asce 1989;115:2617–30.
[23] Ganesan N, Indira PV, Rajendra Prasad S. Strength and behavior of SFRSCC and SFRC wall panels under one-way in-plane action. In: Parra-Montesinos G, Reinhardt H, Naaman AE, editors. High performance fiber reinforced cement composites 6. Netherlands: Springer; 2012. p. 279–86.
[24] Ganesan N, Indira PV, Santhakumar A. Prediction of ultimate strength of reinforced geopolymer concrete wall panels in one-way action. Constr Build Mater 2013;48:91–7.
[25] El-Metwally S, Ashour F, Chen W. Instability analysis of eccentrically loaded concrete walls. J Struct Eng-Asce 1990;116:2862–80.
[26] Doh JH, Loo YC, Fragomeni S. Concrete walls with and without openings supported on three sides. In: Sam Fragomeni SV, Lam Nelson TK, Setunge Sujeeva, editor. Incorporating sustainable practice in mechanics and structures of materials. Taylor & Francis Group; 2010. p. 209–14.
[27] Doh JH, Fragomeni S. Ultimate load formula for reinforced concrete wall panels with openings. Adv Struct Eng 2006;9:103–15.
[28] Fragomeni S, Doh JH, Lee DJ. Behavior of axially loaded concrete wall panels with openings: an experimental study. Adv Struct Eng 2012;15:1345–58.
[29] Fragomeni S, Mendis PA, Grayson WR. Axial load tests on normal and high strength concrete wall panels. Transact Institut Eng, Austr/CE 1994;36:257–63.
[30] Larsson L-E. Bearing capacity of plain and reinforced concrete walls [PhD Thesis]. Göteborg: Chalmers Tekniska Högskola; 1959.
[31] Fragomeni S, Mendis P. Instability analysis of normal- and high-strength reinforced-concrete walls. J Struct Eng 1997;123:680–4.
[32] Mattock AH, Kriz LB, Hognestad E. Rectangular concrete stress distribution in ultimate strength design. ACI Struct J 1961;57:875–928.
[33] Macgregor JG, Breen JE, Pfrang EO. Design of slender concrete columns. ACI Struct J 1970;67:6–28.
[34] Parme AL. Capacity of restrained eccentrically loaded long columns. Symposium of reinforced concrete columns SP-13, American Concrete Institute; 1966. p. 325–67.
[35] Kripanarayanan KM. Interesting aspect of the empirical wall design equation. ACI Struct J 1977;74:204–7.
[36] Leabu VF. Problems and performances of precast concrete wall panels. ACI Struct J 1959;56:287–98.
[37] Oberlender GD, Everard NJ. Investigation of reinforced concrete walls. ACI Struct J 1977;74:256–63.
[38] Zielinski ZA, Troitsky MS, Christodoulou H. Full-scale bearing strength investigation of thin wall-ribbed reinforced concrete panels. ACI Struct J 1982;79:313–21.
[39] ACI Committee 318. Building code requirements for reinforced concrete (ACI 318–77). Detroit: American Concrete Institute; 1977.
[40] Doh JH. Experimental and theoretical studies of normal and high strength concrete wall panels. Australia: PhD Thesis, Griffith University; 2002.
[41] BS8110-1997. Structural use of concrete, Part 1 – Code of practice for Design and Construction. London: British Standards Institution; 1997.
[42] Hegger J, Dressen T, Will N. Load-bearing capacity of plain concrete walls. Mag Concr Res 2009;61:173.
[43] Haller P. Load capacity of brick masonry. Designing. Engineering and constructing with masonry products ed. Houstion, TX, USA: Gulf Publishing; 1969.
[44] Gere JM, Timoshenko SP. Mechanics of materials. 3rd ed. Massachusetts, USA: PWS-KENT; 1990.
[45] Robinson G, Palmeri A, Austin S. Implications of EC2 on the design of simply supported precast RC panels under eccentric axial load. In: Proceedings of fib symposium on concrete engineering for excellence and efficiency; 2011.
[46] Macgregor JG, Simmonds SH, Warwaruk J. Seminar on building code requirements, ACI318-71. University of Alberta, Department of Civil Engineering, Structural engineering report no. 36; 1971.
[47] Westerberg B. Load bearing capacity of unreinforced walls. Second International Workshop in DESIGN OF CONCRETE STRUCTURES AND BRIDGES USING EUROCODES. Bratislava, Slovakia: Slovak University of Technology in Bratislava, Faculty of Civil Engineering; 2011.
[48] Fragomeni S. Review of reinforced concrete wall design formulas. ACI Struct J 1994;91:521–9.
[49] Timoshenko SP, Gere JM. Theory of elastic stability. New York: McGRAW-HILL International Book Co.; 1961.
[50] Aghayere AO, MacGregor JG. Analysis of concrete plates under combined in-plane and transverse loads. ACI Struct J 1990;87:539–47.
[51] Fragomeni S, Mendis P. Improved axial load formulae for normal and high strength reinforced concrete walls. Aust Civ Eng 1996;38:71–81.
[52] Fragomeni S. Design of normal and high strength reinforced concrete walls. Australia: PhD Thesis, University of Melbourne; 1995.
[53] Chen WF, Atsuta T. Strength of eccentrically loaded walls. Int J Solids Struct 1973;9:1283–300.
[54] Kirtschig K, Anstötz W. Knickuntersuchungen an Mauerwerksprosben. In: Proceedings of the 9th international brick/block masonry conference. Berlin: Deutsche Gesellschaft für Mauerwerksbau e.V., Bonn, Germany; 1991. p. 202–9.
[55] Glock C. Traglast unbewehrter Beton- und Mauerwerkswände. TU Darmstadt: Institute for Concrete and Masonry Structures; 2004.
[56] fib Model Code 2010. fib Model Code 2010 for Concrete Structures. Lausanne, Switzerland: Fédération Internationale du Béton; 2013.
[57] EN 1990. Eurocode 0: Basis of structural design. Brussels: COMITÉ EUROPÉEN DE NORMALISATION; 2004.
[58] Lee D-J. Experimental and theoretical study of normal and high strength concrete wall panels with openings. Australia: PhD Thesis, Griffith University; 2008.
[59] Guan H, Cooper C, Lee D-J. Ultimate strength analysis of normal and high strength concrete wall panels with varying opening configurations. Eng Struct 2010;32:1341–55.
[60] Antoniades K, Salonikios T, Kappos A. Tests on seismically damaged reinforced concrete walls repaired and strengthened using fiber-reinforced polymers. J Compos Constr 2005;9:236–46.
[61] Dan D. Experimental tests on seismically damaged composite steel concrete walls retrofitted with CFRP composites. Eng Struct 2012;45:338–48.
[62] Li B, Lim C. Tests on seismically damaged reinforced concrete structural walls repaired using fiber-reinforced polymers. J Compos Constr 2010;14:597–608.
[63] Li B, Qian K. Retrofitting earthquake-damaged RC structural walls with openings by externally bonded FRP strips and sheets. J Compos Constr 2013;17:259–70.
[64] Todut C, Dan D, Stoian V. Numerical and experimental investigation on seismically damaged reinforced concrete wall panels retrofitted with FRP composites. Compos Struct 2015;119:648–65.
[65] El Maaddawy T, Sherif S, El Maaddawy T, Sherif S. FRP composites for shear strengthening of reinforced concrete deep beams with openings. Compos Struct 2009;89:60–9.
[66] Enochsson O, Lundqvist J, Taljsten B, Rusinowski P, Olofsson T. CFRP strengthened openings in two-way concrete slabs – an experimental and numerical study. Constr Build Mater 2007;21:810–26.
[67] Floruţ S-C, Sas G, Popescu C, Stoian V. Tests on reinforced concrete slabs with cut-out openings strengthened with fibre-reinforced polymers. Compos Part B – Eng 2014;66:484–93.

Paper II

The Development of an Experimental Program through Design of Experiments and FEM Analysis: A Preliminary Study

Cosmin Popescu, Gabriel Sas

Published in:

Nordic concrete Research

Vol. 51, December 2014, pp. 29-42

The Development of an Experimental Program through Design of Experiments and FEM Analysis: A Preliminary Study

Cosmin Popescu
M.Sc., Ph.D. Student
NORUT, Rombaksveien E-6 47, N-8517 Narvik, Norway
Department of Infrastructure Structures and Materials
E-mail: cosmin.popescu@norut.no

Gabriel Sas
Ph.D., Assistant Lecturer
Luleå University of Technology, Department of Structural Engineering
SE – 971 87 Luleå, Sweden
E-mail: gabriel.sas@ltu.se

ABSTRACT

This paper presents an experimental test setup which allows investigation of the structural behaviour for axially loaded concrete walls with openings. The test matrix was developed with the help of design of experiments technique. A two-level factorial experiment has been designed resulting in a total of nine wall specimens. Previous research has shown that the ultimate capacity of concrete walls is dependent on the boundary conditions. Therefore, a new test-rig was proposed and designed to work according to the imposed conditions. Nonlinear simulations calibrated on a previous experimental program were used to obtain the reaction forces.

Key words: Concrete walls, openings, design of experiments, FEM, strengthening, test setup

1. INTRODUCTION

In Europe the majority of concrete structures were built before 1970 [1]. These structures are continuously degrading and the need of repair increases exponentially. This increase is closely connected to worldwide population growth, so that new structures are being built and existing structures still need to be used. Replacement is a typical solution for old structures or structures that do not fulfil anymore their intended purpose, however this process requires extended financial effort and is not environmentally friendly.

The following are the main reasons for the need of repair, rehabilitation and strengthening of existing RC structures:

- New design standards are imposed so that the demands of the society regarding structural safety, exploitation and aesthetics can be accommodated
- Changes in use or imposed loading
- Structures are continuously ageing due to material degradation and external environment
- Construction errors are still encountered due to human error

- Conscious human intervention to provide new functionality to a structure requires removing structural elements or creating new openings
- Special events such as accidental explosions and natural disasters

The current project deals with the common situation when new openings are required in existing reinforced concrete (RC) walls due to changing the functionality of the building. In recent years there has been increasing interest in creating large spaces by connecting adjacent rooms through a newly created opening in an existing solid wall. The creation of these openings in walls will change the stress distribution and adversely influence the behaviour of the wall, [2, 3], thus a strengthening of the structure is imposed to recover the initial structural capacity.

There are two traditional methods for strengthening RC walls with openings: (1) creating a frame around the opening using RC/steel frame systems, and (2) increasing the cross section thickness. These methods will increase the weight of the strengthened elements and may create major discomfort by drastically limiting the use of structure during repairs. A better alternative is the use of fiber reinforced polymers (FRP) as externally bonded reinforcement, method that has received worldwide acceptance during the last two decades [4, 5]. This technique implies that thin sheets or plates are bonded to the surface of the structure through an adhesive, so that a composite material is formed. Successful applications of FRP to strengthen openings in structural elements were achieved by several researchers [3, 6, 7].

The research performed on RC walls with openings [8-11] focused on elements designed as if the opening has been initially planned, whereas RC wall panels with cut-out openings is still unexplored. The case when axially loaded RC walls are strengthened by FRP components is still at an incipient level; to the best knowledge of the authors only one study, [3], was performed so far. Mohammed et al. [3] found that the presence of the opening in a solid one-way panel lead to disturbance zones. The discontinuities causing high stresses will force the cracks firstly occur at the corners due to insufficient internal reinforcement. It was concluded that applying FRP around the opening in different patterns, the capacity could be improved by reducing the principal stresses acting on the upper corners of the opening.

A research program is undergoing at Luleå University of Technology where a number of concrete walls with different parameters will be tested. This paper presents the process of defining an experimental program able to describe the structural behaviour of FRP-strengthened walls with cut-out openings. The experimental research found in the available literature was carried out on limited number of tests using customized test-setups because of lack of standardized procedures for testing walls and walls with openings. Therefore, the aim of this study is to investigate how an experimental program can be defined comprehensively using statistical tools and numerical modelling. The type of elements and test procedure, are identical with the ones studied by Lee [12].

The following two objectives were set: (1) determine the number of the specimens to be tested using design of experiments (DOE) technique and (2) propose a new test-rig for laboratory testing based on an accurate finite element modelling (FEM) and comparison with experimental results presented by Lee [12].

2. DESIGN OF EXPERIMENTS

2.1 Theory

A methodology for designing experiments was first proposed by Fischer [13] and is referred in the literature as design of experiments (DOE). The method uses statistical tools to analyse data and predict the system performance [14]. DeCoursey [15] showed that one-factor-at-a-time design would not give precise information about the interaction, and the results from that plan of experimentation might be misleading. Thus, a better alternative is to conduct tests by combining different levels of the factors, which is called a factorial design. By choosing a number of parameters and a fixed number of levels, experiments should be performed with all possible combinations. The entire process for a successful design of experiments is shown in Figure 1.

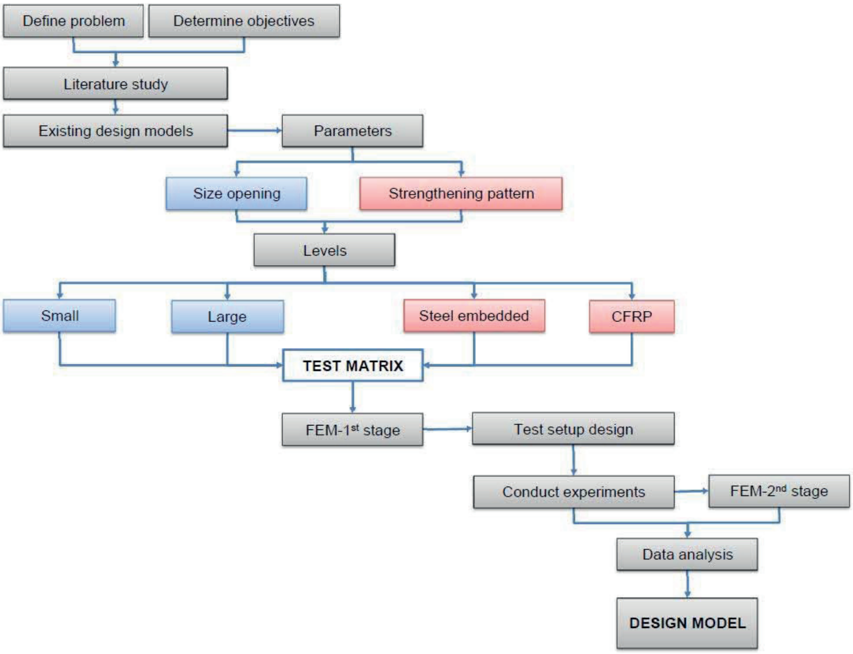

Figure 1 – Development of a design of experiment application

2.2 Proposed experimental program

The parameters that can have a high influence on the axial load capacity of RC walls with openings were identified by studying different models available in the literature. Several models for predicting the axial capacity of RC walls with openings were identified. Among these, the latest formula (Eq. 1) proposed by Doh and Fragomeni [8] was found to give satisfactory results [16]. In equation (1), N_u represents the axial capacity of an identical panel without openings, k_1 and k_2 are constants derived using a standard regression analysis and the factor χ incorporate the effect of the size and location of the opening in the wall.

$$N_{uo} = \left(k_1 - k_2\chi\right) N_u \tag{1}$$

Parameters like eccentricity, side supports, slenderness, aspect ratio and reinforcement ratio have also influence on the ultimate axial strength of a solid RC wall. These parameters have been studied in the past [17-20], thus being out of scope for this experimental program. According to the theory behind factorial design, past experience should contribute in choosing the right parameters to be varied at maximum of two levels. Based on the results from the first stage of experiments (see Figure 1), further tests can be designed logically and may well involve more than two levels for some parameters. Box et al. [21] introduced “the 25% rule” in which not more than one quarter of the budget should be spent in an initial design. Based on the first observations one can run countless experiments for different levels by using computer modelling.

The first set of analyses examines the impact of two parameters: (1) openings size and (2) strengthening pattern. For the first parameter small (S) and large (L) opening will be set as the min/max level and for the second one: (a) steel reinforcement bars embedded into concrete and placed around corners at 45° as it has been initially designed (st) and (b) externally bonded (EB) and near surface mounted (NSM) FRP reinforcement (frp). Consequently, this will require 2^2 different experiments for a complete factorial design. The two levels of these two parameters are presented in Table 1. Besides these tests another three specimens (i.e. wall with and without cut-out openings) used as references will be tested until failure to assess the effectiveness of strengthening alternative. An important factor in experiments, namely replication, would be kept at low level since large elements like walls involve many resources. That means only two identical specimens from those strengthened with FRP will be cast and for the rest of them only one specimen. The tests designed based on the DOE technique are shown in Figure 2.

Table 1 – Level of parameters

Designation	1st parameter [*opening size*]	2nd parameter [*strengthening pattern*]	Description	No. of tests
WSO-st	S	St	Small opening strengthened with steel reinforcement	1
WSO-frp	S	Frp	Small opening strengthened with FRP	2
WLO-st	L	St	Large opening strengthened with steel reinforcement	1
WLO-frp	L	Frp	Large opening strengthened with FRP	2
WSO	S	-	Weakened by small opening	1
WLO	L	-	Weakened by large opening	1
RCW	-	-	Solid slab (without opening)	1

Nine half scale specimens L=1800 mm (length), H=1350 mm (height) and t=60 mm (thickness) resulted from this plan of experimentation having an aspect ratio (H/L), slenderness ratio (H/t) and thickness ratio (L/t) of 0.75, 22.5 and 30, respectively. The cut-outs will represent a door opening centrally placed with 450x1050 mm and 900x1050 mm dimensions for small and large opening, respectively. A concrete with a maximum aggregate size of 16 mm and a C25/30 concrete strength class is used to cast the specimens. The walls are regarded as plain concrete walls in EN 1992-1-1 [22], however, a minimum amount of steel reinforcement are used for durability purposes and to avoid cracks due to creep and shrinkage. The steel ratio was set to 0.3% centrally placed in one layer. An amount of reinforcement equivalent to that interrupted by an opening has to be added at 45° around corners for those elements intended to be strengthened with embedded steel reinforcement. For specimens FRP-strengthened, NSM bars at 45° will be mounted around corners and EBR sheets surrounding the cut-out opening.

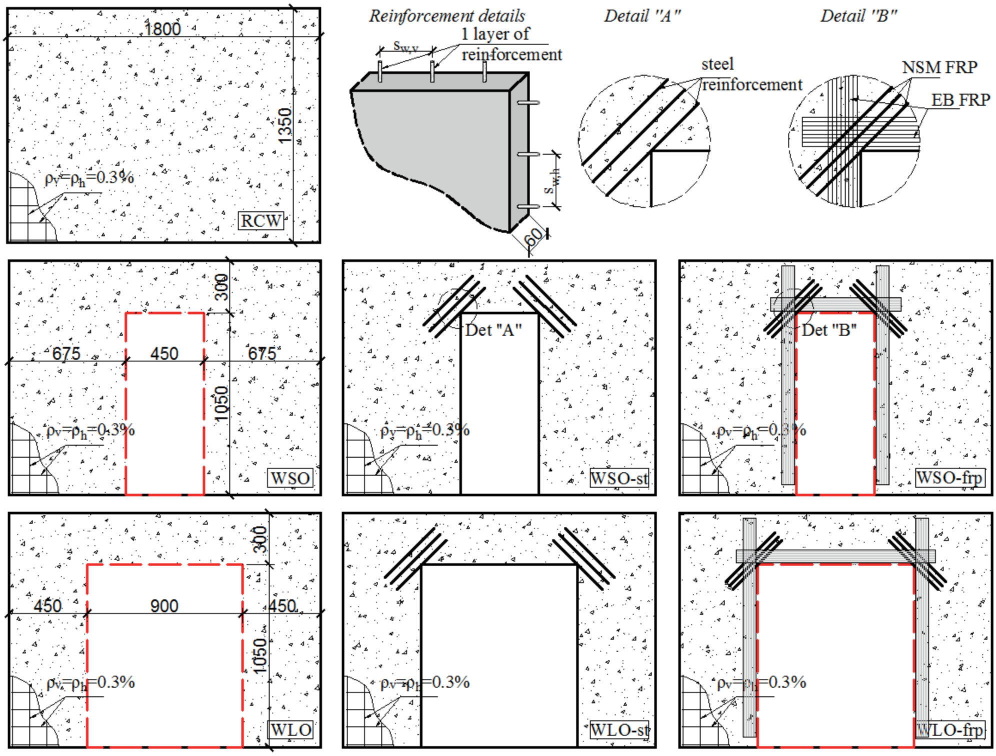

Figure 2 – Details of the specimens

Finally, as soon as the data from the experiments is collected, statistical techniques are used to analyse the data. With the use of computer programs, e.g. MiniTab. [23], the interaction between different parameters and the level for which a parameter plays a significant role could be determined. Moreover, the software is able to plot a model equation that can describe the response of the system.

3. BENCHMARK STUDY

3.1 Summary of the tests performed by Lee [12]

Lee [12] preformed an experimental study on the behaviour of RC walls with openings. The study consisted of forty seven half-scale panels tested in one-way and two-way action. The tested walls had different opening configurations and slenderness ratios and subjected to a uniformly distributed load acting with an eccentricity of one sixth of the wall thickness. The specimens were loaded in increments of 14.7 kN until failure. Ultimate load, deflections and crack pattern were recorded and will be used to compare them with results from the numerical analysis.

Two wall specimens were chosen to be modelled and calibrate the FE-model against them. The window-type openings were symmetrically placed in both one-way (O45W1C1.4) and two-way

(T45W1C1.4) action walls. The wall specimens were reinforced with a single layer of steel bars centrally placed, satisfying the minimum requirements in the AS3600 [24]. The vertical and horizontal reinforcement ratios, ρ_v and ρ_h, were 0.31% with the minimum tensile strength of 500 MPa. To prevent early cracking around openings, three diagonal bars were placed in each corner. The average concrete compressive strengths, f_{cm}, have been determined based on concrete cylinder tests. For O45W1C1.4 wall, the average compressive strength was 32 MPa while for T45W1C1.4 the average compressive strength was 45.5 MPa, determined at day of testing.

The general dimensions of the wall specimen and reinforcement layout are shown Figure 3a. The thickness of the tested element was 40 mm thus, the specimen having both slenderness and thickness ratio equal to 35. These dimensions are identical for both walls, the only difference being in the support conditions, i.e. fixed on two opposite sides (one-way) or on all sides (two way).

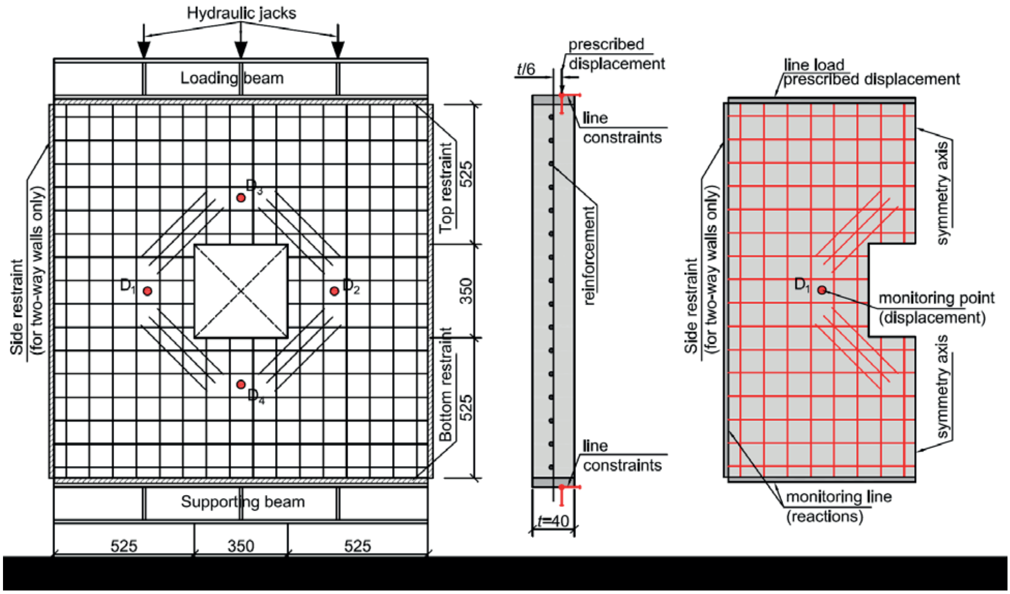

Figure 3 – Details of the test specimen: a) test setup adapted from Lee [12] and b) simplified numerical model

3.2 FE – model

A three-dimensional nonlinear FE-model has been created using ATENA-Science [25] software in order to capture the behaviour of axially loaded RC walls. An iterative solution procedure based on the Newton-Raphson method was adopted in the FEM simulation.

3.3 Material's constitutive laws

Concrete

The material-model used is a fracture-plastic model that combines constitutive models for tensile (fracture) and compressive behaviour (plastic) [26]. Orthotropic smeared crack model based on Rankine tensile criterion is used for concrete cracking while for concrete crushing the yield surface proposed by Menetrey and Willam [27] was employed. The fracture and plastic models are combined together using the strain decomposition method first introduced by De Borst [28] through a return mapping algorithm. The response of the un-cracked material is assumed to be linear-elastic up to peak values of stress in tension, f_t, with E_c the initial elastic modulus of concrete. At this state, the corresponding strain is $\varepsilon_0 = f_t / E_c$. After the tension strength was reached, the stress-strain law of concrete in tension follows a descending branch known as tension softening. The tension softening curve drop exponentially to zero if no tension stiffening effects would be considered, as it is considered in the present case-study.

The tension after cracking is represented by a fictitious crack model based on a crack-opening law and fracture energy in combination with the crack band approach (Figure 4). In the present study fixed crack model was chosen although the software offers the choice of rotated crack model also. The function of crack opening was proposed by Reinhardt et al. [29] and given by Eq. 2:

$$\sigma_t = f_t \left\{ \left[1 + \left(c_1 \frac{w}{w_c} \right)^3 \right] \exp\left(-c_2 \frac{w}{w_c} \right) - \frac{w}{w_c} \left(1 + c_1^3 \right) \exp\left(-c_2 \right) \right\} \qquad (2)$$

where, w is the crack opening, w_c is the crack opening at the complete release of stress, σ is the normal stress in the crack, c_1=3 and c_2=6.93 are material constants valid for normal-weight concrete.

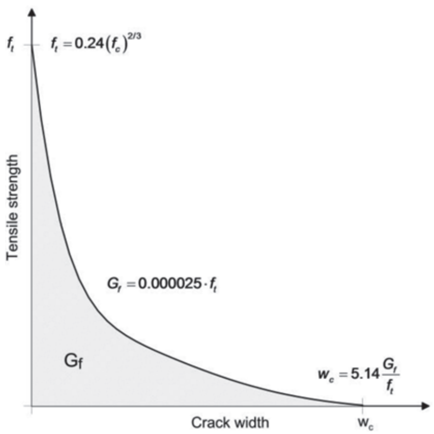

Figure 4 – Exponential crack opening law

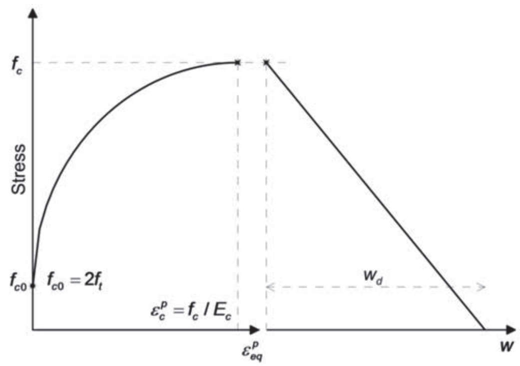

Figure 5 – Hardening/softening laws for concrete in compression

The shape function of the concrete in compression is based on work of van Mier [30]. The hardening law for concrete in compression is elliptical (Eq. 3) and based on strains. The softening law in compression is linearly descending with the end point of the curve defined by means of the plastic displacement w_d, to avoid mesh dependency. The plastic displacement was set to w_d=0.5mm as suggested from experiments of van Mier [30].

$$\sigma_c = f_{c0} + \left(f_c - f_{c0}\right)\sqrt{1-\left(\frac{\varepsilon_c - \varepsilon_c^p}{\varepsilon_c}\right)^2} \tag{3}$$

where, f_{c0} is the onset of nonlinear behaviour, f_c is the compressive strength of concrete, ε_c^p is the plastic strain at compressive strength.

The constitutive model for concrete requires as input important data such as the modulus of elasticity E_c, the tensile strength f_t, and fracture energy G_f. The values from Table 2, evaluated based on the average compression strength f_{cm}, were used in the numerical analysis.

Table 2 – Properties of the concrete material used in FEM analysis

Parameter	Equation	Reference
Elastic modulus [MPa]	$E_c = \left(6000 - 15.5 f_c\right)\sqrt{f_c}$	[31]
Tensile strength [MPa]	$f_t = 0.24 f_c^{2/3}$	[31]
Fracture energy (MN/m)	$G_f = 0.000025 f_t$	[32]

Reinforcement

The reinforcement was modelled as discrete bars using 2D isoparametric truss elements perfectly bonded to the concrete body. The elastic-perfectly plastic (i.e without hardening) behaviour was considered in the analysis with a default value for steel elasticity modulus of E_s = 200 GPa.

3.4 Geometry and boundary conditions

To take advantage of the symmetry of the walls and save processing time, only one half of each model was modelled as shown in Figure 3b. In order to avoid numerical problems due to high stresses concentrations, linear elastic steel plates were added to the model between element edges and the loading points. The load was applied as imposed deformations along the top of the specimens to assure a uniformly distributed load. A load eccentricity of t/6 that would cause an out-of-plane deflection of the wall was included in the analysis.

Displacements were monitored at the same locations where the LVDTs were installed on the tested walls. The ultimate capacity of the specimen was computed by monitoring the line reactions at the bottom of the specimen.

3.5 Element size and mesh sensitivity analysis

Different element types were investigated in order to find suitable elements to simulate the behaviour of slender RC walls with openings. ATENA software offers the possibility to model this problem using shell or solid elements. The concrete element was modelled by 8-nodes brick elements. A mesh sensitivity analysis was undertaken on the control specimens for three different sizes of the finite element per thickness, i.e. 15 mm, 10 mm and 5 mm, respectively.

The element size considered was 10 mm since it provided good results in terms of accuracy and computational time.

4. FE – MODEL VALIDATION

The experimental and numerical load–displacement responses are compared to validate the accuracy of the model proposed and are shown in Figure 6. The ratio between ultimate capacity of experimental and numerical analysis are also shown in Figure 6. Moreover, the crack pattern and the failure mode observed in tests were compared with the one obtained from FEM and shows a good correlation as can be seen from Figure 7 and Figure 8.

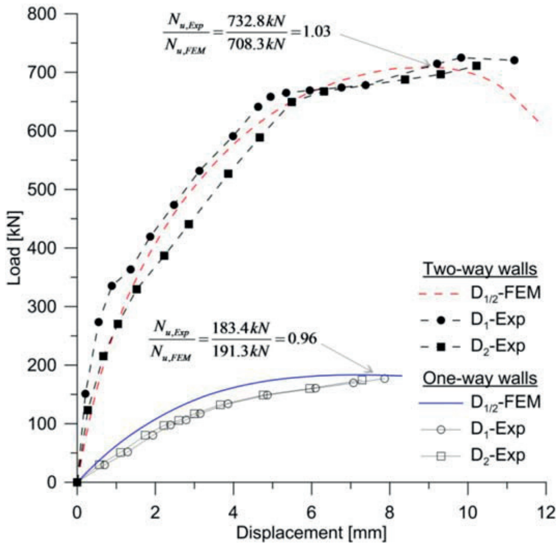

Figure 6 – Load-displacement response: experimental vs. FEM

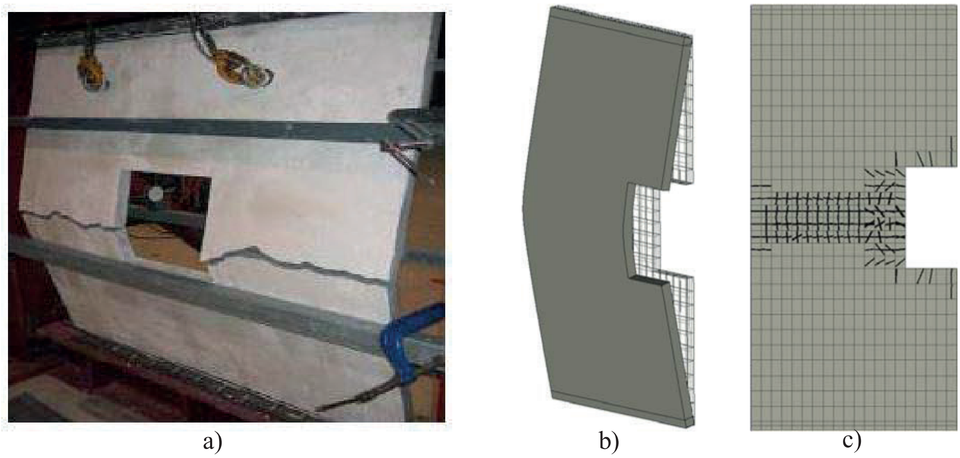

Figure 7 – Crack pattern and failure mode for one-way walls: a) experimental [12]; b) deformed shape - FEM; c) crack pattern - FEM

5. TEST-RIG DESIGN FOR RC WALLS

5.1 Design principles

In practice, the gravitationally loaded walls behave under one-way or two-way action. Walls restrained along top and bottom edges of the wall are denoted as one-way action panels. These panels are developing a single out-of-plane curvature parallel with the load direction and are usually encountered in prefabricated tilt-up concrete structures. Panels restrained along three or all sides are denoted as two-way action panels. The walls in this case deflect in double curvature, in both horizontal and vertical directions, and are usually encountered in monolithic concrete structures. Since the two-way walls are the most encountered in practice and are studied to the same extent as one-way walls, in this study was decided to go further and develop a test-rig who can replicate the boundary conditions met in reality for this kind of walls.

The following assumptions were used for designing the test-rig:

(a) the test-rig has to simulate hinged connections at the boundaries of the specimen;
(b) sufficient rigidity of the lateral edges is needed to prevent any out-of-plane deformations;
(c) the walls are loaded gravitationally with a small eccentricity (one sixth of the wall thickness) to simulate the effect of imperfections;
(d) the design was carried out for the strongest element, i.e. RCW (solid wall).

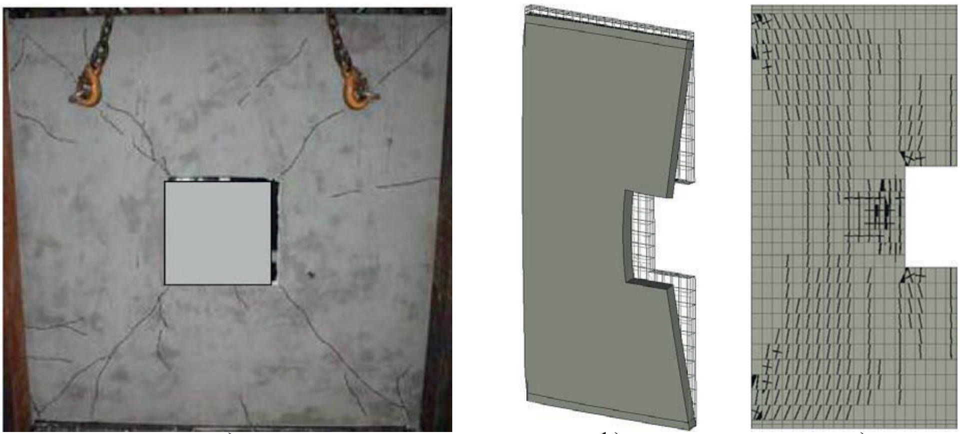

a) b) c)

Figure 8 – Crack pattern and failure mode for two-way walls: a) experimental [12]; b) deformed shape - FEM; c) crack pattern - FEM

5.2 Load reactions and element's design

Considering the good agreement with the experimental results, the FEM model proposed was used to predict the ultimate capacity of the strongest wall, i.e. RCW wall from the matrix proposed (see Figure 2). The ultimate capacity obtained from FEM analysis was 1797 kN. This value was used to find out the required number of the hydraulic actuators. The concentrated force from the actuators was considered to be redistributed through the loading beam with a slope of 1:1 in order to obtain a uniformly distributed load along the wall length. Four hydraulic actuators of 600 kN each were necessary to be above the force obtained from FEM.

By loading to failure the solid wall, the reaction forces acting on the members who simulate the boundary conditions of the specimen were also monitored in FEM model. The reactions at the bottom of the specimen were constant along its length and were used to design the supporting beam. The beam was designed as continuously supported on a strong floor. Reactions along lateral edges of the specimen were used in designing the lateral bracing system of the test rig. Besides some high values at the end of the wall, constant forces acting on the members restraining the specimen from out-of-plane deflections were observed. These reactions were used as input for the simple static system created (see Figure 9) in which both stresses and displacements were checked. All reactions obtained from FEM analysis were multiplied by a factor of 1.4 to cover the difference between the ultimate capacity of the solid wall and the available pressure given by the actuators (see Figure 10).

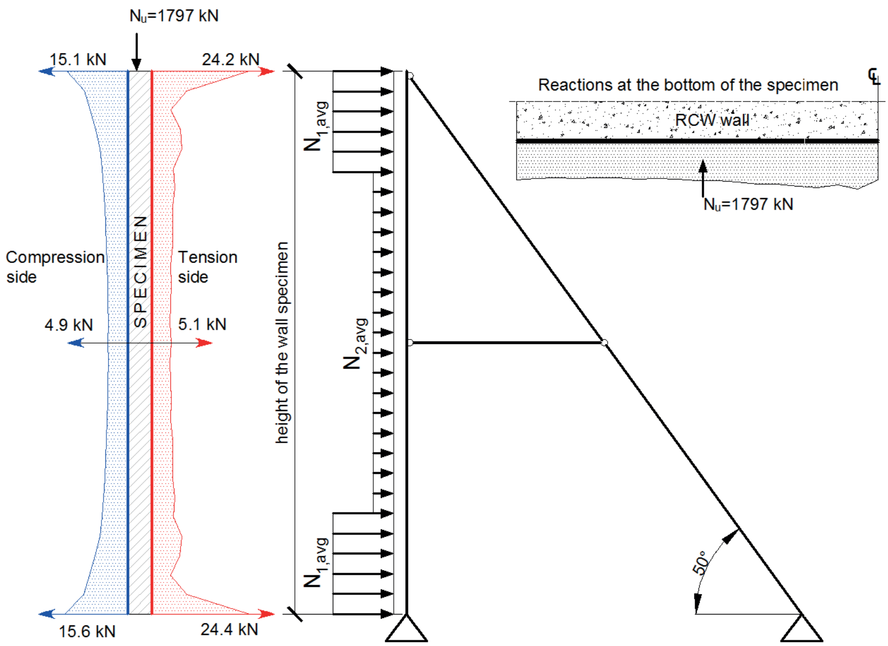

Figure 9 – Load reactions acting on the test rig and its static system

Figure 10 shows the general view of the test-rig with all details. The hinge at the top support is created by the steel rod placed on a thick steel plate along the element edges. In this way the desired eccentricity can also be precisely applied. The wall specimens were restrained along their sides using either equal or unequal leg angles steel profiles.

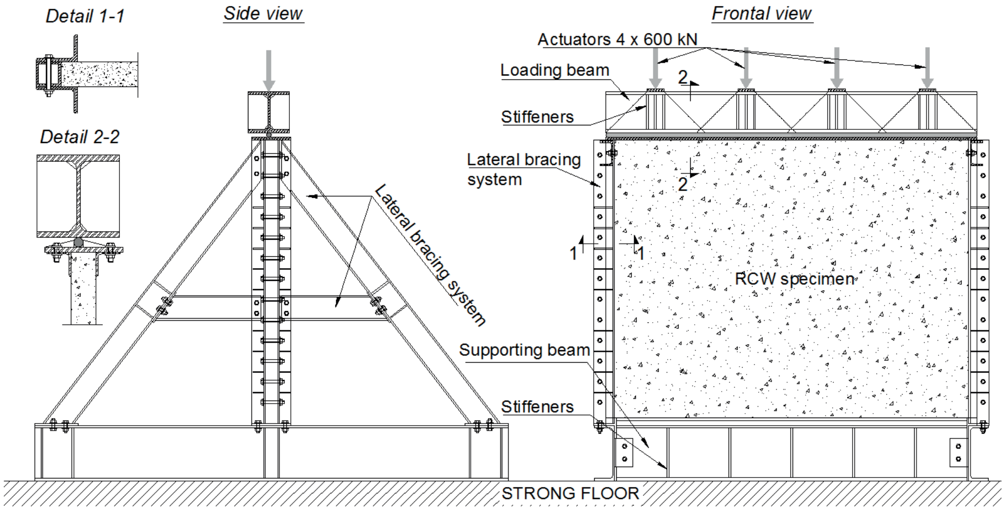

Figure 10 – General view of the test-rig proposed

6. CONCLUSIONS

There are no standardized procedures for testing concrete walls; therefore each experimental programme requires customized design. The experimental program presented in this paper was conceived in accordance with DOE technique. This method has been demonstrated to be a reliable method for research investigations in areas like physics, chemistry or mechanical engineering. However, most of the problems encountered in structural engineering domain are dependent on certain variables; thus, the application of DOE could be useful in a broad range of testing situations.

Two-level factorial design was performed on walls with openings aiming to obtain the test matrix in order to study the influence of opening size and the effectiveness of the strengthening patterns. Two methods for strengthening of RC walls with openings have been proposed: (1) traditional by embedding steel reinforcement and (2) a modern technique using FRP materials.

The design of a new test-rig was presented and analysed through nonlinear simulations. The constitutive model used for concrete was able to predict the axial capacity of concrete walls with openings. Furthermore, the FEM model calibrated on a previous experimental program was used to model the strongest wall from the test matrix. Reaction forces obtained from this simulation were used to design the test-rig. The results from this experimental program will be presented in a future publication.

ACKNOWLEDGEMENTS

The authors would like to acknowledge The Research Council of Norway and Development Fund of the Swedish Construction Industry (SBUF) for financing their work within this project.

REFERENCES

1. Dol, K., Haffner, M., Housing Statistics in the European Union 2010. Delft University of Technology, Netherlands: OTB Research Institute for the Built Environment; 2010.
2. Demeter, I., Seismic retrofit of precast rc walls by externally bonded CFRP composites. Romania: PhD Thesis, Politehnica University of Timisoara; 2011.
3. Mohammed, B., Ean, L. W., Malek, M. A., "One way RC wall panels with openings strengthened with CFRP", *Construction and Building Materials*, Vol. 40, No. 2013, pp. 575-83.
4. Hollaway, L. C., "A review of the present and future utilisation of FRP composites in the civil infrastructure with reference to their important in-service properties", *Construction and Building Materials*, Vol. 24, No. 12, 2010, pp. 2419-45.
5. Täljsten, B., Thomas Blanksvärd, Sas, G., FRP strengthening of existing concrete structures. Design guideline (in Swedish). Luleå, Sweden: Luleå University of Technology, Division of structural engineering,; 2012.
6. El Maaddawy, T., Sherif, S., "FRP composites for shear strengthening of reinforced concrete deep beams with openings", *Composite Structures*, Vol. 89, No. 1, 2009, pp. 60-9.
7. Floruţ, S.-C., Sas, G., Popescu, C., Stoian, V., "Tests on reinforced concrete slabs with cut-out openings strengthened with fibre-reinforced polymers", *Composites Part B: Engineering*, Vol. 66, No. 0, 2014, pp. 484-93.
8. Doh, J. H., Fragomeni, S., "Ultimate Load Formula for Reinforced Concrete Wall Panels with Openings", *Advances in Structural Engineering*, Vol. 9, No. 1, 2006, pp. 103-15.
9. Fragomeni, S., Doh, J. H., Lee, D. J., "Behavior of Axially Loaded Concrete Wall Panels with Openings: An Experimental Study", *Advances in Structural Engineering*, Vol. 15, No. 8, 2012, pp. 1345-58.
10. Guan, H., Cooper, C., Lee, D.-J., "Ultimate strength analysis of normal and high strength concrete wall panels with varying opening configurations", *Engineering Structures*, Vol. 32, No. 5, 2010, pp. 1341-55.
11. Saheb, S. M., Desayi, P., "Ultimate strength of RC wall panels with openings", *Journal of structural engineering*, Vol. 116, No. 6, 1990, pp. 1565-78.
12. Lee, D.-J., Experimental and theoretical study of normal and high strength concrete wall panels with openings. Australia: PhD Thesis, Griffith University; 2008.
13. Fischer, R. A., The design of experiments. Edinburgh, Scotland: Oliver and Boyd; 1935.
14. Wagner Jr, J. R., Mount III, E. M., Giles Jr, H. F. 25 - Design of Experiments. Extrusion (Second Edition). Oxford: William Andrew Publishing; 2014. p. 291-308.
15. DeCoursey, W. J., Statistics and probability for engineering applications with Microsoft Excel. Amsterdam; Boston: Newnes. : ebrary, Inc. Elsevier Science Publishers,; 2003.
16. Popescu, C., Sas, G., Täljsten, B., Blanksvärd, T., "A state of the art review on walls with openings strengthened by use of fiber reinforced polymers", *Proceedings of the 7th International Conference on FRP Composites in Civil Engineering* (CICE 2014). Vancouver, British Columbia, Canada: International Institute for FRP in Construction (IIFC); 2014.
17. Doh, J. H., Fragomeni, S., "Evaluation of Experimental Work on concrete walls in One-Way and Two-Way Action", *Australian journal of structural engineering*, Vol. 6, No. 1, 2005, pp. 37-52.
18. Fragomeni, S., Mendis, P., "Improved axial load formulae for normal and high strength reinforced concrete walls", *Australian Civil Engineering Transactions, Institution of Engineers*, Vol. 38, No. 2/3/4, 1996, pp. 71-81.

19. Pillai, S. U., Parthasarathy, C. V., "Ultimate strength and design of concrete walls", *Building and Environment*, Vol. 12, No. 1, 1977, pp. 25-9.
20. Saheb, S. M., Desayi, P., "Ultimate Strength of R.C. Wall Panels in Two-Way In-Plane Action", *Journal of structural engineering*, Vol. 116, No. 5, 1990, pp. 1384-402.
21. Box, G. E. P., Hunter, W. G., Hunter, J. S., Statistics for experimenters: An introduction to design, data analysis, and model building. New York: John Wiley & Sons; 1978.
22. EN 1992-1-1. Eurocode 2: Design of concrete structures - Part 1–1: General rules and rules for buildings. Brussels: COMITÉ EUROPÉEN DE NORMALISATION; 2004.
23. MiniTab. "MiniTab, Inc.", Vol. State College, PA.
24. AS3600. Concrete Structures. Sydney, Australia: Standards Australia; 2004.
25. ATENA. Advanced Tool for Engineering Nonlinear Analysis, Atena Studio, Cervenka Consulting Ltd., Prague, Czech Republic; 2014.
26. Cervenka, J., Papanikolaou, V. K., "Three dimensional combined fracture-plastic material model for concrete", *International Journal of Plasticity*, Vol. 24, No. 12, 2008, pp. 2192-220.
27. Menetrey, P., Willam, K. J., "Triaxial failure criterion for concrete and its generalization", *ACI Structural Journal*, Vol. 92, No. 3, 1995, pp. 311-8.
28. De Borst, R., Non-linear analysis of frictional materials [Ph.D. Thesis]: Delft University of Technology; 1986.
29. Reinhardt, H., Cornelissen, H., Hordijk, D., "Tensile Tests and Failure Analysis of Concrete", *Journal of structural engineering*, Vol. 112, No. 11, 1986, pp. 2462-77.
30. van Mier, J. M., "Multiaxial strain-softening of concrete", *Materials and Structures*, Vol. 19, No. 3, 1986, pp. 179-90.
31. CEB-FIP Model Code 1990: Design Code. Thomas Telford Ltd.; 1993.
32. Vos, E., "Influence of loading rate and radial pressure on bond in reinforced concrete. A numerical and experimental approach", Dissertation, Delft University Press, 1983

Paper III

Effect of cut-out openings on the axial strength of concrete walls

Cosmin Popescu, Gabriel Sas, Cristian Sabău and Thomas Blanksvärd

Submitted to:
Journal of Structural Engineering - ASCE
July 2015

Effect of cut-out openings on the axial strength of concrete walls

Cosmin Popescu[1,*]; Gabriel Sas[2]; Cristian Sabău[3]; and Thomas Blanksvärd[4]

[1]Ph.D. Candidate, Northern Research Institute – NORUT, Rombaksveien E6-47, N-8517 Narvik, Norway (corresponding author). E-mail: cosmin@norut.no

[2]Associate Senior Lecturer, Dept. of Civil, Environmental and Natural Resources Engineering, Luleå Univ. of Technology, SE-97187, Luleå, Sweden

[3]Ph.D. Candidate, Dept. of Civil, Environmental and Natural Resources Engineering, Luleå Univ. of Technology, SE-97187, Luleå, Sweden

[4]Associate Senior Lecturer, Dept. of Civil, Environmental and Natural Resources Engineering, Luleå Univ. of Technology, SE-97187, Luleå, Sweden

ABSTRACT

Old structures are frequently modified to comply with current living standards and/or legislation. Such modifications may include the addition of new windows or doors and paths for ventilation and heating systems, all of which require openings to be cut into structural walls. However, effects of the required openings are not sufficiently understood. Thus, the objective of the work reported here was to analyze openings' effects on the axial strength of large concrete wall panels. Three half-scaled walls with two opening configurations, corresponding to small and large door openings, were subjected to a uniformly distributed axial load with a small eccentricity. Using a simplified procedure, the load-carrying capacity was predicted using existing design models found in the research literature and design codes. The results may be useful for improving existing design models, assessing requirements for strengthening concrete structures and identifying optimal strengthening procedures.

Author keywords: Concrete walls, Openings, Axial load, Out-of-plane behavior, Digital image correlation

Introduction

Openings are usually avoided in reinforced concrete (RC) structural elements, whenever possible, in order to minimize unfavorable effects of discontinuous regions. However, in recent years there has been increasing interest in enlarging spaces by connecting adjacent rooms through creating openings in existing solid walls. These openings are a source of weakness and can size-dependently reduce the structures' stiffness and load-bearing capacity. It is generally believed that effects of "small" openings can often be neglected, while a "large" opening usually significantly alters the structural system, but there is no clear definition of the size threshold in the literature (Seddon 1956).

Numerous experimental studies have examined the behavior of solid RC walls, but the performance of RC walls with openings has been studied much less intensively, although new openings may be required for various reasons, e.g. to install new doors, windows or paths for ventilation or heating systems. Exceptions include contributions by (Ali and Wight 1991, Taylor, et al. 1998, Wang, et al. 2012, Mosoarca 2014, Todut, et al. 2014). However, the cited studies focused on

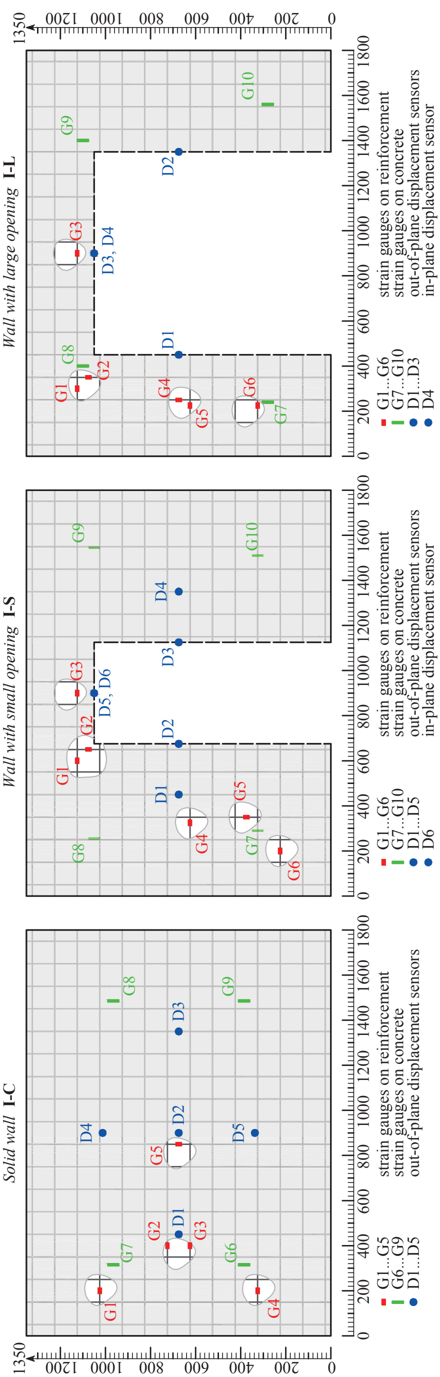

Fig. 1. Instrumentation scheme

structural walls subjected to seismic forces; effects of openings in walls that are only designed to withstand axial compression loads have received much less attention. Literature on the behavior of axially loaded walls has been reviewed by (Fragomeni, et al. 1994) and (Popescu, et al. 2015). Both of these reviews concluded that the performance of walls with openings has not been thoroughly addressed, and some results are conflicting, thus more experimental tests are needed. Furthermore, most relevant research has focused on one-way (OW) action walls (panels restrained only along their top and bottom edges). Walls restrained in this fashion tend to develop a single out-of-plane curvature parallel to the load direction, and are usually encountered in tilt-up concrete structures. Walls or panels restrained along three or four sides are referred to as two-way (TW) action panels. They generally deform in both the horizontal and vertical directions, are usually found in monolithic concrete structures, and their behavior has also received relatively little attention.

However, some aspects of the behavior of OW and TW walls have been addressed, and relevant previous studies include the following. The first systematic study of axially loaded OW and TW concrete walls with openings was reported by Saheb and Desayi (1990a), who examined effects of aspect, thickness, slenderness ratio and steel reinforcement ratios (vertical and horizontal) on their ultimate load. Doh and Fragomeni (2006) and Fragomeni, et al. (2012) subsequently reported two experimental programs on walls with different opening configurations and slenderness ratios, which provided foundations for calibrating simplified design equations for predicting ultimate load capacities (Doh and Fragomeni 2006, Guan 2010). Design codes such as AS3600 (2009) and EN1992-1-1 (2004) provide some guidance.

According to these codes, effects of an opening can be neglected if the wall is restrained on all sides, and the opening's area and height are less than 1/10 and 1/3 of the wall's total area and height, respectively. If these conditions are not met, the portion between a restraining member and opening has to be treated as a separate member, supported on three sides, and areas between openings (if there are more than one) must be treated as being supported on two sides. However, the effect of walls being restrained along all their sides is not recognized by two major codes (ACI318 2011, CAN/CSA-A23.3 2004), and all current design codes ignore the contribution of the steel reinforcement to the axial strength. The validity of ignoring this contribution is supported by some empirical data (Pillai and Parthasarathy 1977), for reinforcement placed within one layer, but not when two reinforcing layers are used (Fragomeni and Mendis 1997).

A recent state-of-the-art review (Popescu, et al. 2015) highlighted gaps in this research field, and aspects that warrant systematic analysis to improve both understanding of the behavior of walls with openings and design provisions. These aspects include effects of the size of openings and steel reinforcement. Thus, they were focal aspects of the work presented here. Three half-scale walls were tested in TW action and subjected to axial loading with small eccentricity. The results were then used to assess the accuracy of current design models. The reported work is part of a larger research program on the effectiveness of fiber-reinforced polymers (FRPs) for strengthening large concrete panels when new openings are made. Use of FRPs has already proved to be a viable solution when cut-out openings are required in structural elements (Li, et al. 2013, Todut, et al. 2015, Florut, et al. 2014), but the ongoing program is expected to significantly extend the findings and their practical utility.

Specimen design and construction

Three specimens designed to represent typical wall panels in residential buildings, at half-scale (1800 mm long, 1350 mm tall and 60 mm thick), were constructed for testing to failure. One was a solid panel, one had a symmetric half-scaled single door-type opening (450 mm x 1050 mm; hereafter small opening) and the other a symmetric half-scaled double door-type opening (900 mm x 1050 mm, hereafter large opening). For convenience, these specimens were designated I-C, I-S and I-L (solid, small opening and large opening, respectively). The specimens' dimensions are illustrated in Fig. 1, together with the positions of installed strain gauges and displacement sensors.

The specimens were all cast as solid panels, i.e. with constant thickness, no voids and no insulating layers. They are considered as load-bearing concrete walls designed to carry vertical loads with no transverse loads between supports or lateral in-plane forces. A predefined eccentricity of one sixth of the wall thickness was applied in the loading, to represent permitted imperfections in several design codes (AS3600 2009, ACI318 2011, CAN/CSA-A23.3 2004). Results obtained from the empirically developed design models may deviate from real values in cases where there is greater eccentricity.

The design codes all specify minimum wall reinforcement, primarily to control cracking due to shrinkage and temperature stresses. For example, the ACI318 (2011) code states that the minimum vertical wall reinforcement does not increase the axial strength of a wall above that of a plain

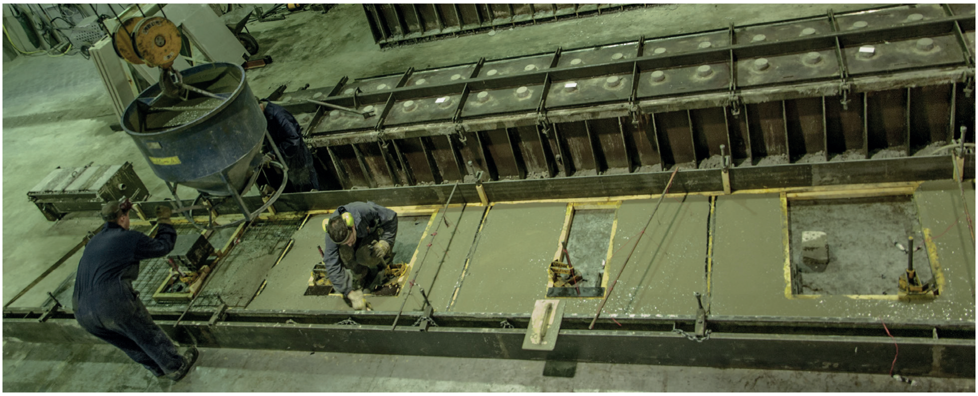

Fig. 2. Casting walls in a long-line form (image by Cosmin

concrete wall, however, the vertical and horizontal reinforcement to cross section area ratios should be at least 0.12% and 0.20%, respectively. Consequently, welded wire fabric reinforcement was used to reinforce the walls, consisting of deformed 5 mm diameter bars with 100 mm spacing in both orthogonal directions and centrally placed in a single layer. The vertical and horizontal steel reinforcement ratios resulting from this configuration are 0.327% and 0.315%, respectively. The specimens with openings were detailed to replicate solid walls with sawn cut-outs, i.e. no additional reinforcement was placed around the edges or corners of the openings.

In order to avoid misalignment of the reinforcement in the molds, the dimensions of the reinforcement mesh were measured from edge to edge of the concrete wall. The leftovers were labeled and kept for material testing. Before casting, electrical resistance strain gauges (KFG-5-120-C1-11L1M2R; 5 mm long, 120 Ω nominal resistance) with pre-attached lead wires (vinyl-coated flat 2-wire cable) were bonded to the reinforcement, after preparation by smoothly sanding the ribs, dusting using an electrical linisher and final cleaning with a soft material soaked in acetone. To avoid malfunction due to agents in the surrounding environment (i.e. water or mechanical damage) the strain gauges were protected by sealing using aluminum foil coated with a 3 mm layer of kneading compound (butyl rubber). The wires were also protected from the gauges to the concrete surface using a small diameter hose. The reinforcement was marked and sent to the precasting plant where the walls were fabricated. The walls were cast in a long-line form in lying position resting on a steel platform. A batch line can accommodate up to five specimens. Wood members were used as spacers to separate the specimens and to create the contours of the openings. Steel rails were used to form the long panel sides (Fig. 2).

Before casting, the formworks were coated with release agents to enable de-molding without damaging the concrete. The compression face of the panel was the one facing the steel platform, as it produces a very smooth surface that facilitates installation of strain gauges on concrete.

The steel reinforcement was then placed into the molds rested on 25 mm high plastic chairs in direct contact with the horizontal reinforcement bars (see Fig. 3) to provide precise concrete cover. Lifting inserts were installed at the top of the specimens to facilitate handling. To avoid risks of premature cracking due to handling (which could have arisen since no additional reinforcing was used) a cast-in steel plate was attached at the bottom of each pier. Then a steel tie was welded to

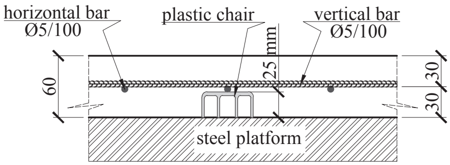

Fig. 3. Arrangement of the reinforcement in the molds

the plate temporarily connecting the piers and effectively stiffening the wall. The tie was removed prior to testing. The walls were manufactured at a local precast concrete plant, in an indoor area with controlled curing conditions. The concrete was transported by in-transit mixers from a nearby batching plant and transferred to the casting platform using a bucket attached to a crane (Fig. 2). The concrete was poured uniformly into all parts of the form and flattened using a screed board. Where additional compaction was required (close to the edge of the form), an edging tool was used. The final step was to further smooth the concrete surface by manual troweling.

The concrete was cured in two stages. First the walls were allowed to harden in the formwork for 48 hours, then after the formwork had been removed the specimens were stored for seven days in the panel racks in a near vertical position before delivery. On reception the specimens were visually inspected for casting defects. No air voids or stains were observed on the exposed surfaces. Regions around openings were also inspected for cracks due to handling. None were found. No tolerances were specified in the technical drawings; the contractor was instructed to follow standard practices for this kind of element.

Material properties

The concrete used to cast the specimens was a self-consolidating mix that could be poured without vibrating it, including dynamon NRG-700, a superplasticizer added to provide high workability and early strength. The target design strength for the concrete (class C32/40) was chosen to reflect standard Swedish construction practices. Information on the mix proportion is provided in Table 1. To determine mechanical characteristics of the concrete (compressive strength and fracture energy), cubes and beams with standardized sizes were cast and cured in identical conditions to the specimens.

The average cubic compressive strength of the concrete (f_{cm}) was 62.8 MPa (coefficient of variation, CoV, 3.2%), according to five cube tests after 28 days. The mean fracture energy (G_F) was 168 N/m (CoV, 11.9%) according to three-point bending tests with five notched beams (150 mm x 150 mm x 600 mm, with a span-to-depth ratio of 3.33, and notch to beam depth ratio of 0.33). In the bending tests the notches were sawn under wet conditions and the loading procedure recommended by RILEM TC 50-FMC (1985) was followed. The ultimate compressive strain in the concrete, ε_{cu}, was computed as function of the cube strength according to EN1992-1-1 (2004).

Table 1. Mix proportion of the concrete

Concrete class	w/c	Cement	Aggregate size		Additives
			1 - 4 mm	8 - 16 mm	
	-	(kg)	(kg)	(kg)	(%) of cement weight
C32/40	0.55	380	1030	630	2.6

Five coupons were taken from the reinforcing steel meshes and tested to determine their stress-strain properties. Their mean yield strength (f_y) and tensile strength (f_u) were 632 MPa (CoV, 0.35%) and 693 MPa (CoV, 0.40%), respectively, at mean strains ε_y and ε_u of 0.28% (CoV, 8.45%) and 4.87% (CoV, 4.82%), respectively.

Test setup and loading strategy

The following considerations were applied when designing the test-rig:

a) It had to simulate hinged connections at the top and bottom boundaries of the specimen and clamped side edges (Fig. 4a and 4b);

b) The side edges had to be sufficiently rigid to prevent excessive out-of-plane deformations;

c) The walls would be loaded gravitationally with a small eccentricity at both ends (one sixth of the wall thickness) to simulate effects of imperfections that occur in normal construction practices and are accounted for in standards.

To apply eccentric loading a steel rod was welded to each loading beam, designed to fit into a guide system attached to the top and bottom of the specimen (see Fig. a). To avoid any unforeseen eccentricities, the wall was vertically aligned using a dual plane levelling and alignment laser tool, with an accuracy of ±0.3 mm/m and self-levelling capability in the range of ±4°. At each contact surface between the specimen and the steel loading beams a 2 mm strap of deformable plywood was introduced to limit local damage due to surface irregularities. Four hydraulic jacks, each with a maximum capacity of 1.4 MN, were networked together to enable a single operator to apply a uniformly distributed load, with controlled total force, along the wall length (through the loading beam with a slope of 1:1). The hydraulic fluid was supplied from a power steering pump with user-adjustable relief valves, allowing the operator to easily set working pressures. Hydraulic load cells were used to measure the induced force, as the load was incrementally increased at 30 kN/min with breaks every 250 kN to allow stress distribution and to monitor the cracks in the specimens. All reactions were transmitted to a reaction frame fixed in a strong floor by three additional pairs of high strength steel rods (prestressed, as the existing anchorage of the reaction frame did not provide sufficient capacity). A general view of the test setup is shown in Fig. 5.

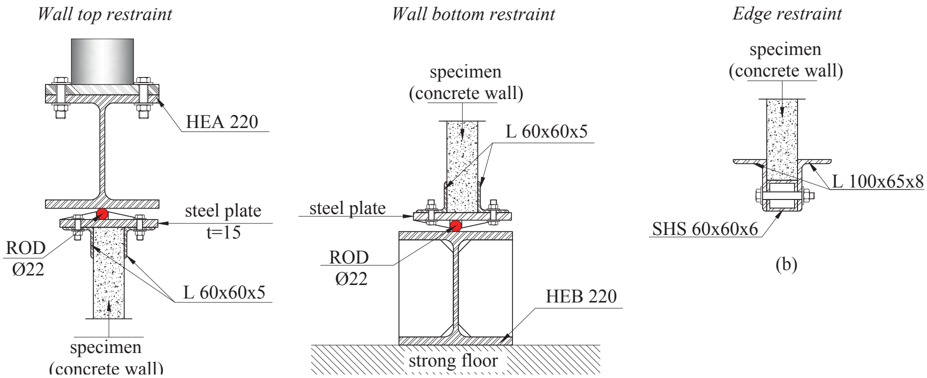

Fig. 4. Specimen edge restraints: (a) top and bottom connections; (b) side edge restraint

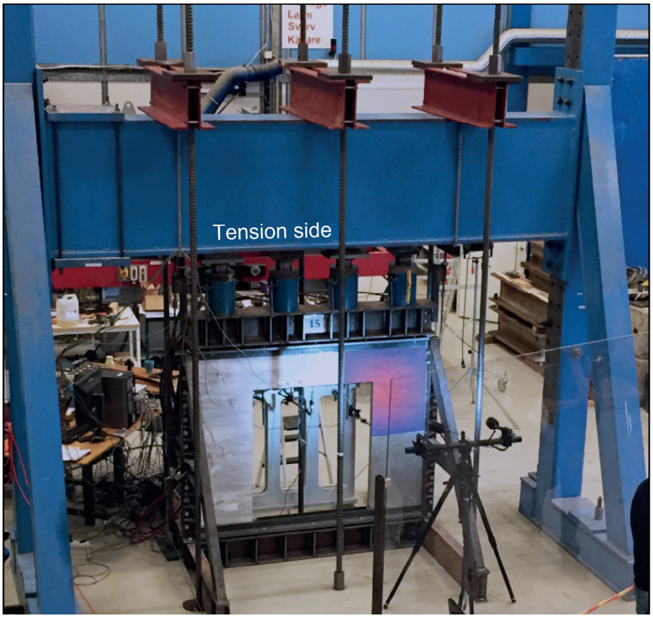

Fig. 5. General overview of the test setup (image by Cosmin Popescu)

Instrumentation

Out-of-plane and in-plane displacements were monitored using linear displacement sensors, a fully active 350 Ω strain-gauge bridge giving the measurements infinite resolution. They were attached on the back side of the wall (hereafter compression side) at locations shown in Fig. 1. Strain gauges intercepting potential yield lines (derived from nonlinear finite element analysis) were installed on the steel reinforcement and compression side of the concrete surface. In addition to yield lines, other relevant information such as crack patterns and ultimate loads was obtained.

To measure the mean strain of the concrete 60 mm gauges (three times longer than the maximum diameter of the aggregate, to even out local strain variations) were selected. To measure tensile stresses of the reinforcement general purpose strain gauges were used. In addition to classical approaches for measuring strains and displacements, optical 3D measurements were also acquired by the digital image correlation (DIC) technique. For this we used a 5M system configuration (GOM mbH) with a strain measuring accuracy of 0.005% to monitor the strain and displacement fields. Ideally a stochastic point pattern should be used, but due to the large area monitored a regular pattern applied using a stencil and spray was utilized here. First a white base layer was applied then a black-dot pattern was sprayed. The area monitored was the right-upper corner on the tension side of the specimen (780 mm x 660 mm, highlighted in Fig. 5), an area of particular interest for monitoring strain and crack development in discontinuous regions. These measurements were supplemented with several video and still camera recordings. To avoid interfering with the optical measurement system the reinforcement was only instrumented with strain gauges on half of each specimen (the left pier, on the tension side), as permitted by the symmetry of the test set-up.

Experimental results

General observations

No anomalies were observed during the specimen loading. The walls behaved as expected, deflecting in both vertical and horizontal directions. The displacements were generally symmetric, with some deviations due to the test rig and random variations in material properties. The lateral bracing of the test rig was designed to be connected to the foundation support through oval holes, to account for variations in the thickness of the wall panels, thus allowing small sliding of the entire system. The crack pattern was also symmetrical, except that the crack patterns in panels with openings only retained symmetry until the onset of failure. When one of the piers failed, triggered failure of the other. The ultimate loads given do not include the weight of the loading beam.

The failure of the specimens can be watched in a multimedia file accessible as supplementary material to the online version of the paper (Video S1).

Solid wall (I-C)

Axial load-displacement relationship

Between 0 and about 500 kN the recorded displacement behaved abnormally, probably due to settlement of the test setup. As the loads were increased to failure the stiffness degradation increased, reflecting opening of the cracks and utilization of the steel reinforcement.

The maximum load capacity was reached at 2363 kN when the out-of-plane displacement registered by D2 was about 18.95 mm (Fig. 6a). An instant jump to 26 mm was recorded immediately after failure when the entire specimen was divided into distinct disks along the yield lines.

Steel reinforcement and concrete strain responses

Four strain gauges (G1-G4) were glued on the horizontal reinforcement and one on the vertical reinforcement (G5). The G5 strain readings increased linearly up to the failure load, when the out-of-plane displacements of the specimens increased rapidly. The compressive strain reached a maximum of 0.68‰. When crushing of the concrete began the neutral axis of the cross-section shifted rapidly and the vertical reinforcement was subjected to tensile forces. All horizontal bars were subjected to tensile strain linearly up to 60-75% of the peak load (Fig 6b). After this the strains were more pronounced with yielding at failure. Four strain gauges (G6-G9) were glued on the compression side of the specimen to monitor the compressive strains (Fig. 6c). The measurements provided good indications of imminent failure of the specimen, with collapse occurring at about 3.2‰ compressive strain. The readings showed consistent patterns, indicating that the loads were transferred uniformly towards the supports.

Failure mode and crack pattern

At up to 85% of its ultimate capacity the solid panel showed no cracks. As the load increased, several major tensile cracks (0.2 mm wide) opened, starting from the corners of the wall at 55° inclination.

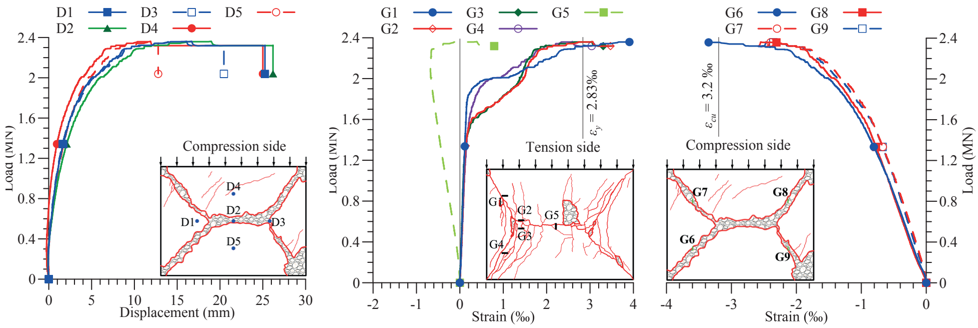

(a) (b) (c)

Fig. 6. Responses of the solid wall (I-C): (a) load-displacement, (b) Strain in steel reinforcement, (c) Strain in concrete. D1-5 and G1-9 refer to displacement sensors and strain gauges, respectively at indicated positions (see Fig. 1 for details)

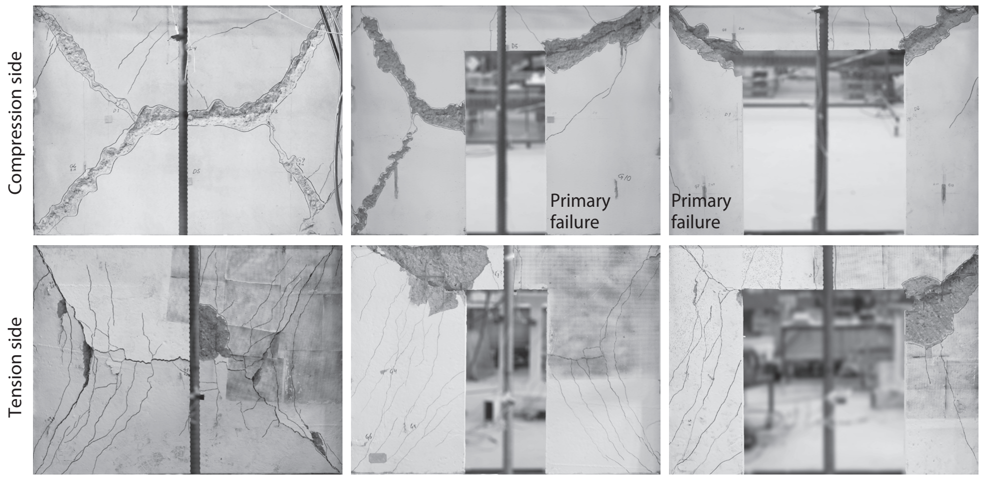

(a) (b) (c)

Fig. 7. Crack pattern and failure mode of the tested specimens: (a) specimen I-C; (b) specimen I-S and (c) specimen I-L (images by Cosmin Popescu)

The wall had a brittle failure due to crushing of concrete with little forewarning (visible out-of-plane deflection) prior to failure. The crack pattern at failure, shown in Fig. 7a for both tension and compression sides, was similar to a pattern previously reported in panels with all sides restrained (Swartz, et al. 1974). Several secondary tensile cracks were distributed parallel to each other around the major tensile cracks, indicating that the reinforcement mesh played an active role in redistributing tensile stresses in the concrete.

Wall with small opening (I-S)

Axial load-displacement relationship

The maximum load capacity of the specimen with a small opening was reached at 1500 kN when the out-of-plane displacements registered by D2 and D3 were about 26.6 mm and 18.4 mm, respectively. The failure occurred on the left pier (corresponding to D3, see Fig. 8a) where the displacements developed more slowly than on the right pier. The differences in displacement symmetry were more pronounced after the first crack appeared in the right pier. Load-displacement diagrams are shown in Fig. 8a.

Steel reinforcement and concrete strain responses

Four strain gauges (G1, G3, G4 and G6) were glued on the horizontal reinforcement and two on the vertical reinforcement (G2 and G5). All horizontal bars were subjected to tensile strains, but recorded strains were low up to 90% of the peak load (Fig. 8b). At G4 and G6 yielding occurred at failure, while ultimate strains recorded by G1 and G3 were below 1.5‰. Strains recorded by G3 (the gauge glued on the first bar above the opening) increased more progressively. As observed in loading of the solid specimen (I-C), the vertical bars were compressed, and G2 (adjacent to the opening) recorded higher strains than G5. However, the maximum compressive strain, reached at failure, did not exceed 1.5‰.

Failure mode and crack pattern

When the specimen was under about 50% of its peak load, a 0.05 mm wide crack opened in the middle of the spandrel, followed by two diagonal cracks from the bottom right corner of the wall with 55° inclination, at 65% of its ultimate capacity. These cracks continued to widen up to 85% of the failure load when several other cracks around the same location began to emerge. For safety reasons, no information regarding the crack opening beyond this load was collected. The wall had a brittle failure due to crushing of concrete with spalling and reinforcement buckling along the line between the corner of the wall and opening corner of one pier (Fig.9a).

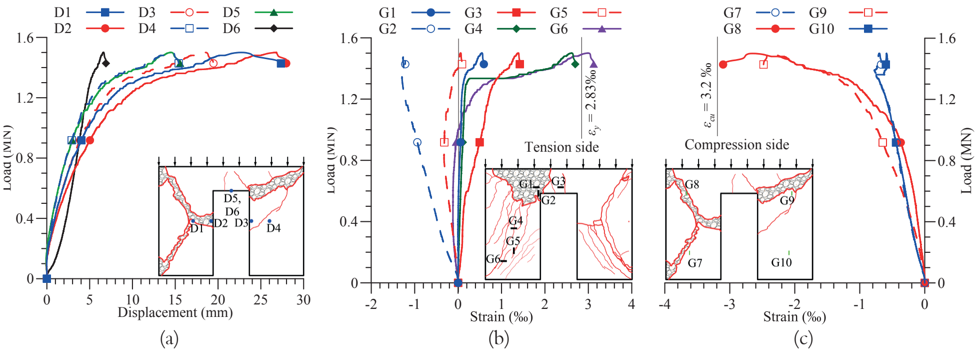

Fig. 8. Responses of the wall with a small opening (I-S): (a) load-displacement; (b) strain in steel reinforcement; (c) strain in concrete. D1-6 and G1-10 refer to displacement sensors and strain gauges, respectively at indicated positions (see Fig. 1 for details)

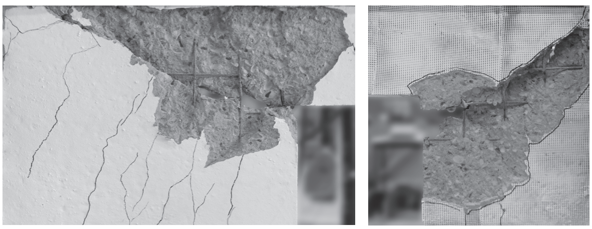

(a) (b)

Fig. 9. Failure at the corner opening with concrete spalling and reinforcement buckling: (a) specimen I-S; (b) specimen I-L (images by Cosmin Popescu)

The other pier failed immediately thereafter, with a typical crack pattern for panels restrained on three sides. Photographs of the crack patterns after collapse in both the tension and compression sides are shown in Fig. 7b.

Wall with large opening (I-L)

Axial load-displacement relationship

The maximum load capacity of the specimen with a large opening was reached at 1180 kN, when the out-of-plane displacements registered by D1 and D2 were about 8.5 mm and 11.2 mm, respectively. The failure occurred on the left pier (where the displacements where smaller), following a very similar pattern to the one observed in the test of the wall with a small opening.

Steel reinforcement and concrete strain responses

Four strain gauges (G1, G3, G5 and G6) were glued on the horizontal reinforcement and two on the vertical reinforcement (G2 and G4). The trends, and strain values, were very similar to those observed in the reinforcement of the specimen with a small opening. The reinforcement bar above the opening was tensioned more than in the panel with a small opening, thus accelerating the redistribution of the forces to piers. Load-strain diagrams for the reinforcement and concrete are shown in Fig. 10b and Fig. 10c, respectively.

Failure mode and crack pattern

The first crack (0.3 mm wide) was identified in the middle of the spandrel early in the load history (at about 20% of its peak load). Another two diagonal cracks (0.05 mm wide) from the bottom corner of the wall with 53° inclination were observed at around 85% of its peak load. The wall had a brittle failure due to crushing of concrete with spalling and reinforcement buckling along the line between the wall corner and opening corner of one pier (Fig. 9b). As in the wall with a small opening, this local failure caused failure of the entire wall with no typical crack pattern in the other pier. Photographs of the crack patterns in both the tension and compression sides after collapse are shown in Fig. 7c.

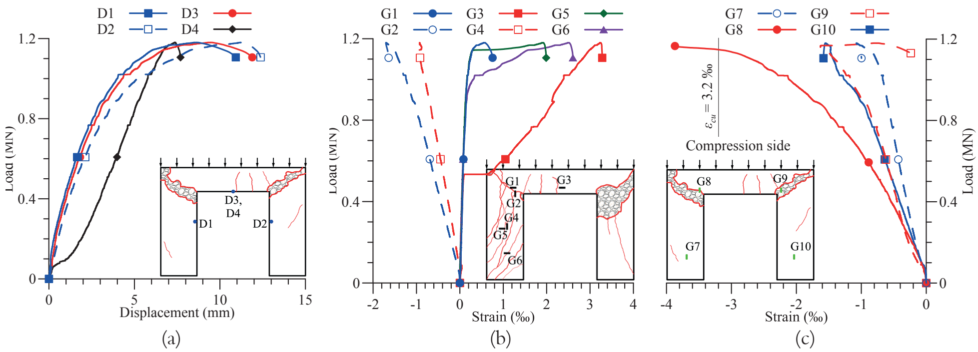

Fig. 10. Responses of the wall with a large opening (I-L): (a) load-displacement; (b) strain in steel reinforcement; (c) strain in concrete. D1-4 and G1-10 refer to displacement sensors and strain gauges, respectively at indicated positions (see Fig. 1 for details)

Analysis of the test results and discussion

Effects of opening size

Displacements of all three specimens (recorded at the same position, D1) were plotted on the same graph (Fig. 11) to assess effects of the size of openings. The results indicate that the 25% and 50% reductions in cross-sectional area of the solid wall caused by introducing the small opening and large opening reduced its load carrying capacity by nearly 36% and 50%, respectively. As shown in Fig. 12, these variables are clearly correlated (as expected), but not linearly. Interestingly, the axial strength ratio (N_{max}/Af_c) responses markedly differed, being very similar for the solid wall and wall with a large opening, but much lower for the wall with a small opening. This may be due to the boundaries being more active as the aspect ratio (height/length) of the piers increases, thereby utilizing the material strength more effectively. This behavior also confirms results of a previous analysis of published data by Saheb and Desayi (1990b).

Numerous simplified procedures have been proposed in the literature for calculating two other highly relevant variables: ductility and energy release at failure. Ductility is commonly expressed in terms of displacements, curvature or rotations (Park 1988). In this study, displacement-based ductility factors (defined as the ratios between elastic and ultimate displacements, $\mu_{\Delta}=d_u/d_e$) were computed. Since a distinct elastic displacement cannot be easily found, a simplified procedure proposed by Park (1988) was adopted. This is based on the assumption that the most realistic approach for RC structures is to compute the elastic displacement for an equivalent elasto-plastic system with reduced stiffness. The reduced stiffness is found as the secant stiffness related to 75% of the peak load (N_e) and the horizontal plateau corresponding to the peak load (N_{max}) of the real system (Fig. 11). The maximum displacement corresponds to the post-peak deformation when the load has decreased by 20% (N_u) or the reinforcement buckles, whichever occurs first. In addition to ductility factors, energy dissipation (E_d) was also evaluated as the area under the load-displacement curves.

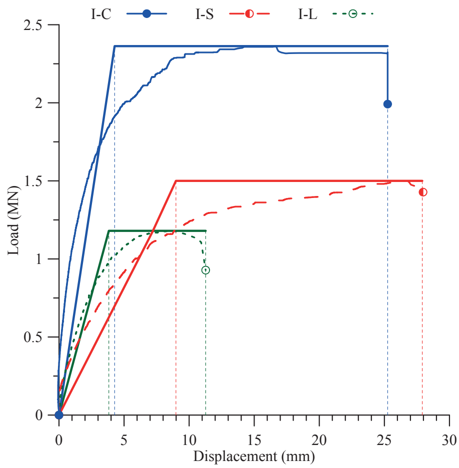

Fig. 11. Load-displacement diagrams for all specimens and idealized elasto-plastic behavior (straight lines)

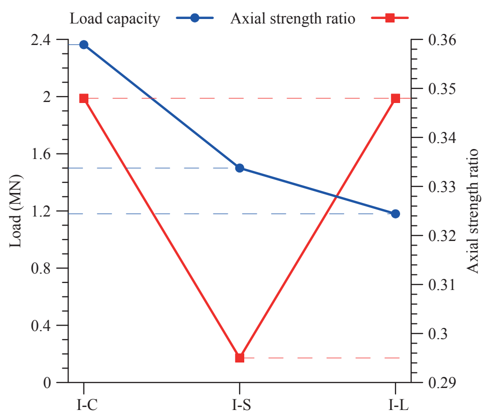

Fig. 12. Ultimate loads and axial strength ratios of the solid wall (I-C) and walls with small (I-S) and large (I-L)

Table 2. Ductility factors and energy release values at failure evaluated according to (Park 1988)

Specimen	N_{max} (kN)	N_e (0.75Nmax) (kN)	N_u (0.75Nmax) (kN)	δ_e (mm)	δ_u (mm)	$\mu_\Delta=\delta_u/\delta_e$	E_d (kNm)
I-C	2363	1772.25	1991.5	4.28	25.25	5.9	55.18
I-S	1500	1125	1277.3	8.98	27.91	3.1 (-47%)	33.77 (-39%)
I-L	1180	885	928.5	3.83	11.27	2.9 (-51%)	10.88 (-80%)

The introduction of the small and large openings resulted in similar, sharp reductions in computed ductility factors (Table 2). However, the differences in size between the openings strongly affected the energy dissipation; the walls with no opening and a small opening could both be classified as "ductile elements" according to Park (1988), having ductility factors between 3 and 6, while the wall with a large opening would be classified as an element with "restricted" ductility (ductility factor < 3).

Contributions of reinforcement

Although the minimum amount of reinforcement prescribed by design codes was used, the tensile or compressive strains that developed in the reinforcement were significant at higher loads, with yielding of some bars occurring at failure. While the vertical bars were more gradually stressed during the specimen loading, none of them yielded at failure. The horizontal reinforcement yielded or was close to yielding and buckled at failure, but no rupture was observed in any of the tests, in contrast to OW specimens tested by Huang, et al. (2015). Another interesting observation was that the failure of the specimens with openings occurred in the pier with lower deformations, presumably at least partly because as geometric nonlinearities increase the reinforcement starts to be more active. El-Metwally, et al. (1990) also showed that the failure mode is sensitive to the initial eccentricity, and here too the reinforcement has a significant effect. Nevertheless, no current design codes recognize the contribution of the steel reinforcement.

Although cracks occurred at late loading stages in the reported tests, the possibility of sustained loads causing cracks should not be neglected, especially around corners of openings if there is no diagonal reinforcement. This is because real structures are subjected to relatively high sustained loads, which tend to impair the performance of slender elements by increasing their long-term deflections (Macgregor, et al. 1971). The study presented here involved only short-term tests, thus, creep effects were not considered.

Digital image correlation

The 3D-DIC system captured well the strain development and distribution around the openings during loading of the specimens, as illustrated by the images in Fig.13 showing strains in the wall with a small opening (I-S) at 30%, 75% and 100% of the peak load and the onset of collapse. Tensile strains appeared first in the spandrel and were concentrated in the piers at later stages. The recorded strain pattern in the pier clearly shows a three-way action behavior with no major strains around the corner of the opening.

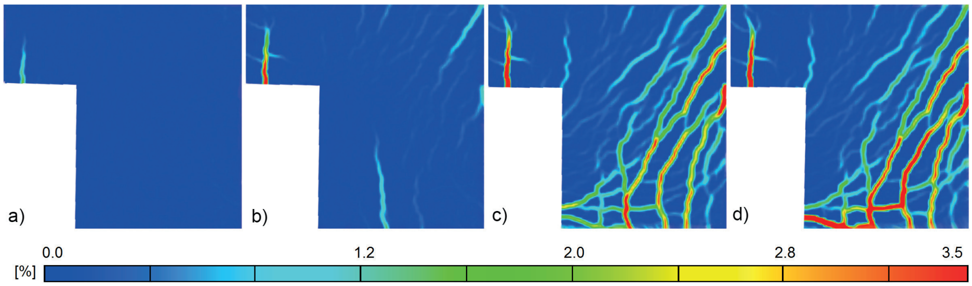

Fig. 13. Principal plane strain development on the tension side of the I-S specimen at: a) 30% of the peak load; b) 75% of the peak load; c) peak load; d) onset of failure

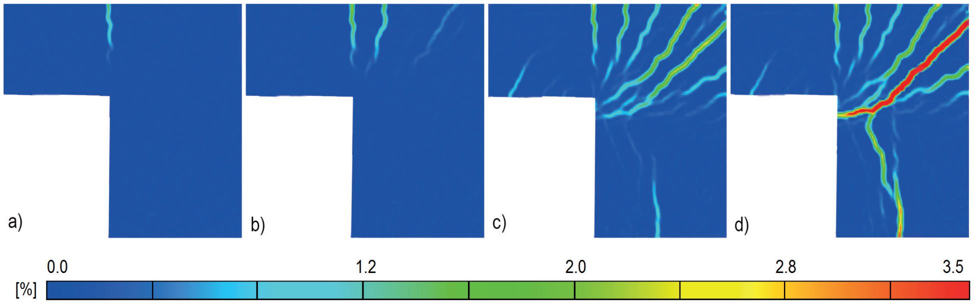

Fig. 14. Principal plane strain development on the tension side of specimen I-L at: a) 30% of the peak load; b) 75% of the peak load; c) peak load; d) onset of failure

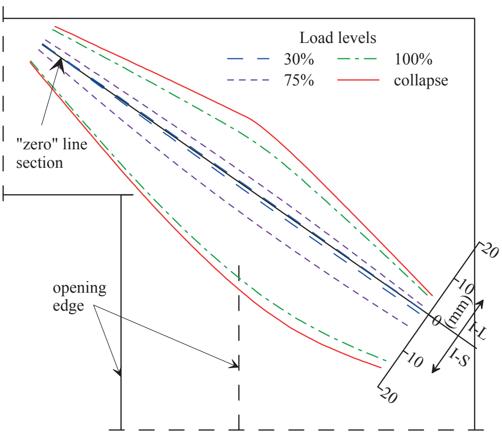

Fig. 15. Displacement profiles along a predefined line for the specimens with large and small openings, above and below the "zero" line section, respectively

The strain distribution and development during the loading of specimen I-L is shown in Fig. 14. Unlike specimen I-S, the strains are more concentrated around the opening corner.

The DIC measurements were also used to compute the out-of-plane displacement profiles along a section line (called the "zero" line section) representative for both specimens with openings (i.e. in the same locations relative to the specimen edge). The resulting profiles for the specimens with large and small openings are shown in Fig. 15, above and below the "zero" line-section, respectively (again at 30%, 75% and 100% of the peak load, and the onset of collapse). The data clearly showed that most displacement occurred after 75% of the peak loading, for specimens with both type of openings. Moreover, the out-of-plane displacements were higher for specimen I-S than specimen I-L. It should be noted that the DIC technique did not record results up to the specimen edges due to the edge restraints (see Fig. 4), which limited the view of the cameras (60 mm from the upper part and 40 mm from the side edge).

Comparison of the test results with existing design models

This section briefly overviews analytical formulas recommended in current design codes and literature for predicting ultimate capacities of walls with or without openings. The experimentally measured ultimate loads for the tested walls are then compared to their axial strengths, as computed using these formulas.

Currently the practical design of RC walls, prescribed in standards such as ACI318 (2011) and AS3600 (2009) is based on empirical models, whereas EN1992-1-1 (2004) is based on calibration against the results of non-linear analysis. Despite numerous relevant subsequent studies, no modifications to the formula presented in ACI318 (2011) have been implemented to incorporate the effect of restraints on all sides. EN1992-1-1 (2004) and AS3600 (2009) are the only major codes that provide methodology to account for the increase in capacity this provides. Numerous studies have attempted to further improve the design models. A comprehensive recent review and assessment of existing design models (Popescu, et al. (2015) concluded that the best models in terms of average deviations between theoretically and experimentally determined capacities were those proposed by Doh and Fragomeni (2006) and Doh and Fragomeni (2005) for walls with and without openings, respectively.

The solid wall

Following EN1992-1-1 (2004), AS3600 (2009) and Doh and Fragomeni (2005), the ultimate load capacity of the solid specimen was computed using Equations 1 to 3, below, and the resulting values are designated N_{EC2}, N_{AS3600} and $N_{D\text{-}F}$, respectively.

$$N_{EC2} = f_c \cdot L \cdot t \cdot \Phi \tag{1}$$

$$\Phi = 1.14\left(1-2\frac{e+e_a}{t}\right) - 0.02 \cdot \frac{H_{eff}}{t} \le \left(1-2\frac{e+e_a}{t}\right)$$

$$N_{AS3600} = 0.6 f_c \left(t - 1.2e - 2e_a\right) L \tag{2}$$

$$N_{D-F} = 2 f_c^{0.7} \left(t - 1.2e - 2e_a\right) L \tag{3}$$

Here: t is wall thickness, L is wall length; f_c is mean concrete compressive strength; e is initial eccentricity, $e = t/6$; and e_a is additional eccentricity due to lateral deflection of the wall.

The additional eccentricity, e_a, accounts for the effect of slenderness, also known as second order (or P–Δ) effects. Several approaches may be used to compute the additional eccentricities, which are a function of the curvature applied to find the maximum deflection at the critical wall section:

$$e_a = \begin{cases} \dfrac{H_{eff}}{400} & \text{EN1992-1-1 (2004)} \\[2ex] \dfrac{\left(H_{eff}\right)^2}{2500t} & \text{AS3600 (2009) \& Doh and Fragomeni (2005)} \end{cases}$$

with H_{eff}=βH being the effective height. Values for the effective height factor β are given for the most commonly encountered restraints depending on the aspect ratio of the wall. According to Fragomeni, et al. (1994), these effective height factors were first introduced by the German code (DIN 1045 1988) and later adopted by EN1992-1-1 (2004) and AS3600 (2009) (see Eq. 4).

$$\beta = \begin{cases} \dfrac{1}{1+\left(\dfrac{H}{3L}\right)^2} & \text{three-sides} \\ \dfrac{1}{1+\left(\dfrac{H}{L}\right)^2} & \text{four-sides with } L \geq H \\ \dfrac{L}{2H} & \text{four-sides with } L < H \end{cases} \tag{4}$$

Doh and Fragomeni (2005) slightly modified the effective height factor to account for loading eccentricities by incorporating an additional eccentricity parameter, α.

$$\alpha = \begin{cases} 1/\left(1+e/t\right) & \text{when } H/t < 27 \\ 18/\left[\left(1-e/t\right)\left(H/t\right)^{0.88}\right] & \text{when } H/t \geq 27 \end{cases} \tag{5}$$

The walls with openings

To the authors' knowledge there are no straightforward methods to evaluate the ultimate capacity of a wall with openings. However, some guidelines are available, such as those in AS3600 (2009) and EN1992-1-1 (2004), which state that effects of an opening on a wall's axial strength can be neglected if the wall is restrained on all sides, while the opening's area and height are less than 1/10 and 1/3 of the wall's total surface area and height, respectively. If these conditions are not fulfilled, areas between openings (if more than one) must be treated as being supported on two sides. Portions between restraining members and openings must be treated as being supported on three sides, according to AS3600 (2009), while EN1992-1-1 (2004) does not clearly prescribe their treatment. In the preceding sections the ultimate capacity of individual elements has been considered, independently of others. However, it is important to evaluate the reliability of entire systems (in this context walls with openings), but design codes do not provide such information or clear methodology for calculating their reliability. Consequently, the following procedure was applied. The entire ensemble may be idealized as a hybrid system, i.e. a combination of series and parallel subsystems. In a series system if one of the components fails, the entire system will fail whereas failure of all components is required for a parallel system to fail (Novak and Collins 2012). In a wall with one or more openings, the piers behave as a parallel system connected in series with the spandrel above the openings, and failure will occur when the axial strength of all piers or the shear-flexural strength of the spandrel is exceeded. Thus, the system's strength is the sum of all the piers' axial strength, assuming that the spandrel continues to distribute the forces until one of the piers fails completely.

Table 3. Comparison of axial loads predicted using formulas from design codes (Eqs. 1-3 and 6) with experimental values

Specimen	Ntest (kN)	N_{EC2} (kN)	Err. (%)	N_{AS3600} (kN)	Err. (%)	N_{D-F} (kN)	Err. (%)
I-C	2363	2220.7	-6.02	2167.6	-8.27	-1945.7	-17.65
I-S	1500	1534	+2.26	1553.6	+3.57	1498.2	-0.12
I-L	1180	1341.6	+13.7	1134.1	-3.89	1045.8	-11.37
Mean percentage error (MPE)		+3.31%		-2.86%		-9.71%	

The experimental results indicate that the spandrel was the first element to fail, as the first crack occurred in it. In reality, failure involves not only the ultimate failure but also excessive deflections and cracks. The loads applied on the spandrel are redistributed directly to the piers until one of the piers fails completely and the whole system collapses. Thus it can be regarded as a parallel system with brittle elements, which will fail if one of the brittle components fails (and the system's strength can be obtained by multiplying the axial strength of the weakest pier by the number of piers).

In order to extend the scope of their design equation, Doh and Fragomeni (2006) proposed a new formula (Eq. 6) for calculating the ultimate capacity of walls with openings:

$$N_{uo} = \left(k_1 - k_2 \chi\right) N_{D-F} \qquad (6)$$

where N_{D-F} is the ultimate load of an identical panel without openings under TW action (Eq. 3).

Here, the constants k_1 and k_2 were obtained by curve-fitting, with k_1= 1.004 and k_2= 0.933. Effects of the size and location of openings are taken into account through a dimensionless parameter, χ, defined as,

$$\chi = \left(A_0 / A + a / L\right) \qquad (7)$$

where A_0 and A are horizontal cross-sectional areas of the opening (i.e. $A_0 = L_0 t$) and the solid wall (i.e. $A = Lt$), respectively. All parameters involved in Eq. (7) can be easily determined from Fig. 16.

The test results are summarized in Table 3, together with the failure loads predicted by the presented design models.

Design models overestimated somewhat the ultimate capacity of the tested specimens. However, the model proposed by Doh and Fragomeni (2006) provides more conservative results being on the safe side. It should be noted that a safety factor, ϕ, of 1 was applied in all design equations, while a carefully chosen safety factor should be used in practice.

Conclusion and future work

The effects of steel reinforcement and the presence of cut-out openings on axially loaded concrete walls were examined in the presented experimental program. The main conclusions were as follows:

1. Recorded strains in the steel reinforcement indicate that it may make no significant contribution at serviceability limit states, but yielding may occur close to failure when second order effects start to be more active, thus contributing to the overall ductility. It is not clear how much the

reinforcement contributes to the overall load-bearing capacity of walls with openings.
2. Reducing the cross-sectional area by 25% and 50% by cutting out openings led to 36% and 50% reductions in peak loads, respectively. The specimen with a large opening was stiffer than the specimen with a small opening (and hence lower ductility and energy release at failure).
3. The 3D DIC system has proved to be a reliable non-contact tool for monitoring strain and displacement fields in regions of interest. The observed strain patterns indicate that the specimen with a large opening behaved more like an RC frame than an RC wall, with all major strains oriented towards the opening corner. In order to set suitable thresholds for "small" and "large" openings in walls (with negligible and non-negligible effects, respectively), and the optimal transition point between RC walls and RC frames in design codes for structural elements, more tests are required including walls with intermediate size openings.
4. The Doh and Fragomeni equations, which address the axial strength of walls with and without openings, provided good predictions of the test results. Considering the procedure proposed for evaluating the systems' capacity, formulas in the design codes also provided good agreement with the test results, although they overestimated overall capacity somewhat.

The findings open new avenues for studying the behavior of concrete walls with openings and may provide foundations for future research. Nonlinear analysis could be applied with a larger test matrix to assess effects of other important parameters (e.g. higher eccentricities, asymmetric openings and/or different boundary conditions). However, despite the clear need to extend the analyses, the presented results may be useful for improving existing design models, assessing requirements for strengthening concrete structure and identifying optimal strengthening procedures.

Acknowledgements

The authors would like to acknowledge The Research Council of Norway (RFF), Development Fund of the Swedish Construction Industry (SBUF) and Skanska for financing the presented work and associated, ongoing project.

Supplemental Data

Video S1 (video by Cosmin Popescu) is available online in the ASCE Library.

References

ACI318 (2011). "Building code requirements for structural concrete and commentary (ACI 318–11)." American Concrete Institute (ACI), Farmington Hills, USA.

Ali, A., and Wight, J. (1991). "RC Structural Walls with Staggered Door Openings." Journal of Structural Engineering, 117(5), 1514-1531.

AS3600 (2009). "Concrete structures." Standards Australia, Sydney, Australia.

CAN/CSA-A23.3 (2004). "Design of concrete structures." Canadian Standards Association, Mississauga, Ontario.

DIN 1045 (1988). "Reinforced concrete structures: Design and construction." Berlin.

Doh, J., and Fragomeni, S. (2005). "Evaluation of experimental work on concrete walls in one-way and two-way action." Aust J Struct Eng, 6, 37–52.

Doh, J. H., and Fragomeni, S. (2006). "Ultimate load formula for reinforced concrete wall panels with openings." Advances in Structural Engineering, 9(1), 103-115.

El-Metwally, S. E., Ashour, A. F., and Chen, W. F. (1990). "Instability Analysis of Eccentrically Loaded Concrete Walls." Journal of Structural Engineering, 116(10), 2862-2880.

EN1992-1-1 (2004). "Eurocode 2: design of concrete structures – Part 1–1: General rules and rules for buildings." Comité Européen de Normalisation (CEN), Brussels, Belgium.

Florut, S.-C., Sas, G., Popescu, C., and Stoian, V. (2014). "Tests on reinforced concrete slabs with cut-out openings strengthened with fibre-reinforced polymers." Composites Part B: Engineering, 66C(0).

Fragomeni, S., Mendis, P. A., and Grayson, W. R. (1994). "Review of reinforced concrete wall design formulas." ACI Materials Journal, 91(5), 521-529.

Fragomeni, S., and Mendis, P. (1997). "Instability Analysis of Normal- and High-Strength Reinforced-Concrete Walls." Journal of Structural Engineering, 123(5), 680-684.

Fragomeni, S., Doh, J. H., and Lee, D. J. (2012). "Behavior of Axially Loaded Concrete Wall Panels with Openings: An Experimental Study." Advances in Structural Engineering, 15(8), 1345-1358.

GOM mbH "ARAMIS - Optical 3D Deformation Analysis." <http://www.gom.com/metrology-systems/system-overview/aramis.html>. (2015-05-20).

Guan, H. (2010). "Ultimate strength analysis of normal and high strength concrete wall panels with varying opening configurations." Engineering Structures, 32(5), 1341-1355.

Huang, Y., Hamed, E., Chang, Z.-T., and Foster, S. J. (2015). "Theoretical and Experimental Investigation of Failure Behavior of One-Way High-Strength Concrete Wall Panels." Journal of Structural Engineering, 141(5), 04014143.

Li, B., Kai Qian, and Tran, C. T. N. (2013). "Retrofitting earthquake-damaged RC structural walls with openings by externally bonded FRP strips and sheets." Journal of Composites for Construction, 17(2), 259-270.

Macgregor, J. G., Simmonds, S. H., and Warwaruk, J. (1971). "Seminar on building code requirements, ACI318-71." Structural engineering report no. 36, University of Alberta, Department of Civil Engineering.

Mosoarca, M. (2014). "Failure analysis of RC shear walls with staggered openings under seismic loads." Engineering Failure Analysis, 41(0), 48-64.

Novak, A. S., and Collins, K. R. (2012). Reliability of Structures, Second Edition, CRC Press/Taylor & Francis Group, Boca Raton

Park, R. (1988). "State of the art report: ductility evaluation from laboratory and analytical testing." Proceedings of Ninth World Conference on Earthquake Engineering., Vol.VIII, Tokyo-Kyoto, Japan, 605-616.

Pillai, S. U., and Parthasarathy, C.V. (1977). "Ultimate strength and design of concrete walls." Building and Environment, 12(1), 25-29.

Popescu, C., Sas, G., Blanksvärd, T., and Täljsten, B. (2015). "Concrete walls weakened by openings as compression members: A review." Engineering Structures, 89(0), 172-190.

RILEM TC 50-FMC (1985). “Determination of the fracture energy of mortar and concrete by means of three-point bend tests on notched beams.” Materials and Structures, 18(4), 287-290.

Saheb, M., and Desayi, P. (1990a). “Ultimate strength of RC wall panels with openings.” Journal of Structural Engineering, 116(6), 1565-1578.

Saheb, M., and Desayi, P. (1990b). “Ultimate Strength of R.C. Wall Panels in Two-Way In-Plane Action.” Journal of Structural Engineering, 116(5), 1384-1402.

Seddon, A. E. (1956). “The strength of concrete walls under axial and eccentric loads.” In: Andrew RP, editor. Symposium on the strength of concrete structures: Cement and Concrete Association, London, UK;, 445-486.

Swartz, S. E., Rosebraugh, V. H., and Rogacki, S. A. (1974). “A method for determining the buckling strength of concrete panels.” Experimental Mechanics, 14(4), 138-144.

Taylor, C. P., Cote, P. A., and John, W. W. (1998). “Design of Slender Reinforced Concrete Walls with Openings.” ACI Structural Journal, 95(4).

Todut, C., Dan, D., and Stoian, V. (2014). “Theoretical and experimental study on precast reinforced concrete wall panels subjected to shear force.” Engineering Structures, 80(0), 323-338.

Todut, C., Dan, D., and Stoian, V. (2015). “Numerical and experimental investigation on seismically damaged reinforced concrete wall panels retrofitted with FRP composites.” Composite Structures, 119(0), 648-665.

Wang, J., Sakashita, M., Kono, S., and Tanaka, H. (2012). “Shear behaviour of reinforced concrete structural walls with eccentric openings under cyclic loading: experimental study.” The Structural Design of Tall and Special Buildings, 21(9), 669-681.

Paper IV

Concrete walls with cut-out openings strengthened by FRP-confinement

Cosmin Popescu, Gabriel Sas, Thomas Blanksvärd and Björn Taljsten

Manuscript prepared for submission to:

Journal of Composites for Construction - ASCE

Concrete walls with cut-out openings strengthened by FRP-confinement

Cosmin Popescu[1,*]; Gabriel Sas[2]; Thomas Blanksvärd[3]; and Björn Täljsten[4]

[1]Ph.D. Candidate, Northern Research Institute – NORUT, Rombaksveien E6-47, N-8517 Narvik, Norway (corresponding author). E-mail: cosmin@norut.no

[2]Associate Senior Lecturer, Dept. of Civil, Environmental and Natural Resources Engineering, Luleå Univ. of Technology, 971 87, Luleå, Sweden

[3]Associate Senior Lecturer, Dept. of Civil, Environmental and Natural Resources Engineering, Luleå Univ. of Technology, 971 87, Luleå, Sweden

[4]Professor, Dept. of Civil, Environmental and Natural Resources Engineering, Luleå Univ. of Technology, 971 87, Luleå, Sweden

Abstract

Redesigning buildings to improve their space efficiency and allow changes in use is often essential during their service lives to comply with shifts in living standards and functional demands. This may require the introduction of new openings in elements such as beams, walls and slabs, which inevitably reduces their structural performance, and hence necessitates repair or strengthening. However, there are uncertainties regarding both the effects of openings and the best remedial options. Here we report an experimental investigation of the effectiveness of fiber-reinforced polymer (FRP)-based strengthening for restoring the axial capacity of a solid reinforced concrete wall after cutting openings. Nine half-scale specimens, designed to represent typical wall panels in residential buildings with and without door-type openings, were tested to failure. FRP-confinement and mechanical anchorages increased the axial capacity of walls with small and large openings (which had 25% and 50% reductions in cross-sectional area, respectively) by 34-50% and 13-27%, to 85-94.8% and 56.5-63.4% of their pre-cutting capacity, respectively.

Author keywords: Strengthening, Fiber-reinforced polymers, Concrete walls, Openings, Axial strength, Eccentricity, Mechanical anchorages, Confinement, Disturbed regions

Introduction

Openings in reinforced concrete (RC) structural elements such as beams, slabs or walls are often needed for technical or functionality reasons, i.e. to improve their space efficiency and/or meet shifts in functional requirements. However, openings have clear negative effects, as addressed in numerous studies – recent examples include (Mohammed, et al. 2013, Florut, et al. 2014, Todut, et al. 2014, Popescu, et al. 2015a) – through the introduction of disturbed regions that significantly decrease the elements' ultimate load capacity, stiffness and energy dissipation. Thus, effects of any opening must be carefully considered in design stages, and addressed by specifying appropriate reinforcement detailing around the edges. However, when openings must be introduced in structures that have already been built the scope for such detailing is very limited. Instead, repair is often required (defined here as actions that fully or partially restore the structure's load-carrying capacity). New repair options are being developed and applied, but both further development of innovative approaches and more knowledge of their effects is needed.

European (EN1992-1-1 2004) and Australian (AS3600 2009) design codes provide some guidance regarding the design of walls with openings subjected to vertical loads. Both assume that the effects of a "small" opening (with area and height less than 1/10 and 1/3 of the wall's total area and height, respectively) on the structural integrity of the element can be neglected if the wall is restrained on all sides. For a "large" opening exceeding these proportions, each remaining portion should be separately considered. The portion between a restraining member and opening should be treated as a separate member, supported on three sides, while areas between openings (if there are more than one) must be treated as being supported on two sides. Several other empirical models have also been proposed (Saheb and Desayi 1990, Doh and Fragomeni 2006, Guan 2010), calibrated using data from limited numbers of one-way (OW) and two-way (TW) action tests, with loading eccentricity up to one sixth of the wall thickness (Popescu, et al. 2015b). One-way and two-way action refer here to cases where, due to eccentricity, flexure occurs in one and two directions, respectively, as in panels restrained along the top and bottom edges (which develop out-of-plane curvature parallel to the load direction), and panels restrained along three or four sides (which generally deform in both horizontal and vertical directions).

The aim of the study presented here was to contribute to efforts to develop a convenient new repair system that can substantially restore the axial strength of concrete walls after openings have been cut. Traditionally RC walls with openings have been strengthened by either installing a frame around the openings using RC/steel members (Engel n.d.) or increasing the elements' cross-sectional thickness (Delatte 2009). Nowadays, intervention in existing buildings must be minimal in order to minimize inconvenience due to limitations in use of the structure during repairs. An option is to use externally bonded fiber-reinforced polymers (FRP). This has been successfully tested by several authors in seismic retrofitting contexts (Demeter 2011, Li, et al. 2013, Todut, et al. 2015). Thus, the strengthening schemes proposed in the cited studies may not be suitable for repairing gravitationally loaded walls, and more research regarding their effects on elements' responses to vertically applied loads is required (Popescu, et al. 2015b).

The performance of non-seismically designed walls with openings strengthened with FRP has only been examined by Mohammed, et al. (2013), who strengthened OW, 1/3-scale RC walls with openings varying in size from 5% to 30% of the total wall area by placing carbon FRP (CFRP) sheets around edges of the openings. As expected, the walls' load-carrying capacity increased as the principal stresses on the opening corners decreased. A limitation of the study by Mohammed, et al. (2013) was that it only involved OW walls with no strengthening procedures for walls in TW action. Furthermore the failure mode (concrete crushing) of unstrengthened TW walls with openings observed in experimental tests (Popescu, et al. 2015a) indicates that the strengthening configuration proposed by Mohammed, et al. (2013) would not be suitable for them, and a better strengthening solution may be confinement.

Confinement with FRP has proved to be an efficient strategy for enhancing the strength and ductility of axially loaded members, although its effects are the most effective only for elements with circular cross-sections. For elements with rectangular cross-sections only parts of the cross-section are effectively confined (Mirmiran 1998, Pessiki 2001, Wu and Wei 2010, Liu, et al. 2015).

Design/analysis-oriented models developed by various researchers, reviewed by (Lam and Teng 2003, Rocca, et al. 2008), have shown that as the aspect ratio of the cross-section increases the enhancement of compressive strength provided by FRP-confinement decreases. Members with aspect ratios higher than 3:1 are usually regarded as wall-like columns. Creating a new opening in a concrete wall inevitably increases the aspect ratio of the remaining portions, hereafter piers (or wall-like column), and reduces the effectiveness of FRP-confinement. Few studies have addressed this problem. However, it has been shown that the axial strength and ductility of short (1.5 m) columns with an aspect ratio of 3.65 to 1 can be increased by confinement using longitudinal and transversal FRP sheets in combination with placing fiber anchor spikes along the wider faces of the column (Tan (2002) or adding semi-cylindrical attachments (high-strength mortar) to increase the cross-sectional area (Tanwongsval, et al. (2003). In addition, quadri-directional CFRP can improve seismic performance, but not other strength parameters, according to (Prota, et al. (2006). Adding heavy anchor spikes or cross-sectional enlargement with high-strength mortar can also double the confining effect of circumferential FRP, but excessively light fiber anchor spikes fail prematurely and thus have little effect on strength as with no anchors (Triantafillou, et al. (2015). In contrast to these findings, Luca, et al. (2013) found that confining wall-like columns with an aspect ratio of 2.92 to 1 with FRP (but no longitudinal or anchor fibers) could enhance the axial ductility, but not axial capacity. Hence it is necessary to use a hybrid method (FRP-confinement and longitudinal FRP fibers, anchors or increases in cross-section) when it is necessary to increase both the axial strength and ductility of wall-like columns.

Before such an approach can be used with confidence more information about response of the overall system is required. Hence, in the presented study the effectiveness of FRP-confinement with mechanical anchorages for increasing the axial strength of concrete walls weakened by cut-out openings was investigated. Increases in axial strength, ductility, steel reinforcement and FRP strain utilization were measured to improve understanding of such elements' structural behavior. The results provide information that it is believed will assist efforts to develop a new design model capable of capturing complicating effects such as load eccentricity and large aspect ratios of elements' cross-sections.

Experimental testing

Specimen design and test matrix

Half-scale walls designed to represent typical wall panels in residential buildings with and without cut-out openings (1800 mm long, 1350 mm wide and 60 mm thick), were constructed for testing to failure. The specimens are designed to carry vertical loads with no transverse loads between supports or lateral in-plane forces. The walls were tested in TW action and subjected to axial loading with small eccentricity (1/6 of the wall thickness), as typically found in practice and applied in previous studies. Moreover, the simplified design formulas found in the literature were calibrated for eccentricity up to one sixth of a wall's thickness to ensure that the resultant of all loads passes through the middle-third of the wall's overall thickness. Thus, the selected eccentricity facilitates comparison of results with those of previous tests and further development of published equations.

Minimum wall reinforcement was provided according to American and Australian design codes (ACI318 2011, AS3600 2009). In the European code (EN1992-1-1 2004) such specimens are treated as lightly reinforced or un-reinforced elements, as the sections contain reinforcement placed within a single layer, thus not contributing to the overall capacity. Consequently, welded wire fabric reinforcement was used to reinforce the walls, consisting of deformed 5 mm diameter bars with 100 mm spacing in both orthogonal directions and centrally placed in a single layer. The vertical and horizontal steel reinforcement ratios resulting from this configuration are 0.327% and 0.315%, respectively. The specimens with openings were detailed to replicate solid walls with sawn cut-outs, i.e. no additional reinforcement was placed around the edges or corners of the openings. More details about the fabrication process are given in (Popescu, et al. 2015a).

The test matrix can be divided into three stages, designated I-III, in which reference (unstrengthened) specimens, pre-cracked specimens strengthened by FRP and uncracked specimens strengthened by FRP (duplicated to increase the reliability of the data) were tested, respectively. As mentioned above, all of these specimens were 1800 mm long, 1350 mm wide and 60 mm thick.

Three specimens were loaded to failure in stage I: a solid panel, a panel with a "small" symmetric half-scaled single door-type opening (450 mm x 1050 mm), and a panel with a "large" symmetric half-scaled double door-type opening (900 mm x 1050 mm). The results are illustrated in Fig. 1. The small and large openings represent 25% and 50% reductions, respectively, in the cross-sectional area of the solid wall. Thus, these tests enabled evaluation of effects of introducing new openings in a solid wall. The damage level was evaluated in terms of ultimate load, crack pattern, displacement profiles, strains in concrete and steel reinforcement, ductility, and energy release at failure. Detailed results have been published in (Popescu, et al. 2015a).

In stage II, two specimens (one with a small opening and one with a large opening) were first loaded to the point required to create a significant crack based on nonlinear finite element analyses and observations of the reference specimens in stage I. Of course, the significance of a crack

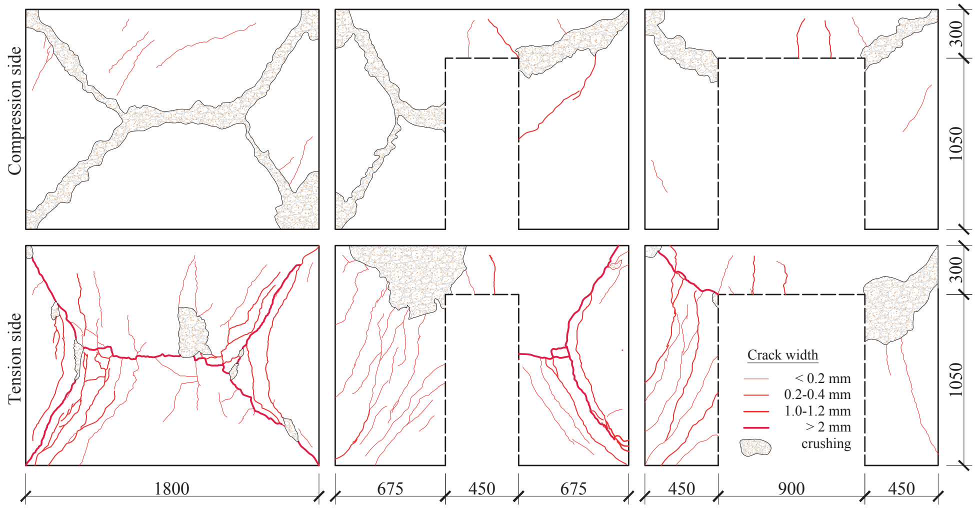

Fig. 1. Crack patterns and failure modes of the unstrengthened specimens of a solid wall (left) and walls with a small opening (center) and large opening (right) at failure

depends on many factors, including the building's functions and environmental exposure. However, according to ACI 224R-01 (2001) a crack wider than 0.15 mm may require repair. To create cracks of this width the specimens were loaded up to 75% of their unstrengthened axial capacity. They were subsequently completely unloaded then strengthened by FRP and tested to failure. This procedure mimics scenarios in which the creation of openings and subsequent presence of a sustained load results in degradation of a wall.

In stage III duplicated specimens with openings of each size were strengthened with the FRP system in an uncracked state then loaded to failure.

For convenience, the specimens are designated according to the stage when they were tested (I, II or III), their type (C, S or L: for solid wall, and walls with small and large openings, respectively) and (for specimens used in stage III) serial number. It should be noted that "small" and "large" are used here as convenient designations rather than as clearly delimited terms with specific thresholds and implications.

CFRP strengthening

Design method

Information obtained from analysis of failure modes of unstrengthened walls reported by (Popescu, et al. 2015a) was used to identify a suitable FRP configuration. In all cases, the walls had a brittle failure due to crushing of concrete with spalling and reinforcement buckling. High resolution pictures of both the tension and compression sides after collapse were imported into CAD software to map and display the cracks (Fig. 1). In order to increase the axial strength of walls with openings, confinement strengthening was designed as follows. First, the decrease in capacity caused by introducing new openings was found by testing the unstrengthened elements. The results indicate that the 25% and 50% reductions in cross-sectional area of the solid wall caused by introducing the small and large opening reduced the load carrying capacity by nearly 36% and 50%, respectively.

Next, the EC2 (EN1992-1-1 2004) design model for TW walls was used to find the confined compressive strength (f_{cc}) needed to restore the capacity of the solid wall. The resulting value was then used in conjunction with the model presented by Lam and Teng (2003) to estimate the required thickness of FRP jacket.

For FRP-wrapped rectangular concrete columns, Lam and Teng (2003) proposed an analytical relationship, Eq. (1), which considers the effect of non-uniformity of confinement through a shape factor (k_{s1}):

$$\frac{f_{cc}}{f_c} = 1 + k_1 k_{s1} \frac{f_l}{f_c} \tag{1}$$

where f_c is compressive strength of the unconfined concrete, f_{cc} is compressive strength of the confined concrete; $k_1 = 3.3$ is the confinement effectiveness coefficient and f_l is confining pressure.

$$k_{s1} = \left(\frac{b}{h}\right)^2 \frac{A_e}{A_c} \tag{2}$$

The effective confinement area ratio A_e/A_c is calculated as:

$$\frac{A_e}{A_c} = \frac{1 - \left[\left(b/h \right) (h - 2R)^2 + (h/b)(b - 2R)^2 \right] / 3A_g - \rho_{sc}}{1 - \rho_{sc}} \tag{3}$$

where b and h are width and height of the cross-section, respectively, A_e is effective confinement area, A_c is total area of the cross-section, R is corner radius, r_{sc} is cross-sectional area proportion of longitudinal steel, and A_g is gross area of the column section with rounded corners.

$$f_l = \frac{2 \cdot f_{frp} \cdot t_{frp}}{D'} = \frac{2 \cdot f_{frp} \cdot t_{frp}}{\sqrt{h^2 + b^2}} \tag{4}$$

where f_{frp} and t_{frp} are the tensile strength and thickness of the FRP jacket, respectively.

As the model is not valid for members with high cross-section aspect ratios the following procedure was employed. The transverse fiber sheets were fixed using steel bolts in a configuration that created virtual cross-sections with an aspect ratio limited to 2:1 (60 x 120 mm² starting from the edge of the opening, see Fig. 2). Following the assumption by Tan (2002), that such internal transverse links provide additional anchor points for FRP jackets, the effectively confined area for pure compression is shown in Fig. 2. Based on required thicknesses of FRP layers under these conditions back-calculated from Eq. (4), two and three 0.17 mm thick FRP layers were used to strengthen the specimens with small and large openings, respectively. The authors are aware that loading eccentricity (included in the tests to mimic imperfections in routine construction practices), may reduce the axial strength, but the lack of better models prevented the incorporation of appropriate parameters to simulate its effects. Thus, as noted by Mukherjee (2004) more tests are required to extend current confinement models to account for loading imperfections.

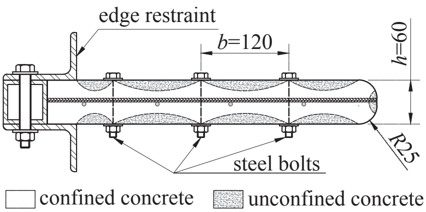

Fig. 2. Effectively confined area of a wall pier (dimensions in mm)

Specimen preparation and material properties

The walls were cast in a long-line form, in lying position resting on a steel platform that can accommodate up to five specimens, in two batches: the specimens used in stages I and II in the first batch, and those used in stage III in the second batch. The concrete used to cast the specimens was a self-consolidating mix that could be poured without vibrating it, including dynamon NRG-700, a superplasticizer added to provide high workability and early strength. To determine mechanical characteristics of the concrete (compressive strength and fracture energy), five cubes and beams from each batch with standardized sizes were cast and cured in identical conditions to the specimens. The average cubic compressive strength of the concrete was determined in accordance with (SS-EN 12390-3:2009 2009) while the fracture energy was determined following recommendations in RILEM TC 50-FMC (1985). In addition, five coupons were taken from the reinforcing steel meshes and tested according to SS-EN ISO 6892-1:2009 (2009) to determine their stress-strain properties.

Table 1 Mechanical properties of the concrete and steel reinforcement

<table>
<tr><td>Batch</td><td colspan="4">Concrete</td><td colspan="8">Steel reinforcement</td></tr>
<tr><td></td><td colspan="2">Compressive strength</td><td colspan="2">Fracture energy</td><td colspan="4">Yield</td><td colspan="4">Tensile</td></tr>
<tr><td></td><td colspan="2"></td><td colspan="2"></td><td colspan="2">Strength</td><td colspan="2">Strain</td><td colspan="2">Strength</td><td colspan="2">Strain</td></tr>
<tr><td></td><td>f_{cm} (MPa)</td><td>CoV (%)</td><td>G_F (N/m)</td><td>CoV (%)</td><td>f_y (MPa)</td><td>CoV (%)</td><td>ε_y (‰)</td><td>CoV (%)</td><td>f_u (MPa)</td><td>CoV (%)</td><td>ε_u (‰)</td><td>CoV (%)</td></tr>
<tr><td>Batch 1</td><td>62.8</td><td>3.2</td><td>168</td><td>11.9</td><td rowspan="2">632</td><td rowspan="2">0.35</td><td rowspan="2">2.8</td><td rowspan="2">8.45</td><td rowspan="2">693</td><td rowspan="2">0.40</td><td rowspan="2">4.87</td><td rowspan="2">4.82</td></tr>
<tr><td>Batch 2</td><td>64.4</td><td>2.8</td><td>228</td><td>12.5</td></tr>
</table>

The results (means and corresponding coefficients of variation, CoV) are given in Table 1.

Temporary timber supports were created for all six specimens to replicate the vertical positions of the elements in a structure and provide access around the specimens. The concrete surfaces were prepared by grinding and cleaning with compressed air (see Fig. 3a-b). The corners adjacent to the opening edge were rounded with a corner radius of 25 mm to avoid premature failure of the FRP and increase the effect of confinement. The strength enhancement relies on the continuity (fully wrapped) of the fiber sheets in the transverse direction. The as-built boundary conditions limited access to lateral edges of the cross-section. Therefore, we applied U-shaped CFRP sheets fixed with mechanical anchorages, installed in 8 mm holes drilled through the wall at positions pre-marked on the concrete surface.

The sheets were applied using the wet lay-up procedure as illustrated in Fig.3c-d. A two-component epoxy primer (StoPox 452 EP) was applied to the prepared surfaces of the specimens, while CFRP (StoFRP IMS300 C300) sheets were impregnated with StoPox LH two-component epoxy resin (elastic modulus, 2 GPa) then applied approximately 6 hours later.

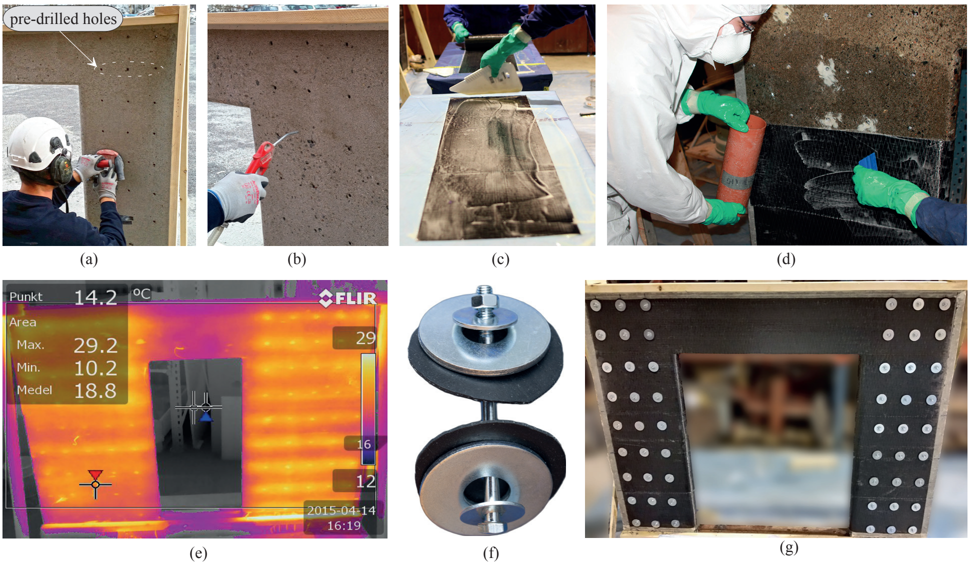

Fig. 3. Strengthening process: (a) grinding the concrete surface, (b) cleaning with compressed air, (c) impregnating the fibers, (d) applying the fibers to the specimen, (e) thermal image indicating positions of the holes, (f) mechanical anchorage, (g) specimen prepared for testing

These sheets have uni-directional fibers, high tensile strength (5500 MPa) and intermediate elastic modulus (290 GPa) according to the supplier. The specimens were stored indoors at around 18°C for about 7 days to allow the epoxy resin to cure. The surface of each specimen surface was then locally heated with a heat gun and a thermal imaging camera (FLIR T-series) was used to look for areas with poor adhesion or air voids (none were detected) and find the pre-drilled holes (Fig. 3e). Steel anchorage bolts, M6S 8.8 – SS-EN ISO 4014 (2011), were then inserted into pre-drilled holes and prestressed with a torque estimated from the clamp load as 75% of the proof load as specified in SS-EN ISO 898-1 (2013). Neoprene padding was placed between the 50 mm steel washers providing the anchorage and CFRP to avoid shearing of the fibers. The whole strengthening process is illustrated in Fig. 3. The strengthening entirely covers the concrete surface, so humidity and moisture issues may arise. However, the panels used in this study were intended to mimic indoor elements, classified as environmental Class 0 (i.e. structures located in a dry environment with low humidity) according to Täljsten (1999). The strengthening was applied without any sustained load due to permanent and partly due to imposed load.

Test setup and instrumentation

All specimens were tested gravitationally in a test-rig designed to represent the as-built boundary conditions. The test rig had to simulate hinged connections at the top and bottom edges of the specimen and clamped side edges. The axial load was applied eccentrically (at 1/6 of the wall thickness) in increments of 30 kN/min with inspection stops every 250 kN to monitor cracks in the specimens. The eccentricity was induced by a 22 mm diameter steel rod welded to each loading beam (HEB220). Four hydraulic jacks, each with a maximum capacity of 1.4 MN, were networked together to apply a uniformly distributed load along the wall length. More details about the design of the test rig are given in (Popescu, et al. 2015a). A general view of the test setup is shown in Fig. 4.

Out-of-plane and in-plane displacements were monitored using linear displacement sensors, and strain gauges intercepting potential yield lines (obtained from nonlinear finite element analysis)

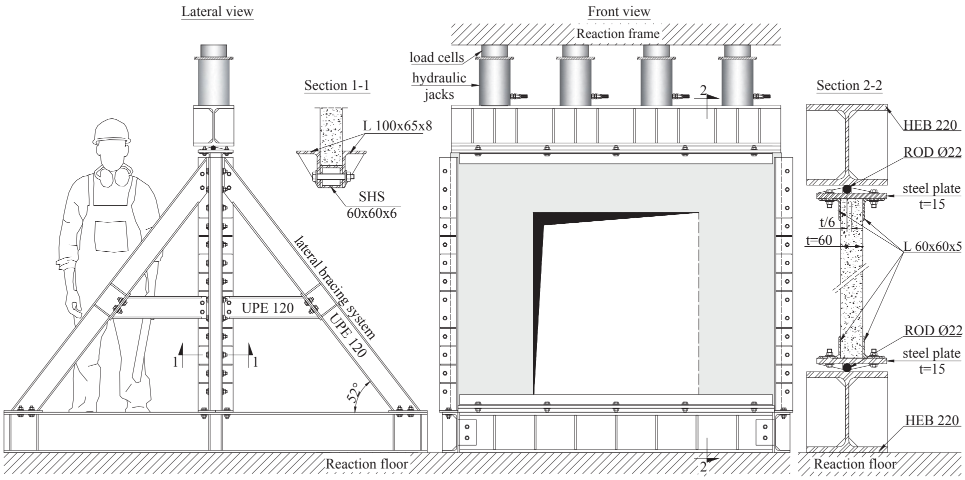

Fig. 4. Test setup and boundary conditions (all dimensions in mm)

Note: Sections 1-1 and 2-2 scaled up to show details were installed on the steel reinforcement and CFRP. Data obtained from the strain gauges and linear displacement sensors were then supplemented by measuring full-field strain distributions, using digital image correlation (DIC) technique. A system (GOM mbH) capable of capturing three-dimensional displacements was then used to facilitate the DIC measurements. The area of each specimen monitored by the optical DIC system was the right-upper corner on the tension side (780 mm x 660 mm, see Fig. 5), an area of particular interest for monitoring strain and crack development in discontinuous regions. Patterning of the monitored surfaces (required for this equipment) was applied using a stencil and spray for unstrengthened specimens, and manually for strengthened elements since access to the surface was obstructed by the anchorages. A regular pattern was obtained when the stencil was used, while a random pattern was manually applied. To avoid interference with the optical measurement system the reinforcement and outer FRP layer were only instrumented with strain gauges on half of each specimen (the left pier, on the tension side), as permitted by the symmetry of the test set-up. The instrumentation scheme for walls with openings is shown in Fig. 5. The arrangement of the monitoring system for the solid wall differed, but the position of D1 was identical to enable comparison of all specimens.

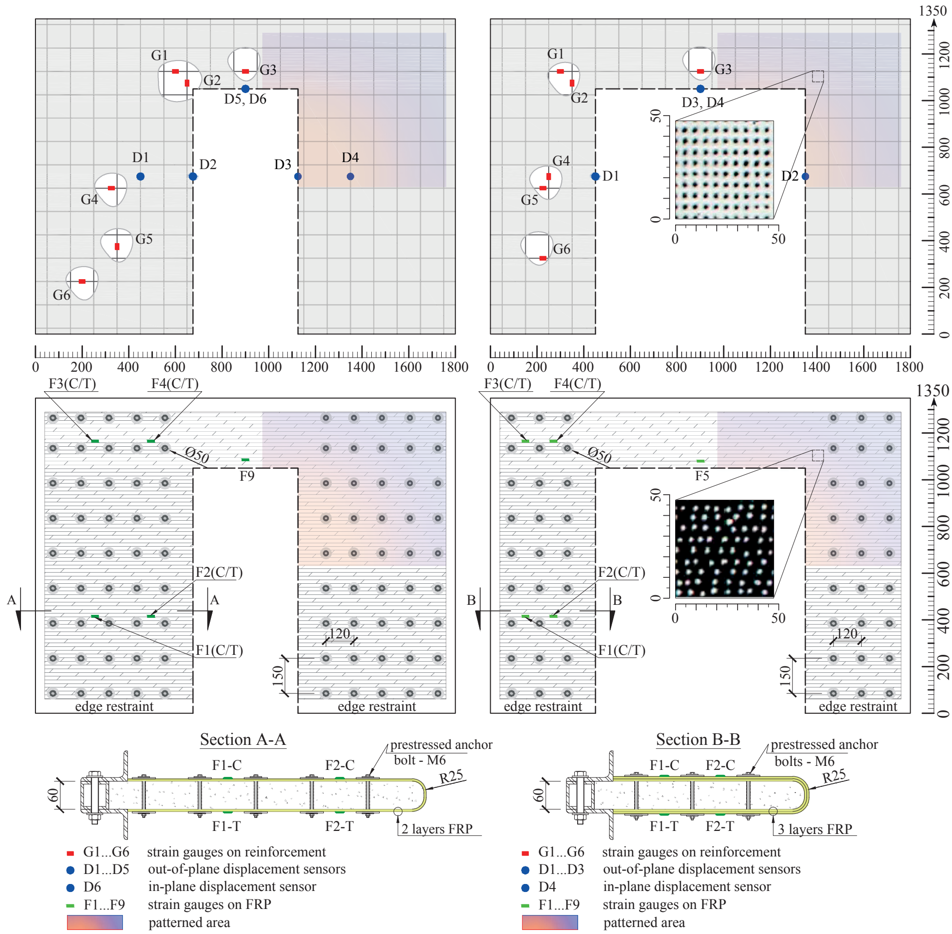

Fig. 5. Specimens' configurations, reinforcement and FRP strengthening details, and instrumentation (all dimensions in mm)

Test results and discussion

Tests on reference specimens. Stage I

This section briefly summarizes results from stage I, i.e. tests with reference specimens, which behaved typically for elements restrained on all sides, deflecting in both horizontal and vertical directions. The displacements were generally symmetric, but there were some asymmetries due to variations in material properties. All specimens failed by concrete crushing with spalling and reinforcement buckling. Cracks opened late in the loading of the solid wall (at 85% of the peak load), and earlier in the loading of specimens with both small and large openings (at 50% and 20% of peak load, respectively). The peak loads are presented in Table 2, and the effects of opening size in the load-displacement curves for the three specimens (recorded at the same position, D1) shown in Fig. 6. Crack patterns at failure were mapped and quantified in terms of crack widths using a graduated magnifying device (see Fig. 1). Strain responses in steel reinforcement and concrete were also recorded and are given elsewhere (Popescu, et al. 2015a), but strains in the reinforcement at selected load levels are given in comparison with those from strengthened specimens to evaluate the strain utilization.

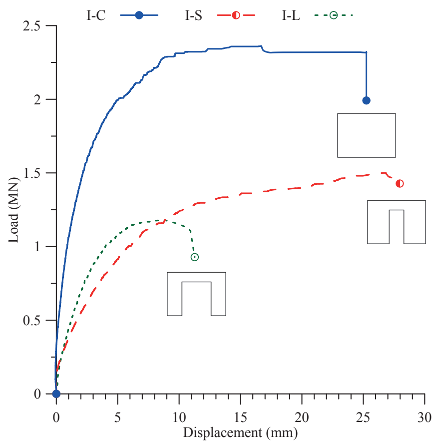

Fig. 6. Load-displacement responses of the three reference specimens showing effects of opening size

Table 2 Summary of test results

Specimen	N_{test} (kN)	$\varepsilon_{u.frp}$ (‰) F1 T	F1 C	F2 T	F2 C	F3 T	F3 C	F7 T	F7 C	F9 T	δ_e (mm)	δ_u (mm)	μ_Δ	E_d (kNm)
I-C	2363										4.3	25.3	5.89	55.18
I-S	1500					-					9.0	28.0	3.11	33.77
I-L	1180										3.8	11.3	2.94	10.88
II-S	2241	0.88	0.23	0.87	0.10	0.70	0.08	1.38	– 0.18	1.51	9.1	18.0	1.97	31.23
II-L	1497	0.46	0.21	0.21	0.13	0.27	0.21	0.39	0.08	1.24	4.1	5.0	1.23	4.66
III-S1	2178	0.80	0.20	0.96	0.20	0.73	– 0.25	0.95	0.20	1.89	8.2	15.9	1.94	26.61
III-S2	2009	0.94	– 0.02	0.81	0.22	0.99	0.37	1.64	– 0.11	1.57	4.6	15.5	3.38	29.89
III-L1	1334	0.24	0.05	0.22	0.18	0.47	0.25	0.88	– 0.14	1.63	8.0	8.4	1.05	6.60
III-L2	1482	N/A	0.11	N/A	0.10	N/A	0.53	0.54	0.44	1.48	3.4	7.4	2.18	9.66

Tests on strengthened specimens. Stages II & III

Pre-cracking

The specimens used in stage II were loaded up to 75% of the reference walls' axial capacity. At this point the strains recorded in the steel reinforcement were lower than yielding. The maximum values were -0.63‰ (compressed bar) and 0.43‰ (tensioned bar) for the specimen with a small opening and -0.91‰ and 2.25‰ for the specimen with a large opening. A few cracks were observed, mainly in the spandrel above the opening followed by other diagonal cracks from the bottom corner of the wall with approximately 50° inclination, similar to those reported for the reference specimens.

When the target damage (pre-cracking) level was reached, the specimens were completely unloaded and removed from the test setup to apply the strengthening. Thus the pre-cracks were nearly closed during this manipulation.

Failure modes

No cracks could be seen in the following loading cycles because the specimens were fully covered by FRP sheets. Thus, in contrast to the reference specimens, for which increases in deformations and cracking provided clear visual warnings of imminent failure, sounds provided more warnings of the imminent failure of strengthened specimens. Crushing of the concrete accompanied by debonding of the FRP sheets occurred at failure. In all but one of the tests (III-S2, see below)) the primary failure occurred at the bottom of one of the piers, and was immediately followed by bulging of the FRP on the diagonally opposite side, i.e. the region around the opening's corner. The debonding of the FRP started in regions between steel anchorage rows (see Fig. 7), highlighting the need for vertical strips or even bi-directional fibers to improve utilization of the CFRP fibers and further increase the element's axial strength.

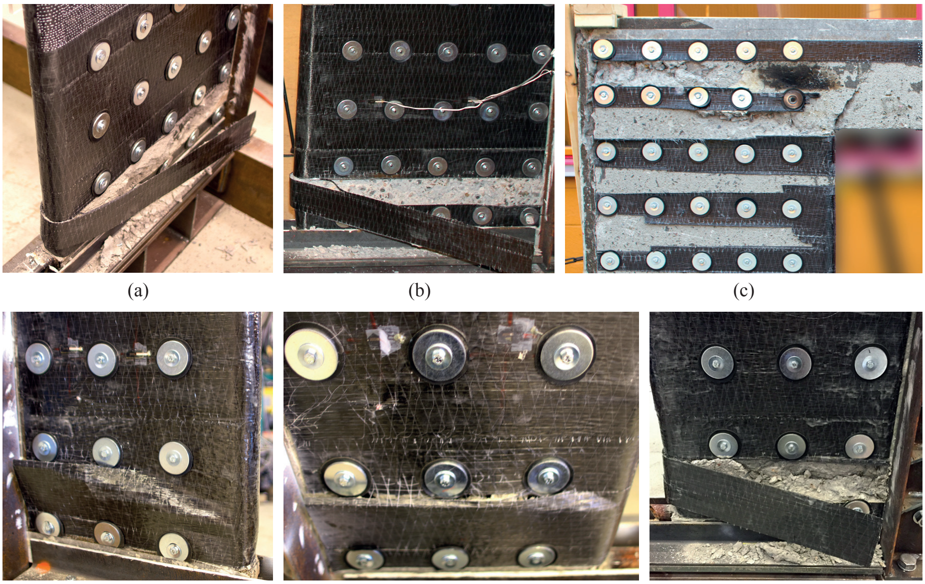

(a) (b) (c)

(d) (e) (f)

Fig. 7. Failure of the strengthened specimens: a) II-S, b) III-S1, c) III-S2, d) II-L, e) III-L1 and f) III-L2

After each test the FRP sheets were removed to observe crack patterns. None were detected part from those located around the failure region. However, as already mentioned, specimen III-S2 had a different failure mode, with crushing of concrete and debonding of the FRP along the line between the wall corner and opening corner of one pier (Fig. 7c). After stripping the FRP jacket (Fig. 7c) another diagonal crack was revealed on the spandrel starting from the re-entrant corner. The failure modes of all specimens, both pre-cracked and un-cracked, were similar.

Axial load versus displacements response

Figure 8 shows load-displacement data recorded at the D1 location (identical for all specimens) of both strengthened and reference elements. As shown in Table 2, the strengthening increased maximum loads at failure of pre-cracked specimens with small and large openings by 49% and 27%, respectively. Slightly lower increases were observed for uncracked specimens: 45% and 34% for specimens III-S1 and III-S2 with small openings, respectively, and 13% and 26% for specimens III-L1 and III-L2 with large openings, respectively. Thus, FRP strengthening seems to be most effective for pre-cracked elements. The FRP strengthening also changed the initial stiffness of the elements, but less for the pre-cracked specimens than for uncracked specimens. Similar behavior was reported by Wu, et al. (2014) for FRP-confined concrete cylinders with varying damage levels.

The increase in axial strength and initial stiffness of specimen III-L1 were relatively low due to an error during the test. The lateral bracing of the test rig was designed to be connected to the foundation support through oval holes, to account for variations in the thickness of the wall panels, thus allowing a little sliding of the entire system. The bolts were then prestressed to obtain high friction between the foundation support and lateral bracing elements. However, the bolts were accidentally loosened for specimen III-L1, thus friction was lost, permitting higher deformation of the specimen's lateral edges. This was detected by analyzing the measurements on the lateral bracing system, which for the sake of brevity are not plotted here.

The strengthening did not increase the load carrying capacity of any of the specimens with openings to that of a solid wall. The axial strength of specimens with a small opening were between 85-94.8% of that of a solid wall (target I-C, Fig. 8), while the axial strength of specimens with a large opening were 56.5-63.4% of that of a solid wall (target I-C) and 88.9-99.8% of that of a wall with a small opening (target I-S, Fig. 8). The higher increase in capacity of specimens with a small opening can be attributed to the larger aspect ratios of the piers. Thus, both dilatation of concrete in compression and yield lines of the concrete in tension contribute to the increase in capacity.

Steel reinforcement and FRP strain responses

It was believed that the strengthening method would affect local performance measures such as demands on the steel reinforcement. Thus, before casting electrical resistance strain gauges with pre-attached lead wires were bonded to the reinforcement to monitor such demands. Selected strain values at certain loadings (50%, 75% and 100% of the peak load) are compared with those obtained for the reference specimens in Figs.9 and 10. Unfortunately, the connections between some of these wires and the strain gauges were damaged during the strengthening process (e.g. grinding of the concrete surface). These gauges are indicated with asterisks in the figures.

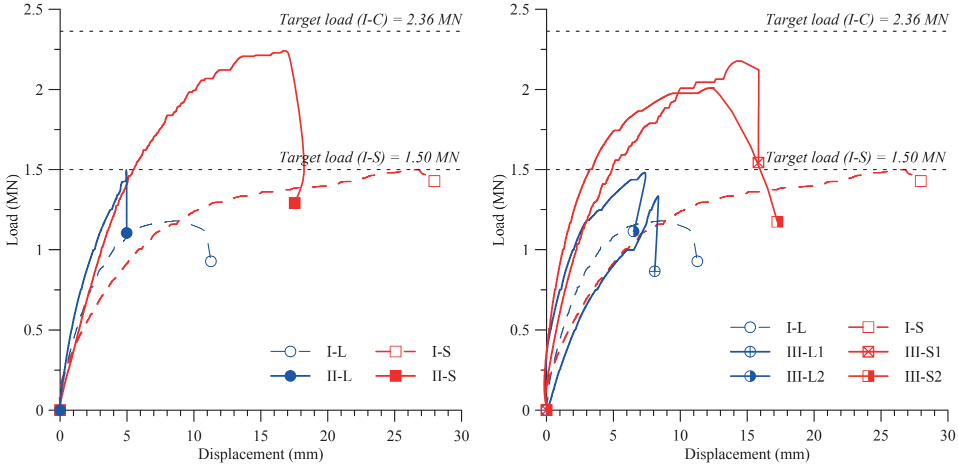

(a) (b)

Fig. 8. Load-displacement curves for reference (stage I) specimens and: (a) pre-cracked strengthened (stage II) specimens and b) uncracked strengthened specimens (stage III)

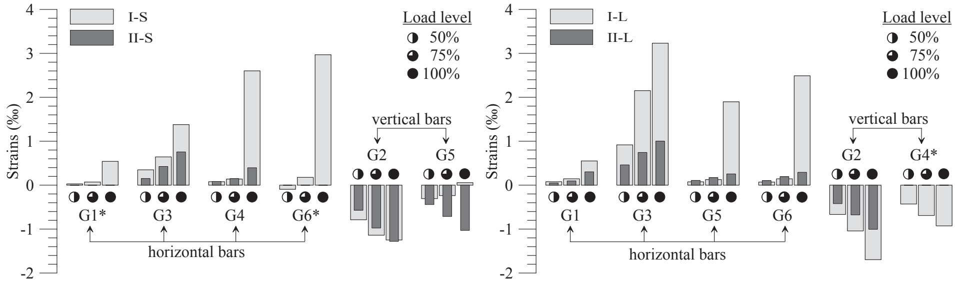

(a) (b)

Fig. 9. Strain utilization of the steel reinforcement for reference specimens (Stage I) and pre-cracked strengthened specimens (Stage II): a) with a small opening (I/II-S) and b) with a large opening (I/II-L)

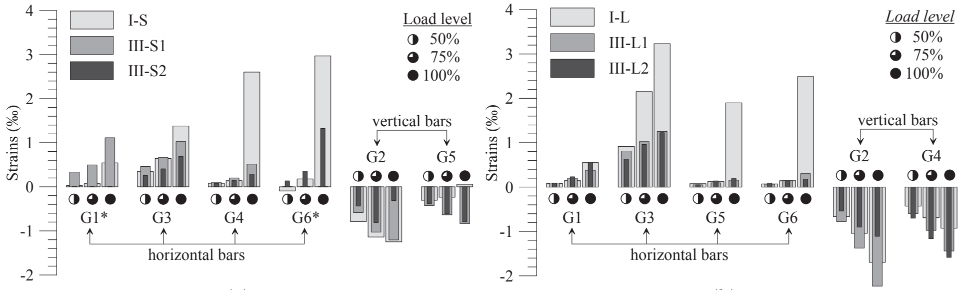

(a) (b)

Fig. 10. Strain utilization of the steel reinforcement for reference specimens (Stage I) and uncracked strengthened specimens (Stage III): a) with a small opening (I/III-S) and b) with a large opening (I/II-L)

* *Strains not recorded for strengthened specimens due to malfunction of the strain gauge*

The comparison is plotted as bar charts in Fig. 9 for pre-cracked, strengthened specimens and Fig. 10 for un-cracked, strengthened specimens. Overall, the FRP strengthening reduced strain in the steel reinforcement during the tests. It should be noted that Figs. 9 and 10 compare strains recorded at the same proportions of the specimens' peak loads. Thus, as peak loads were higher for the strengthened specimens, the effectiveness of the strengthening in this respect was even greater than the figures visually indicate.

Some of the strains recorded for reference specimens reached the yielding point at failure with buckling of the reinforcement, specifically of horizontal bars G4 and G6 located in the pier of the wall with a small opening, and G3 located in the midspan – bottom bar of the spandrel for the wall with large opening. Above the 75% load level the strains increased rapidly for all horizontal bars regardless of the opening size while a more gradual increase was observed for vertical bars.

For strengthened elements the demands on the steel reinforcement were somewhat lower during the specimen loading, and more evident as failure approached. The strains in these cases gradually increased, with no sudden jumps or either yielding or buckling of the reinforcement. The amelioration provided by the FRP fibers is less evident for vertical bars because the fibers had been aligned only horizontally, and thus provided relatively little vertical contribution. Strains were reduced (relative to those in corresponding unstrengthened specimens) particularly strongly in the horizontal bar above the opening, and most strongly in the specimens with large openings since the stresses on the reinforcement (and hence utilization of the composite material) increase with increases in the spandrel's span. No noticeable differences in these observations were detected between pre-cracked and uncracked specimens.

Strains in the FRP of strengthened specimens at peak load were also recorded, as listed in Table 2, where (for instance) F1-T and F1-C indicate strains recorded at position "F1" in the wall's plane at tension and compression sides of the element, respectively (see Fig. 5). The tension side is defined as the specimens' surface where tensile cracks occur due to load eccentricity. In a hypothetical eccentrically loaded one-dimensional element strain gauges located on the compression side would register higher strains, but the current problem is better described three-dimensionally, and strains in the examined specimens were higher on the tension side. In the design process this effect of non-uniformity in strain efficiency was not taken into consideration, which may explain why lower than predicted ultimate loads were registered for the strengthened elements. On average, strains on the tension side were more than two times higher than the readings on the compression side for specimens with large openings and more than six times higher for specimens with small openings. The strain gauge located at the midspan of the spandrel (F9) recorded the highest strains, peaking at about 1.89‰.

It should be noted that these values are measured strains and not necessarily the highest in the specimens since the strain paths may have differed from those expected. Moreover, single point information is not as valuable as full-field information. Therefore, we also examined full-field surface displacements and transformed them into surface strain fields. To reduce the computation time, areas around the anchorages (slightly larger than in reality to avoid their contours complicating analysis) were masked and ignored. Major strains in other areas of each specimen at the peak load were plotted (Fig. 11) to gain insights into the full strain field around the corner openings.

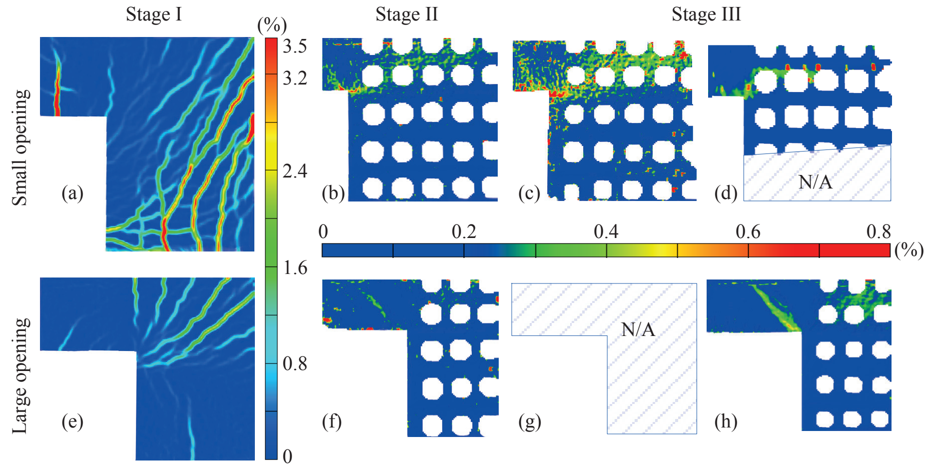

Fig. 11. Major strains detected by 3D-DIC analysis at peak loads of specimens: (a) I-S; (b) II-S; (c) III-S1; (d) III-S2; (e) I-L; (f) II-L (90% of peak load); (g) III-L1 and (h) III-L2

Cracks were denser and more distinct in unstrengthened specimens (Fig. 11a and e), than in strengthened specimens, where they were more scattered. Furthermore, in all strengthened specimens the major strains tended to form a diagonal path through the spandrel, indicating that the arching effect cancelled by introducing the opening is re-activated through addition of strengthening material. This effect is clearest for walls with large openings. For unstrengthened specimens 3D-DIC also offers more detailed, and valuable, information on crack patterns than the manually reproduced patterns shown in Fig. 1. This is partly because some cracks closed after failure and partly because hairline cracks are difficult to observe with the naked eye, especially during specimen loading.

Ductility factors and energy dissipation at failure

Displacement-based ductility factors (defined as the ratios between elastic and ultimate displacements, $\mu_\Delta = d_e/d_u$) were computed and are reported in Table 2. A simplified procedure proposed by Park (1988) was adopted to identify a distinct elastic displacement. The method assumes that the elastic displacement should be computed for an equivalent elasto-plastic system with reduced stiffness (arguably the most realistic approach for RC structures). The reduced stiffness is found as the secant stiffness related to 75% of the peak load and the horizontal plateau corresponding to the peak load of the real system. The maximum displacement corresponds to the post-peak deformation when the load has decreased by 20% or the reinforcement buckles, whichever occurs first. In addition to ductility factors, energy dissipation (E_d) was also evaluated as the area under the load-displacement curves.

Neither ductility factors nor energy dissipation were improved by the strengthening with FRP. In fact, in most cases reductions were noted for the strengthened specimens in relation to the corresponding unstrengthened specimens. The introduction of the small and large openings in a solid wall resulted in similar, sharp reductions in computed ductility factors and energy dissipation.

Conclusion and future work

The main conclusions drawn from the reported tests on the effectiveness of FRP-confinement of walls with cut-out openings can be briefly summarized as follows:

- Creating new openings in solid walls dramatically reduces their axial strength. The "small" and "large" openings in these tests resulted in 36% and 50% reductions, respectively. More tests are required, including walls with intermediate size openings, to identify optimal size thresholds and transition points between RC walls and RC frames in design codes for structural elements.

- The strengthening method increased the axial strength of specimens with small and large openings by 34-50% and 13-27% relative to that of corresponding unstrengthened specimens. However, the FRP strengthening method did not fully restore the axial strength of a solid wall in any of the tests. The type of FRP sheet used to strengthen the specimens was uni-directional, but bi-directional fibers or vertical strips may have been more effective. Also, anchoring the FRP sheets to the wall foundation and adjacent elements (i.e. transverse walls or floors) may delay debonding, thereby increasing the axial strength. The optimal distances between steel anchorages, and potential effects of the prestressing force of the bolts, should be further investigated.

- The strengthening did not avoid brittle failure, i.e. concrete crushing. However, it could avoid buckling of the reinforcement and the explosive failure mode observed in unstrengthened specimens.

- Reductions in energy dissipation and ductility factors of strengthened specimens, relative to corresponding unstrengthened specimens, reduce the system's effectiveness.

The lateral restraints transformed the problem into a three-dimensional rather than one-dimensional problem. It is therefore necessary to develop a design model that can better describe current stress states. In this study the design of the FRP strengthening was based on one-dimensional element with no load eccentricity assumptions. However, it may be possible to develop disk theory (Nielsen 1999) to derive a theoretical model that provides better estimates of capacities of FRP-strengthened walls with openings.

Acknowledgements

The authors would like to acknowledge the Research Council of Norway (RFF), Development Fund of the Swedish Construction Industry (SBUF) and Skanska for financing the work in this project. Special thanks are due to the technicians of CompLab, the structural engineering laboratory at Luleå University of Technology (LTU). The authors would also like to express gratitude to others who provided help during this research program, including: Dr. Dan Diaconu from Politehnica University Timisoara for helping with the strengthening work, and PhD students Cristian Sabau and Niklas Bagge (both from LTU) for providing help with optical measurements and fruitful discussions, respectively.

Notations

The folowing symbols are used in this paper:

A_c = Cross-sectional area of concrete
A_e = effective confinement area
A_g = the gross area of a column section with rounded corners
E_d = energy dissipation
G_F = fracture energy
N_{test} = peak load
R = corner radius
b = width of a cross-section
f_c = compressive strength of unconfined concrete
f_{cc} = compressive strength of confined concrete
f_{cm} = mean value of concrete cube compressive strength
f_{frp} = tensile strength of a FRP jacket
f_l = confining pressure
f_u = mean value of tensile strength of reinforcement
f_y = mean value of yield strength of reinforcement
h = height of the cross-section
k_1 = confinement effectiveness coefficient
k_{s1} = shape factor for strength enhancement
t_{frp} = thickness of a FRP jacket
δ_e = elastic displacement
δ_u = ultimate displacement
δ_u = mean value of tensile strain of reinforcement

References

ACI318 (2011). "Building code requirements for structural concrete and commentary (ACI 318–11)." American Concrete Institute (ACI), Farmington Hills, USA.

ACI 224R-01 (2001). "Control of Cracking in Concrete Structures." American Concrete Institute (ACI). ACI Committee 224.

AS3600 (2009). "Concrete structures." Standards Australia, Sydney, Australia.

Delatte, N. (2009). *Failure, Distress and Repair of Concrete Structures*, Woodhead Publishing.

Demeter, I. (2011). "Seismic retrofit of precast RC walls by externally bonded CFRP composites." Politehnica University of Timisoara, Romania: PhD Thesis.

Doh, J. H., and Fragomeni, S. (2006). "Ultimate load formula for reinforced concrete wall panels with openings." *Advances in Structural Engineering*, 9(1), 103-115.

EN1992-1-1 (2004). "Eurocode 2: design of concrete structures – Part 1–1: General rules and rules for buildings." Comité Européen de Normalisation (CEN), Brussels, Belgium.

Engel, P. (n.d.). "General rehabilitation techniques using steel." <http://www.constructalia.com/english/renovation_with_steel/ii_general_rehabilitation_techniques_using_steel#.VMPsNP6G9Wg>. (2015.01.23).

Florut, S.-C., Sas, G., Popescu, C., and Stoian, V. (2014). "Tests on reinforced concrete slabs with cut-out openings strengthened with fibre-reinforced polymers." *Composites Part B: Engineering*, 66C, 484–493.

GOM mbH "ARAMIS - Optical 3D Deformation Analysis." <http://www.gom.com/metrology-systems/system-overview/aramis.html>. (2015-05-20).

Guan, H. (2010). "Ultimate strength analysis of normal and high strength concrete wall panels with varying opening configurations." *Engineering Structures*, 32(5), 1341-1355.

Lam, L., and Teng, J. G. (2003). "Design-Oriented Stress-Strain Model for FRP-Confined Concrete in Rectangular Columns." *Journal of Reinforced Plastics and Composites*, 22(13), 1149-1186.

Li, B., Kai Qian, and Tran, C.T. N. (2013). "Retrofitting earthquake-damaged RC structural walls with openings by externally bonded FRP strips and sheets." *Journal of Composites for Construction*, 17(2), 259-270.

Liu, H.-X., Liu, G.-J., Wang, X.-Z., and Kong, X.-Q. (2015). "Effect of cross-sectional aspect ratio and basalt fiber-reinforced polymer-confined number on axial compression behavior of short columns." *Journal of Reinforced Plastics and Composites*, 34(10), 782-794.

Luca, A. D., Nardone, F., Lignola, G., Prota, A., and Nanni, A. (2013). "Wall-Like Reinforced Concrete Columns Externally Confined by Means of Glass FRP Laminates." *Advances in Structural Engineering*, 16(4), 593-604.

Mirmiran, A., Shahawy, M., Samaan, M., Echary, H., Mastrapa, J., Pico, O. (1998). "Effect of Column Parameters on FRP-Confined Concrete." *Journal of Composites for Construction*, 2(4), 175-185.

Mohammed, B., Ean, L. W., and Malek, M. A. (2013). "One way RC wall panels with openings strengthened with CFRP." *Construction and Building Materials*, 40, 575-583.

Mukherjee, A., Boothby, T., Bakis, C., Joshi, M., and Maitra, S. (2004). "Mechanical Behavior of Fiber-Reinforced Polymer-Wrapped Concrete Columns—Complicating Effects." *Journal of Composites for Construction*, 8(2), 97-103.

Nielsen, M. P. (1999). *Limit analysis and concrete plasticity, Second Edition*, CRC Press.

Park, R. (1988). "State of the art report: ductility evaluation from laboratory and analytical testing." *Proceedings of Ninth World Conference on Earthquake Engineering., Vol. VIII,* Tokyo-Kyoto, Japan, 605-616.

Pessiki, S., Harries, K., Kestner, J., Sause, R., Ricles, J. (2001). "Axial Behavior of Reinforced Concrete Columns Confined with FRP Jackets." *Journal of Composites for Construction*, 5(4), 237-245.

Popescu, C., Sas, G., Sabau, C., and Blanksvärd, T. (2015a). "Effect of cut-out openings on the axial strength of concrete walls." *Submitted to Journal of Structural Engineering.*

Popescu, C., Sas, G., Blanksvärd, T., and Täljsten, B. (2015b). "Concrete walls weakened by openings as compression members: A review." *Engineering Structures*, 89, 172-190.

Prota, A., Manfredi, G., and Cosenza, E. (2006). "Ultimate behavior of axially loaded RC wall-like columns confined with GFRP." *Composites Part B: Engineering*, 37(7–8), 670-678.

RILEM TC 50-FMC (1985). "Determination of the fracture energy of mortar and concrete by means of three-point bend tests on notched beams." *Materials and Structures*, 18(4), 287-290.

Rocca, S., Galati, N., and Nanni, A. (2008). "Review of design guidelines for FRP confinement of reinforced concrete columns of noncircular cross sections." *Journal of Composites for Construction*, 12(1), 80-92.

Saheb, M., and Desayi, P. (1990). "Ultimate strength of RC wall panels with openings." *Journal of Structural Engineering*, 116(6), 1565-1578.

SS-EN 12390-3:2009 (2009). "Testing hardened concrete – Part 3: Compressive strength of test specimens." Swedish Standards Institute (SIS), Stockholm, Sweden.

SS-EN ISO 898-1 (2013). "Mechanical properties of fasteners made of carbon steel and alloy steel - Part 1: Bolts, screws and studs with specified property classes - Coarse thread and fine pitch thread (ISO 898-1:2013)." Swedish Standards Institute (SIS), Stockholm, Sweden.

SS-EN ISO 4014 (2011). "Hexagon head bolts - Product grades A and B (ISO 4014:2011)." Swedish Standards Institute (SIS), Stockholm, Sweden.

SS-EN ISO 6892-1:2009 (2009). "Metallic materials – Tensile testing – Part 1: Method of test at room temperature (ISO 6892-1:2009)." Swedish Standards Institute (SIS), Stockholm, Sweden.

Tan, K. (2002). "Strength Enhancement of Rectangular Reinforced Concrete Columns using Fiber-Reinforced Polymer." *Journal of Composites for Construction*, 6(3), 175-183.

Tanwongsval, S., Maalej, M., and Paramasivam, P. (2003). "Strengthening of RC wall-like columns with FRP under sustained loading." *Materials and Structures*, 36(5), 282-290.

Todut, C., Dan, D., and Stoian, V. (2014). "Theoretical and experimental study on precast reinforced concrete wall panels subjected to shear force." *Engineering Structures*, 80, 323-338.

Todut, C., Dan, D., and Stoian, V. (2015). "Numerical and experimental investigation on seismically damaged reinforced concrete wall panels retrofitted with FRP composites." *Composite Structures*, 119, 648-665.

Triantafillou, T. C., Choutopoulou, E., Fotaki, E., Skorda, M., Stathopoulou, M., and Karlos, K. (2015). "FRP confinement of wall-like reinforced concrete columns." *Materials and Structures*, 1-14.

Täljsten, B. (1999). "Strengthening of existing concrete structures with carbon fibre fabrics or laminates. Design, material and execution." *Extract from Swedish National Railroad and Road Codes.*

Wu, Y.-F., and Wei, Y.-Y. (2010). "Effect of cross-sectional aspect ratio on the strength of CFRP-confined rectangular concrete columns." *Engineering Structures*, 32(1), 32-45.

Wu, Y.-F., Yun, Y., Wei, Y., and Zhou, Y. (2014). "Effect of Predamage on the Stress-Strain Relationship of Confined Concrete under Monotonic Loading." *Journal of Structural Engineering*, 140(12), 04014093.